



Search for dimuon resonance in the 35 to 75 GeV mass range using 140 fb^{-1} of 13 TeV pp collisions with the ATLAS detector

The ATLAS Collaboration

A model-independent search for low-mass resonances decaying into pairs of oppositely charged muons is presented. The analysis uses proton–proton collision data corresponding to an integrated luminosity of 140 fb^{-1} , recorded by the ATLAS detector at the Large Hadron Collider between 2015 and 2018. The search targets hypothetical dimuon resonances in the invariant mass range from 35 GeV to 75 GeV. The modelling of this mass region is particularly challenging for conventional analytic background parameterisations. To address this, a Gaussian process regression technique is used to model the background. The dimuon mass spectrum is analysed for potential signals, and no statistically significant excess is observed. Upper limits at the 95% confidence level are set on the fiducial production cross-section of new resonances decaying promptly into muons, ranging from 20 fb to 110 fb, depending on the resonance mass. These results are further interpreted in the context of dark-photon and dark-matter-mediator models, leading to new constraints on their parameter spaces.

Contents

1	Introduction	2
2	ATLAS detector	4
3	Data and Monte Carlo samples	5
3.1	Data sample	5
3.2	Simulation of signal processes	6
3.3	Simulation of background processes	7
4	Object and event selection	8
5	Signal modelling	8
5.1	Acceptance and efficiency	9
5.2	Parameterisation of the dimuon invariant mass	10
6	Systematic uncertainties	11
7	Background modelling and signal yield extraction	11
7.1	Signal extraction procedure with GPR-based background modelling	12
7.2	Hyper-parameters tuning of GPR	13
8	Statistical interpretation and limit setting	14
9	Results	15
10	Conclusions	20

1 Introduction

Many strategies are employed to search for physics beyond the Standard Model (BSM), motivated by the open questions that remain in particle physics. Model-independent searches for low-mass resonances are of considerable interest due to their potential to reveal new phenomena, such as possible dark-matter interactions. Among the possible final states, the dimuon channel provides a clean and well-understood signature, offering high sensitivity to a broad class of BSM scenarios.

BSM scenarios involving dark matter (DM) provide a compelling motivation for such searches. While there is convincing cosmological evidence for the existence of dark matter [1–4], its fundamental nature remains one of the most pressing open questions in both particle physics and cosmology. Although no interactions between DM and Standard Model (SM) particles beyond gravity have yet been observed, many theoretical models predict that DM could interact very weakly with SM particles [5]. These scenarios often introduce a hidden sector of particles, with interactions mediated by a new vector or axial-vector boson. If such interactions exist, these mediators could be produced in proton–proton (pp) collisions at the Large Hadron Collider (LHC) [6] and subsequently decay into SM particles.

While the search presented in this paper is designed to be model independent, two benchmark theoretical scenarios are used for interpretation, illustrating possible DM realisations leading to low-mass dimuon

resonances. A standard benchmark for LHC DM searches [7] involves extending the SM with an additional U(1) gauge symmetry, under which the DM particle carries a charge. If certain SM particles are also assumed to carry charges under this new gauge group, a new gauge boson, commonly denoted as Z' , could mediate interactions between SM and DM particles. Within the framework of a simplified s -channel exchange model, these interactions can be described by the following Lagrangians, incorporating both vector and axial-vector couplings:

$$\mathcal{L}_V \supset \frac{1}{2}m_{Z'}^2 V_\mu V^\mu - g_q V_\mu \bar{q}_i \gamma^\mu q_i - g_l V_\mu \bar{l}_i \gamma^\mu l_i - g_\chi V_\mu \bar{\chi} \gamma^\mu \chi \quad (1)$$

$$\mathcal{L}_A \supset \frac{1}{2}m_{Z'}^2 V_\mu V^\mu - g_q V_\mu \bar{q}_i \gamma^\mu \gamma^5 q_i - g_l V_\mu \bar{l}_i \gamma^\mu \gamma^5 l_i - g_\chi V_\mu \bar{\chi} \gamma^\mu \gamma^5 \chi \quad (2)$$

where $m_{Z'}$ is the mass of the Z' boson (V_μ). The couplings g_q and g_l are taken to be universal across all quark and lepton flavours, respectively, and g_χ represents the coupling between the mediator and the DM particle (χ).

An alternative, theoretically well-motivated framework introduces kinetic mixing between a dark Abelian gauge symmetry, $U_D(1)$, and the SM hypercharge, $U_Y(1)$ [8]. The relevant gauge terms in the Lagrangian are:

$$\mathcal{L} \supset -\frac{1}{4}B_{\mu\nu}B^{\mu\nu} - \frac{1}{4}Z_{D\mu\nu}Z_D^{\mu\nu} + \frac{1}{2}\frac{\epsilon}{\cos\theta}Z_{D\mu\nu}B^{\mu\nu} + \frac{1}{2}m_{Z_D,0}^2 Z_D^\mu Z_{D\mu}.$$

where the $U_Y(1)$ and $U_D(1)$ field strengths are defined as $B_{\mu\nu} = \partial_\mu B_\nu - \partial_\nu B_\mu$ and $Z_{D\mu\nu} = \partial_\mu Z_{D\nu} - \partial_\nu Z_{D\mu}$, respectively, and θ is the Weinberg mixing angle. In this model, the resonance, referred to as a dark photon, Z_D , has a mass m_{Z_D} , denoted as $m_{Z_D,0}$ before mixing with the SM. While the dark photon has no direct couplings to SM particles, the kinetic mixing parameter ϵ induces an effective coupling between the two sectors.

This analysis searches for new resonances decaying into pairs of muons, using the dimuon invariant mass as the primary discriminating variable. Benchmark signal models include a Z' and a Z_D , which could be directly produced via the Drell–Yan (DY) mechanism in pp collisions and subsequently decay promptly into a pair of oppositely charged muons, as illustrated in Figure 1. These benchmark signals serve as representative scenarios for evaluating the sensitivity of the search.

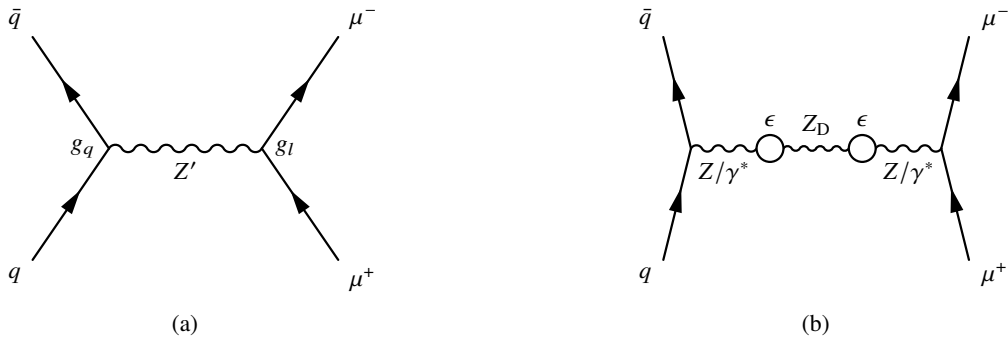


Figure 1: Feynman diagrams for Drell–Yan production of (a) a generic resonance Z' and (b) a kinetically mixed dark photon Z_D .

Searches for low-mass dimuon resonances have been performed by the CMS [9, 10] and LHCb [11] Collaborations, covering mass ranges of 1.1–7.9 GeV, 11.5–75 GeV and 110–200 GeV for CMS, and

0.214–70 GeV for LHCb. Building on similar strategies, this analysis employs a data-driven approach to estimate the dominant, smoothly varying background from Z/γ^* induced dimuon production and to search for new resonances appearing as localised deviations on top of this background spectrum using ATLAS data [12]. The mass region from 35 to 75 GeV is investigated. This range is selected based on signal-extraction capability and is explored for the first time in a resonance search with ATLAS data.

A key innovation of this study is the use of Gaussian process regression (GPR) [13–15], a flexible non-parametric method that is novel in the context of modelling the background shape in resonance searches. This replaces the traditional analytic functions used, for example, in Refs. [9–11, 16–18], to describe the background in simultaneous signal-plus-background fits, and provides a robust description of the full mass range accessible with standard, unrescaled muon triggers.

The signal is extracted through a binned simultaneous profile likelihood fit to the signal and background components observed in data. In the absence of a significant excess, upper limits are set on the fiducial production cross-section times branching ratio to the dimuon final state of a new resonance, as a function of its mass. These model-independent fiducial cross-sections are then parameterised into the coupling parameters of the DM mediator and dark photon models, described above, from which upper limits on these theoretical parameters are derived.

The structure of this paper is as follows. Section 2 provides a brief description of the ATLAS detector. Section 3 presents the data and Monte Carlo (MC) simulation samples used in the analysis. The event reconstruction and selection criteria are detailed in Section 4. Section 5 discusses the modelling of the signal and the associated systematic uncertainties. The background estimation and signal extraction based on GPR are described in Section 7. Section 8 outlines the statistical interpretation and limit-setting procedure. The results and their interpretations in the context of benchmark models are presented in Section 9, and the conclusions are summarised in Section 10.

2 ATLAS detector

The ATLAS detector [12] at the LHC covers nearly the entire solid angle around the collision point.¹ It consists of an inner tracking detector surrounded by a thin superconducting solenoid, electromagnetic and hadronic calorimeters, and a muon spectrometer incorporating three large superconducting air-core toroidal magnets.

The inner-detector system (ID) is immersed in a 2 T axial magnetic field and provides charged-particle tracking in the range of $|\eta| < 2.5$. The high-granularity silicon pixel detector covers the vertex region and typically provides four measurements per track [19, 20]. It is followed by the semiconductor tracker (SCT), which usually contributes eight measurements per track. These silicon detectors are complemented by the transition radiation tracker (TRT), which extends track reconstruction capabilities to a radial distance corresponding to $|\eta| = 2.0$. The TRT also provides electron identification information based on the fraction of hits (typically 30 in total) above a higher energy-deposit threshold corresponding to transition radiation.

¹ ATLAS uses a right-handed coordinate system with its origin at the nominal interaction point (IP) in the centre of the detector and the z -axis along the beam pipe. The x -axis points from the IP to the centre of the LHC ring, and the y -axis points upwards. Polar coordinates (r, ϕ) are used in the transverse plane, ϕ being the azimuthal angle around the z -axis. The pseudorapidity is defined in terms of the polar angle θ as $\eta = -\ln \tan(\theta/2)$ and is equal to the rapidity $y = \frac{1}{2} \ln \left(\frac{E+p_z}{E-p_z} \right)$ in the relativistic limit. Angular distance is measured in units of $\Delta R \equiv \sqrt{(\Delta y)^2 + (\Delta \phi)^2}$.

The calorimeter system covers $|\eta| < 4.9$. Within $|\eta| < 3.2$, electromagnetic calorimetry is provided by barrel and endcap high-granularity lead/liquid-argon (LAr) calorimeters, with an additional thin LAr presampler covering $|\eta| < 1.8$ to correct for energy loss in material upstream of the calorimeters. Hadronic calorimetry is provided by the steel/scintillator-tile calorimeter within $|\eta| < 1.7$, and two copper/LAr hadronic endcap calorimeters in $1.5 < |\eta| < 3.2$. The solid angle coverage is completed with forward copper/LAr and tungsten/LAr calorimeter modules optimised for electromagnetic and hadronic energy measurements, respectively.

The muon spectrometer (MS) comprises separate trigger and high-precision tracking chambers measuring the deflection of muons in a magnetic field generated by the superconducting air-core toroidal magnets. The field integral of the toroids ranges between 2.0 and 6.0 T m across most of the detector. Three layers of precision chambers, each consisting of layers of monitored drift tubes, cover the region $|\eta| < 2.7$, complemented by cathode-strip chambers in the forward region, where the background is highest. The muon trigger system covers the range $|\eta| < 2.4$ with resistive-plate chambers in the barrel, and thin-gap chambers in the endcap regions.

Events were selected by the first-level trigger system implemented in custom hardware, followed by selections made by algorithms implemented in software in the high-level trigger [21]. The first-level trigger accepted events from the 40 MHz bunch crossings at a rate close to 100 kHz, which the high-level trigger further reduced in order to record complete events to disk at about 1.25 kHz.

A software suite [22] is used in data simulation, in the reconstruction and analysis of real and simulated data, in detector operations, and in the trigger and data acquisition systems of the experiment.

3 Data and Monte Carlo samples

3.1 Data sample

The data were recorded by the ATLAS detector during the period 2015–2018. After selecting data-taking periods corresponding to good detector conditions [23] and applying standard data-quality requirements, the total integrated luminosity amounts to 140 fb^{-1} [24, 25]. Events were selected using unprescaled single-muon and dimuon triggers [26].

For single-muon triggers, two types of trigger were employed, one with an isolation requirement and one without. The single-muon trigger with the isolation condition selected muons with transverse momentum $p_T > 26 \text{ GeV}$ that satisfied medium identification and isolation criteria [27]. To enhance acceptance for high-momentum muons, an additional non-isolated single-muon trigger requiring $p_T > 50 \text{ GeV}$ was also used, avoiding the isolation requirement whose efficiency decreases at high p_T .

Two dimuon triggers were employed, one with symmetric and the other with asymmetric p_T requirements on the two muons. The symmetric trigger required two muons with $p_T > 14 \text{ GeV}$, while the asymmetric configuration required one muon with $p_T > 22 \text{ GeV}$ and the other with $p_T > 8 \text{ GeV}$. Neither of the dimuon triggers applied isolation requirements to the muons.

3.2 Simulation of signal processes

Dedicated MC samples were produced for the benchmark signal models involving the Z' and dark photon (Z_D) resonances. These samples are used to model the signal acceptance, efficiency, and invariant-mass distributions. The simplified DM model was used for the MC production of the Z' signal samples, in which the Z' boson couples to SM and DM particles through either vector or axial-vector interactions, as defined in Eqs. (1) and (2). The two interaction types are denoted as Z'_V and Z'_A , respectively. To study one of the most commonly considered scenarios [5], the mass of the DM particle is set to 10 TeV, thereby kinematically forbidding the decay of the Z' boson into DM particles.

The simulations are based on a *Universal FeynRules Output* (UFO) [28, 29] implementation of the DMSimp model [30], generated using FeynRules [29]. The original model was modified to include couplings to leptons [31]. Signal events were generated at leading order (LO) using MADGRAPH 5 [8] with the A14 set of tuned parameters (tune) [32] and the NNPDF2.3LO [33] parton distribution function (PDF) set, followed by parton showering with PYTHIA 8 [34].

The differences in acceptance and mass shape modelling between the Z'_A and Z'_V models are found to be negligible. Therefore, signal sample production focuses on the axial-vector interaction case, while results for the vector case can be obtained by reinterpretation, using the relationship between couplings and cross-sections.

To explore different regions of parameter space, MC samples were generated over a range of Z' masses and intrinsic widths. For mass modelling, benchmarks were set between 35 GeV to 75 GeV, in 5 GeV intervals, with both g_l and g_q set to 0.1. To study intrinsic width effects, two representative mass points (45 GeV and 65 GeV) were chosen, and the coupling strength was varied from 0.1 to 0.3, maintaining $g_l = g_q$. This corresponds to intrinsic-width ratios of $\Gamma/m_{Z'} \approx 0.4\% - 4\%$.

The spacing between simulated mass points is validated as sufficient for interpolating the signal modelling, enabling a continuous parameterisation across the mass and width ranges of interest. The upper range of the coupling scan is chosen such that the intrinsic width becomes comparable to the detector resolution, allowing an evaluation of width effects on the analysis sensitivity. The intrinsic width Γ used is calculated according to theoretical predictions for Z'_A [31], which account for contributions from decays into leptons, quarks, and neutrinos, given by:

$$\begin{aligned}\Gamma^{q\bar{q}} &= \frac{g_q^2 m_{Z'}}{4\pi} (1 - 4z_q)^{3/2}, \\ \Gamma^{\ell\bar{\ell}} &= \frac{g_\ell^2 m_{Z'}}{12\pi} (1 - 4z_\ell)^{3/2}, \\ \Gamma^{\nu\bar{\nu}} &= \frac{g_\ell^2}{24\pi} m_{Z'},\end{aligned}$$

where $z_i = m_i^2/m_{Z'}^2$, with $i = q, \ell$.

LO Z_D samples were generated between 35 GeV to 75 GeV, in 5 GeV intervals, using the hidden Abelian Higgs model (HAHM v3) [8] implemented in MADGRAPH 5, in order to quantify the results in terms of the dark-photon interpretation. The input parameters for MADGRAPH 5 were derived from the chosen Z_D mass (m_{Z_D}), together with the corresponding width (Γ_{Z_D}) and branching ratio ($\mathcal{B}_{\ell\ell}$), calculated including three-loop quantum chromodynamics (QCD) corrections as reported in Ref. [8]. In the (HAHM v3) configuration used in this analysis, no hidden-sector states lighter than the Z_D are assumed, and therefore

the Z_D decays exclusively into Standard Model fermions. The NNPDF2.3LO [33] PDF set was used for the matrix-element calculation. Parton showering and hadronisation were performed by PYTHIA 8 [35], using the A14 tune and the NNPDF2.3LO [36] PDF set. Signal samples for both models were simulated using the ATLAS fast simulation framework (AtlFast-II) [37].

For both the Z' and Z_D signals, cross-sections were evaluated at LO and corrected to next-to-next-to-leading order (NNLO) using a common k-factor [38].

The effect of multiple interactions in the same and neighbouring bunch crossings (pile-up) for all simulated signal and background (described below) samples was modelled by overlaying the simulated hard-scattering events with inelastic pp events generated with PYTHIA 8.186 [35], the NNPDF2.3LO PDF set and the A3 tune [39]. Simulated events were reweighted to match the pile-up conditions in data. All samples were reconstructed and processed with the same trigger and reconstruction algorithms as used in data.

3.3 Simulation of background processes

To validate the statistical analysis for the data-driven background estimation, simulated SM background processes are used. The dominant contribution arises from DY $Z/\gamma^* \rightarrow \mu^+\mu^-$ production, with smaller contributions from $Z/\gamma^* \rightarrow \tau^+\tau^-$, top-quark pair ($t\bar{t}$) production, and diboson processes. Background events from the DY $Z/\gamma^* \rightarrow \mu\mu$ and $Z/\gamma^* \rightarrow \tau\tau$ process were simulated with SHERPA 2.2.1 [40] employing next-to-leading-order (NLO) accurate matrix elements for up to two partons, and LO-accurate matrix elements for up to four partons. These were calculated with the COMIX [41] and OPENLOOPS [42, 43] libraries and used the NNPDF3.0NNLO PDF set [44]. Parton showering was performed using the SHERPA parton shower [45] with MEPS@NLO matching [46–49]. Diboson processes (WW , WZ , and ZZ) were simulated with a similar set-up in SHERPA 2.2.1. The $t\bar{t}$ samples were generated at NLO using POWHEG BOX [50, 51] with the NNPDF3.0NLO PDF set interfaced to PYTHIA 8 for parton showering and hadronisation with the A14 tune. All background MC samples were processed by the full ATLAS detector simulation based on GEANT4 [52].

Typically, the equivalent integrated luminosity of the fully simulated background samples is 5–20 times higher than that of the data. To validate the signal extraction procedure with a smooth background template, an additional large DY sample was produced using a generator-smearing technique, following the method used in the ATLAS $H \rightarrow \mu\mu$ analysis [53]. In this technique, generator-level muons are smeared using parameterised detector resolutions that include non-Gaussian tails to emulate reconstruction effects. The generator-smearing simulation was performed with PYTHIA 8.244. Only $Z \rightarrow \mu\mu$ and $Z \rightarrow \tau\tau$ decays were enabled. To speed up event generation without affecting the final-state muon kinematics, multi-parton interactions and hadronisation were disabled. The A14 tune, together with the NNPDF2.3LO PDF set, was used as the baseline. Final-state radiation photons were simulated using the default PYTHIA 8 QED parton shower. The equivalent integrated luminosity of the generator-smearing sample corresponds to approximately 30 ab^{-1} . Residual mismodelling in the generator-smearing sample was corrected by reweighting its mass spectrum to match that of the fully simulated DY sample, using a high-order polynomial to avoid propagating statistical uncertainties from the fully simulated sample.

4 Object and event selection

Proton–proton interaction vertices are reconstructed from events containing at least two tracks associated with the ID, each with transverse momentum $p_T > 0.5$ GeV. Track reconstruction in the ID is performed using a combinatorial Kalman filter algorithm, seeded by hit triplets in the pixel and silicon microstrip detectors, with additional recovery of tracks formed from segments in the TRT. The primary hard-scatter vertex is defined as the vertex with the largest $\sum p_T^2$ of its associated tracks [54].

Most muon candidates are reconstructed using a combined track from the ID and the MS. To increase the muon reconstruction efficiency within the region $|\eta| < 1$, where the MS coverage is limited, additional muon candidates are reconstructed by matching an ID track to either calorimeter hits consistent with a minimum-ionising particle or to a single MS track segment.

Corrections are applied to the reconstructed muon momentum in simulation to ensure precise agreement with data. These corrections to the simulated momentum scale and resolution are parameterised as an expansion in powers of the muon p_T , with each coefficient determined as a function of η and ϕ [55].

Muon candidates are required to satisfy medium identification criteria [27]. To reduce the contribution from fake muons originating from light-jet misidentification, a particle-flow-based isolation criterion [56] is applied. In addition, to suppress muons from non-prompt heavy-flavour hadron decays, muon candidates must satisfy $|d_0/\sigma_{d_0}| < 3$ and $|z_0 \sin \theta| < 0.5$ mm, where d_0 is the transverse impact parameter measured relative to the measured beamline position, σ_{d_0} is its uncertainty, and z_0 is the longitudinal distance between the point of closest approach in the transverse plane and the primary vertex. Muon candidates are required to have $p_T > 3$ GeV and $|\eta| < 2.4$.

Events are selected if they contain at least two muon candidates. The two muons with the highest p_T are chosen to form the dimuon pair and are required to have opposite electric charges. To ensure that the trigger operated in its efficiency plateau region, dedicated selection criteria on p_T are applied to the muons matched to the corresponding trigger objects. These requirements are summarised in Table 1.

The overall trigger matching [26] is performed by applying a logical OR of the criteria listed for the various trigger types in Table 1. An event is considered matched if it satisfies the requirements of at least one trigger type. The signal region is defined by the invariant mass of the dimuon pair being within the range 30–80 GeV.

Table 1: Summary of matching criteria ensuring the events are in the trigger efficiency plateau.

Trigger type	Matching criteria	p_T [GeV]
Single muon	At least one muon matched to a single-muon trigger	> 27
Asymmetric dimuon	Leading muon matched to the high- p_T trigger object	> 23
	Subleading muon matched to the trigger low- p_T object	> 10
Symmetric dimuon	Both muons matched to the two trigger objects	> 15

5 Signal modelling

Building on the event selection outlined in the previous section, the expected signal contribution is modelled to assess the sensitivity of the analysis to possible new resonances. The modelling of the signal shape, and the evaluation of the acceptance and efficiency within the fiducial region are presented in this section.

5.1 Acceptance and efficiency

Following the detector-level selection, the signal production cross-section is evaluated within a fiducial volume defined by applying the muon selection criteria at particle level, as summarised in Table 2. These criteria are defined after final-state radiation and are designed to reflect the acceptance of the corresponding trigger matching applied at the reconstruction level. Three overlapping categories, single-muon, asymmetric-dimuon and symmetric-dimuon are defined to emulate the respective trigger requirements. An event is considered to be within the fiducial region if it satisfies the conditions of at least one of these three categories.

Table 2: Definition of fiducial regions. Each event is required to contain two muons (labelled as μ_1 and μ_2) that satisfy all listed selection criteria.

Fiducial categories	$p_T^{\mu_1}$ [GeV]	$p_T^{\mu_2}$ [GeV]	$ \eta^{\mu_1} $	$ \eta^{\mu_2} $
Single muon	> 27	> 3	< 2.4	< 2.4
Asymmetric dimuon	> 23	> 10	< 2.4	< 2.4
Symmetric dimuon	> 15	> 15	< 2.4	< 2.4

The fiducial regions, defined in Table 2, provide the framework for evaluating signal acceptance and selection efficiency. The acceptance (\mathcal{A}) is defined as the fraction of all generated signal events that satisfy the fiducial selections at particle level. The efficiency (ε) is defined as the probability that a fiducial event also passes the full reconstruction-level selection, including all object- and event-level requirements. These quantities are used to extrapolate the measured signal yield to the fiducial phase space and to interpret the results in terms of theoretical parameters.

The overall acceptance and efficiency of the signal depend strongly on the mass of the new resonance. Figure 2 presents both the acceptance times efficiency ($\mathcal{A} \times \varepsilon$) and the standalone efficiency as a function of the new resonance mass. To model their mass dependence, a second-order polynomial is fitted to $\mathcal{A} \times \varepsilon$, while a third-order polynomial is used to describe ε . As the acceptance and efficiency are found to be similar for the Z' and Z_D signals, a common parameterisation is adopted for both cases.

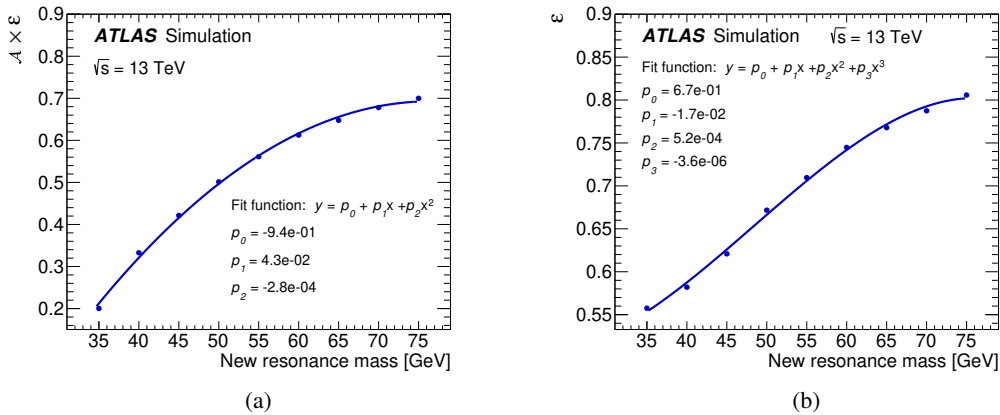


Figure 2: Parameterisation of the acceptance and efficiency for the new resonance. (a) The product of acceptance and efficiency ($\mathcal{A} \times \varepsilon$) as a function of the resonance mass, fitted with a second-order polynomial. (b) The detector correction factor (efficiency, ε) as a function of the resonance mass, fitted with a third-order polynomial.

5.2 Parameterisation of the dimuon invariant mass

The invariant mass ($m_{\mu\mu}$) distribution of the signal resonance is modelled using a Breit–Wigner (BW) function convolved with a double-sided Crystal Ball (DSCB) function [57–59]. The generator-level lineshape of the signal is described by the BW function, as:

$$f(x) \propto \frac{1}{(x - m_X)^2 + \left(\frac{1}{2}\Gamma\right)^2}$$

where m_X is the new resonance mass and Γ is the intrinsic width, which is described in Section 3. The DSCB function is used to model the detector resolution, featuring a Gaussian distribution core with power-law tails on both sides.

In the dark photon model, the intrinsic width is expected to be sufficiently small to be negligible [8]. Therefore, the narrow width approximation (NWA) is used to test this model.

The parameters of the DSCB function are extracted by fitting simulated signal samples. The width of the Gaussian core (σ), which reflects the detector resolution, varies from approximately 0.6 GeV to 1.3 GeV, depending on the new resonance mass. To enable a smooth scan over the full mass range from 35 GeV to 75 GeV, a continuous signal model is constructed by interpolating the fitted parameters obtained from a set of discrete mass point simulations, as shown in Figure 3(a). Figure 3(b) presents a representative comparison between the simulated dimuon mass distribution and the parameterised signal shape, demonstrating the accuracy of the signal modelling.

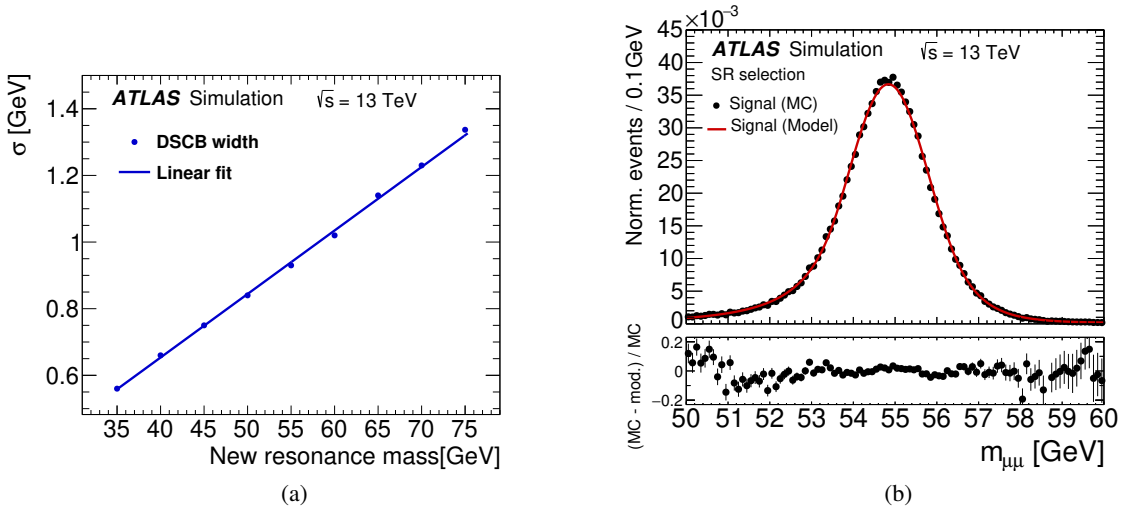


Figure 3: (a) Width of the DSCB Gaussian core as a function of the new resonance mass (solid markers), with a linear fit overlaid. (b) Simulated dimuon mass distribution for a hypothetical Z' resonance with a mass of 55 GeV and a width $\Gamma = 0.21$ GeV (solid markers), overlaid with the signal model, defined as a Breit–Wigner distribution convolved with a DSCB function and obtained from a parametric fit to the signal template. The lower panel displays the relative difference between the MC simulation and the signal model.

6 Systematic uncertainties

Systematic uncertainties affecting both the fitted signal yield and shape are considered. These include theoretical, experimental, and background-modelling uncertainties. The latter play a dominant role in the analysis and are discussed in detail in Section 7.2.

To estimate theoretical uncertainties in the signal yield, systematic variations are applied to account for uncertainties in the choice of QCD renormalisation (μ_R) and factorisation (μ_F) scales, as well as in the PDFs. The QCD scales are varied independently by factors of 0.5 and 2.0 relative to their nominal values, with the largest observed deviation taken as the systematic uncertainty. Following PDF4LHC recommendations [60], PDF uncertainties are estimated by using the envelope of variations across different PDF sets.

As discussed in Section 3, the signal cross-section is normalised to the NNLO prediction, and uncertainties from Ref. [38] are used to estimate cross-section uncertainties. The NNLO cross-section uncertainty, together with the effects of QCD scale and PDF variations on the acceptance, is considered only when interpreting the cross-section limits as constraints on the coupling parameters.

Experimental systematic uncertainties related to the reconstructed physics objects also affect expected yields. In addition, uncertainties in the muon momentum scale and resolution impact the signal mass distribution. The experimental uncertainties considered include muon reconstruction and identification efficiencies, efficiencies related to the trigger, isolation and impact-parameter requirements, and the muon momentum scale and resolution [26, 27, 61]. The uncertainty in the combined 2015–2018 integrated luminosity is 0.83% [24], derived using the LUCID-2 detector [25] for the primary luminosity measurements. The overall relative experimental uncertainty in the dimuon event selection efficiency is estimated to be below 1%, while the total uncertainty in the dimuon mass resolution is approximately 3.5%.

All systematic uncertainties impacting the final dimuon invariant mass distribution are implemented as nuisance parameters, constrained by Gaussian likelihood terms in the statistical analysis described in Section 7.1.

7 Background modelling and signal yield extraction

The analysis adopts a bump-hunting strategy, fitting the mass spectrum using a data-driven estimation of the background. However, as shown in Figure 4, the mass spectrum exhibits a non-trivial structure, including threshold effects from the muon triggers that are most visible in the 30–45 GeV region. This complexity makes it difficult to model the background using traditional analytic functions typically used for smoothly falling spectra.

To overcome these challenges, GPR is employed. GPR, a well-established machine-learning technique typically used for smoothing procedures [16], provides a flexible yet robust framework for background modelling. In this analysis, it is used innovatively to model the background within a simultaneous signal-plus-background (S+B) fit, enabling signal extraction.

The GPR assumes that bin-to-bin correlations in the background $m_{\mu\mu}$ spectrum follow a multivariate Gaussian distribution. Under this assumption, the background distribution is modelled as a Gaussian random process, with the covariance matrix determining the degree of correlation between bins.

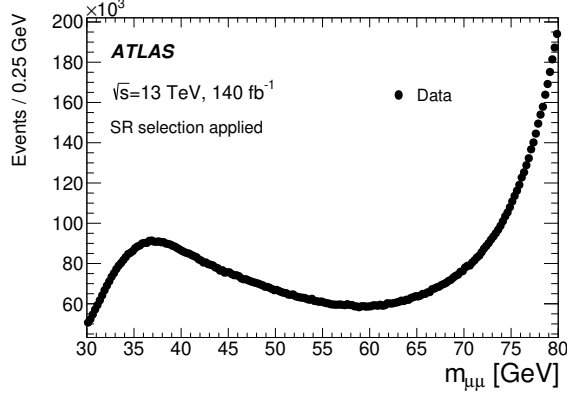


Figure 4: The dimuon mass, $m_{\mu\mu}$, distribution in the range 30–80 GeV, after applying the selections described in Section 4.

The flexibility of the GP is governed by the covariance matrix, derived from the chosen kernel function, and the prior mean function. The radial basis function (RBF) kernel is selected for its simplicity and its clear interpretation, with the correlation decreasing as a function of the distance between bins:

$$C_{ij} = c(x_i, x_j) = k \exp\left(-\frac{(x_i - x_j)^2}{\ell^2}\right), \quad (3)$$

where k and ℓ are the covariance strength and length scale, respectively. The tuning of these hyperparameters, aimed at optimising sensitivity and minimising bias, is detailed in Section 7.2. The prior mean is parameterised by a ninth-degree polynomial function fitted to the generator-smearred samples. As the prior mean is determined before any reweighting of these samples, as described at the end of Section 3.3, the resulting bias in the uncertainty estimation from background modelling (Section 7.2) is negligible and does not artificially improve the agreement between the background model and the data.

7.1 Signal extraction procedure with GPR-based background modelling

The GPR is applied to the $m_{\mu\mu}$ distribution, binned as (m_i, N_i) for $i = 1, \dots, n$, where m_i is the bin centre and N_i is the observed yield. Signal extraction is incorporated into the fit through the following likelihood:

$$L(\text{data}|\mu, \theta) = \left(\prod_{i \in \text{bins}} G\left(N_i^{\text{background}}(\mu, \theta) \mid N_i^{\text{GP}}, \sqrt{N_i^{\text{GP}}}\right) \right) \\ \times (G(N_{\text{GP}} \mid \mathbf{b}_0, \mathbf{C}_0)) \\ \times \left(\prod_{i \in \text{systematics}} G(\theta_i \mid \theta_i^{\text{aux}}, \sigma(\theta_i^{\text{aux}})) \right)$$

where the background yield in bin i is given by

$$N_i^{\text{background}} = N_i^{\text{data}} - N_i^{\text{signal}}(\mu, m_X, \Gamma, \theta)$$

Here, N_i^{data} is the observed data yield in bin i , $N_i^{\text{signal}}(\mu, m_X, \Gamma, \theta)$ denotes the expected signal yield for the given signal hypothesis and μ is the signal strength, relative to a reference signal yield. The first term in the likelihood compares the GP background model (N_i^{GP}) to the observed background ($N_i^{\text{background}}$) across different bins. The second term, introduced by the GPR, constrains the background prediction to the prior mean function (\mathbf{b}_0) through the covariance matrix (\mathbf{C}_0) determined by the kernel function in Eq. (3), where \mathbf{N}_{GP} denotes the binned vector of the predicted yields from GP. The third term applies Gaussian constraints to the nuisance parameters θ_i , each associated with an auxiliary measurement θ_i^{aux} and its corresponding uncertainty $\sigma(\theta_i^{\text{aux}})$. These constraints incorporate systematic uncertainties into the likelihood and enable a simultaneous fit to signal and background within a data-driven framework, ensuring a statistically well-defined treatment of all sources of uncertainty. Based on this likelihood, the best-fit mean and covariance functions, derived from the GP using the input histogram, define the background shape.

The parameter of interest extracted from the likelihood fit is the signal strength μ , which serves as a scaling factor for the total event yield predicted by the signal model. This is subsequently converted into the fiducial cross-section using a correction factor for the detection efficiency.

7.2 Hyper-parameters tuning of GPR

The GP kernel function captures the correlation structure across bins in the likelihood fit. The choice of kernel hyper-parameters is critical, as it controls the flexibility and smoothness of the background modelling. In the RBF kernel used in this analysis, the hyper-parameter k defines the correlation strength across bins, while ℓ characterises the correlation length scale, i.e., how far neighbouring bins influence each other.

The choice of hyper-parameters is guided by their ability to model the background shape reliably while maintaining a balance between flexibility and robustness. The values of k and ℓ are selected to achieve a smooth yet accurate background model, following the procedure outlined below. The optimisation is performed on mass-spectrum templates reweighted from the generator-smearing sample to the fully simulated sample, as described in Section 3.3. The criteria for choosing suitable hyper-parameters include the requirement that only hyper-parameter sets yielding a χ^2 probability greater than 1% when fitting the simulation template are retained. For the final choice of parameters, the background-only fit χ^2 probability is in the range of 5–20% when evaluated in a $\pm 3\sigma$ mass window around each tested mass point, where σ is the detector resolution at that mass.

To validate the signal extraction procedure, a series of signal injection tests is performed. These include scenarios with varying injected signal strengths as well as a null injection case. The response to a null signal injection, referred to as a spurious signal (SS) [62], is evaluated by fitting signal-plus-background models to background-only templates. Any non-zero fitted signal yield in this context indicates an intrinsic bias in the background modelling in the absence of a true signal. The magnitude of the SS is treated as a systematic uncertainty associated with the background model. Following recommendations for smooth background modelling [63], the background model is optimised to ensure that the SS yield satisfies $N_{\text{SS}} < 0.5\sigma_{\text{fit}}$, where σ_{fit} is the statistical uncertainty in the fitted signal yield. This criterion ensures that any potential bias remains within the range covered by the modelling uncertainty controlled via nuisance parameters.

Additional validation tests are conducted by injecting signals of varying strengths on top of the background-only template. The linearity between the injected and extracted signal yields is verified by fitting the response curve, and the fitted slope is required to remain within 3% of unity during hyper-parameter

optimisation. Any residual deviation is treated as an additional systematic uncertainty associated with the signal extraction procedure.

Among the hyper-parameter configurations meeting the established criteria, the final choice is made by selecting the set that minimises the total uncertainty in the extracted signal yield. This total uncertainty is defined as the quadrature sum of the statistical uncertainty from the fit and the systematic contribution from the SS, thereby ensuring optimal overall sensitivity.

Different hyper-parameter configurations are used for distinct resonance mass ranges, as summarised in Table 3. The optimal values depend on the resonance mass, reflecting variations in the background shape and signal resolution; consequently, no single set of hyper-parameters provides an adequate description across the entire mass range. The parameter k correlates with the behaviour of the spectrum shown in Figure 4. Larger k values are used near the rapidly varying edges of the mass range to constrain the GP prediction around the prior mean, while smaller values in the central region allow greater flexibility. The correlation length ℓ is primarily driven by the signal resolution and generally increases with the resonance mass, except in the few GeV at the upper edge of the mass range, where smaller ℓ values are required to capture the steeply varying spectrum. The resulting SS values after optimisation are shown in Figure 5 as a function of the resonance mass. The envelope of the SS distribution is obtained as the magnitude of the analytic signal constructed from the quadrature sum of the original signal and its Hilbert-transformed [64] counterpart, and is subsequently smoothed with a Savitzky–Golay filter. This envelope defines the final systematic uncertainty associated with the background model, and its symmetrised band is taken as the systematic uncertainty in the background modelling.

Table 3: RBF kernel hyper-parameter sets optimised for different m_X mass hypotheses, tuned using spurious signal and linearity tests.

m_X [GeV] range	k	ℓ [GeV]
$35 \leq m_X < 38$	4×10^9	4.4
$38 \leq m_X < 40$	2×10^8	8.0
$40 \leq m_X < 55$	2×10^8	7.1
$55 \leq m_X < 68$	2×10^8	8.7
$68 \leq m_X < 71.5$	5×10^8	12.1
$71.5 \leq m_X < 75$	5×10^8	11.4

8 Statistical interpretation and limit setting

Hypothesis testing of the signal strength μ is based on the profile likelihood ratio [65], with the test statistic for the limit-setting:

$$q_\mu = \begin{cases} -2 \ln \frac{L(\text{data}|\mu, \hat{\theta}(\mu))}{L(\text{data}|0, \hat{\theta}(0))}, & \hat{\mu} < 0 \\ -2 \ln \frac{L(\text{data}|\mu, \hat{\theta}(\mu))}{L(\text{data}|\hat{\mu}, \hat{\theta})}, & 0 \leq \hat{\mu} \leq \mu \\ 0, & \hat{\mu} > \mu \end{cases} \quad (4)$$

Here, $\hat{\mu}$ and $\hat{\theta}$ denote the unconditional maximum-likelihood (ML) estimators of the signal strength and nuisance parameters, while $\hat{\theta}(\mu)$ and $\hat{\theta}(0)$ are the corresponding conditional estimators obtained under the signal-plus-background and background-only hypotheses, respectively. The likelihood function L

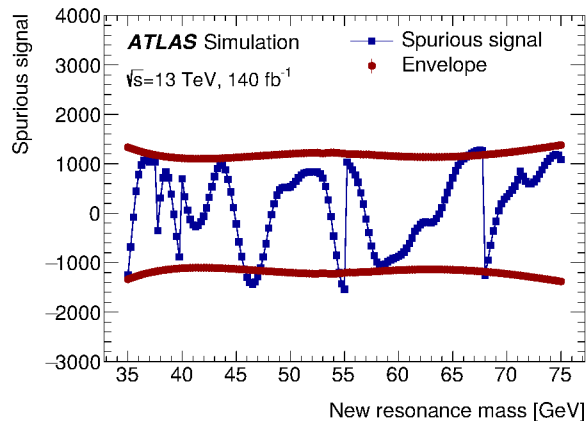


Figure 5: Spurious signal yield as a function of the new resonance mass, obtained by fitting signal-plus-background models to background-only templates. The points represent the fitted signal yields, with vertical error bars indicating the corresponding statistical uncertainties. The thick curves denote the symmetrised envelope, which defines the systematic uncertainty associated with the background modelling. Discontinuities in the spurious signal reflect transitions between different Gaussian process hyper-parameter configurations.

incorporates all sources of systematic uncertainty through nuisance parameters and their correlations. For significance and p -value evaluations, the corresponding one-sided test statistic q_0 is used, following the asymptotic formalism in Ref. [65].

The significance of a potential excess is first quantified with the p_0 value, defined as the probability that the background could fluctuate to the observed excess:

$$p_0 = P(q_0 > q_0^{\text{obs}} \mid \mu = 0)$$

For discovery tests, the one-sided statistic q_0 is defined analogously to Eq.(4), restricted to positive signal-strength estimates ($\hat{\mu} > 0$) [65]. The p_0 value is converted into a local significance, expressed as the equivalent number of Gaussian standard deviations (σ) assuming a one-sided normal distribution.

Upper limits on the signal strength are evaluated using the CL_s method [66]. A signal strength μ is considered excluded at the 95% confidence level when the resulting CL_s value falls below 0.05.

Since the measurement is performed within a fiducial phase-space region (defined in Section 4), to facilitate reinterpretation, the number of signal events N_S is parameterised in terms of the fiducial cross-section times branching ratio to derive upper limits:

$$\sigma_{\text{fid}} \times \mathcal{B}(X \rightarrow \mu\mu) = \frac{N_S}{\varepsilon \times \mathcal{L}},$$

where the \mathcal{L} is the integrated luminosity and ε is the correction factor accounting for the detector efficiency, described in Section 5.

9 Results

The signal extraction is performed by fitting the dimuon invariant mass spectrum in the range of 30–80 GeV, which corresponds to events satisfying the signal-region (SR) selection defined in Section 4. The search for

a potential resonance is carried out within the narrower range of 35–75 GeV to avoid potential edge effects from the fit boundaries. The dimuon mass distributions, overlaid with signal-plus-background fits using various GP hyperparameter configurations, are shown in Figure 6 for several representative resonance mass hypotheses.

The p_0 values and local significance, corresponding to the background-only hypothesis, are scanned across a range of hypothesised new resonance masses, as shown in Figure 7. The methodology for this calculation is detailed in Section 8. The minimum p_0 value is observed at a mass of 57.5 GeV, corresponding to a local significance of 2.3σ , while the global significance is negligible. The ranking of systematic uncertainties is dominated by the SS contribution, followed by theoretical and experimental sources.

The observed and expected 95% confidence level (CL) upper limits on the production fiducial cross-section times branching ratio, $\sigma_{\text{fid}} \times \mathcal{B}(X \rightarrow \mu\mu)$, as a function of the resonance mass are shown in Figure 8. The limits are derived under the narrow-width approximation ($\Gamma = 0$). The results remain valid for resonances with relative intrinsic widths $\Gamma/m_X < 1\%$, covering a broad class of new-physics scenarios with perturbative couplings. The primary factors limiting the sensitivity are the size of the recorded data sample and uncertainties associated with the background modelling. Discontinuities in the limit curve reflect transitions between different sets of hyper-parameters used in the GP background modelling.

Assuming a coupling of 0.1 between the Z' and quarks, an upper limit on the coupling (g_l) between Z' and leptons is derived by varying the intrinsic signal width as described in Section 3.2. As shown in Figure 9(a), the limits on g_l range from 4×10^{-4} to 1.4×10^{-3} , depending on the assumed Z' mass.

A similar search strategy can be applied to models involving dark photons, where the coupling to SM particles is characterised by the kinetic mixing parameter ϵ . In such models, the production cross-section scales as ϵ^2 . The experimental sensitivity is thus expressed as an upper limit on ϵ^2 . The resulting limits, shown in Figure 9(b), range from 1×10^{-6} to 9×10^{-6} . As noted in Section 5.2, the narrow-width approximation is applicable to these models.

The search sets stringent constraints on the dark-photon kinetic mixing in the mass range 35–75 GeV, complementing results from CMS [9] and LHCb [11]. An improvement in sensitivity is achieved in the 35–45 GeV region, where the CMS results [9] were obtained using a scouting data acquisition scheme. This improvement is driven by the mass-shape modelling capability provided by GPR, which enables the use of standard, unrescaled muon triggers together with the standard offline p_T selection, thereby suppressing backgrounds.

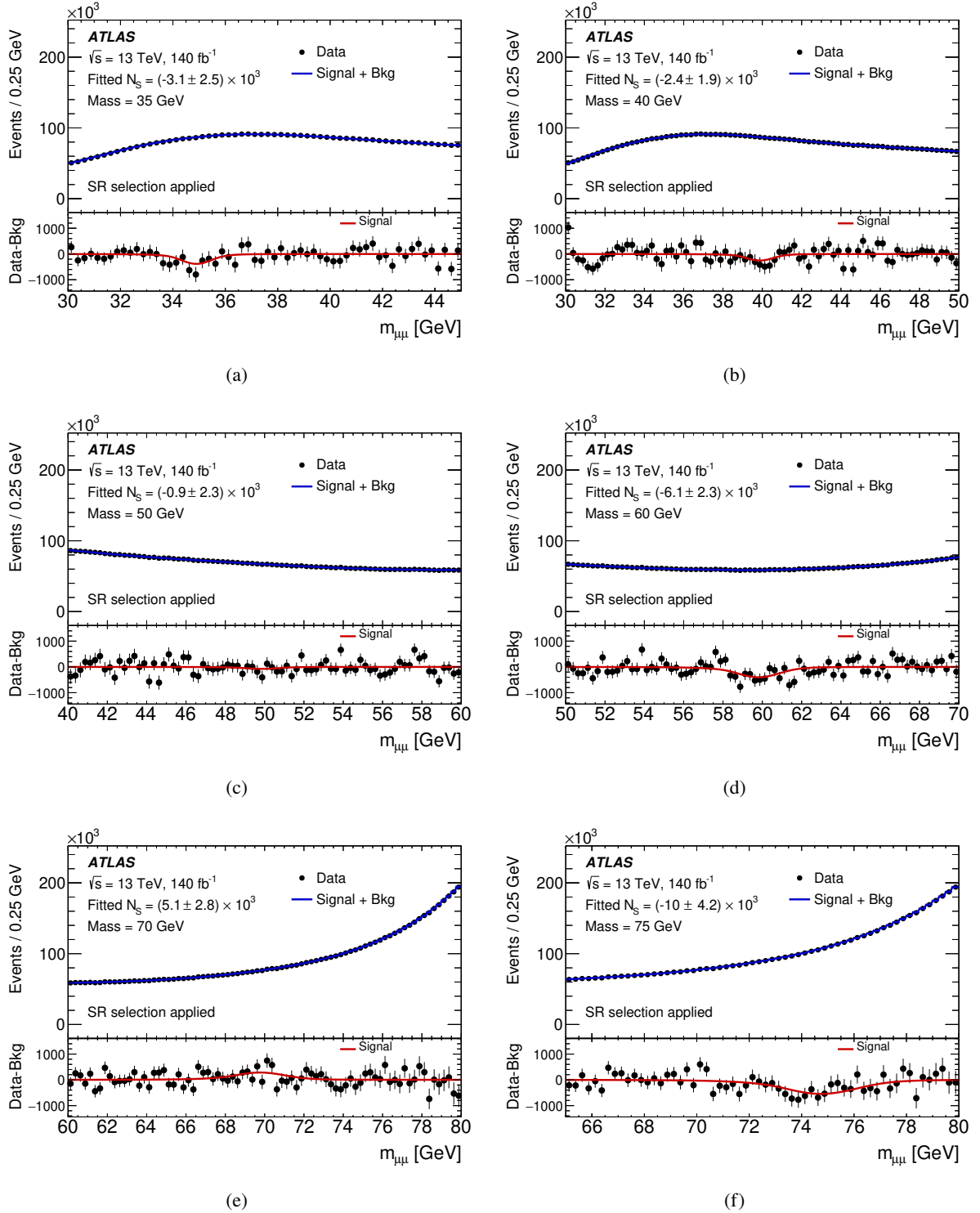


Figure 6: Fit results for various new resonance mass hypotheses. Each plot shows the $m_{\mu\mu}$ distribution in data overlaid with the fitted signal-plus-background model. The lower panels display the data-minus-background residuals (points), obtained by subtracting the estimated background component of the fit model from the data, and the extracted signal component (line). The N_S in the plots refers to the extracted signal yield. The fits are performed in the range of 30 GeV to 80 GeV, but only the region around the signal hypothesis is shown. The plots correspond to different resonance mass hypotheses: (a) 35 GeV, (b) 40 GeV, (c) 50 GeV, (d) 60 GeV, (e) 70 GeV, and (f) 75 GeV.

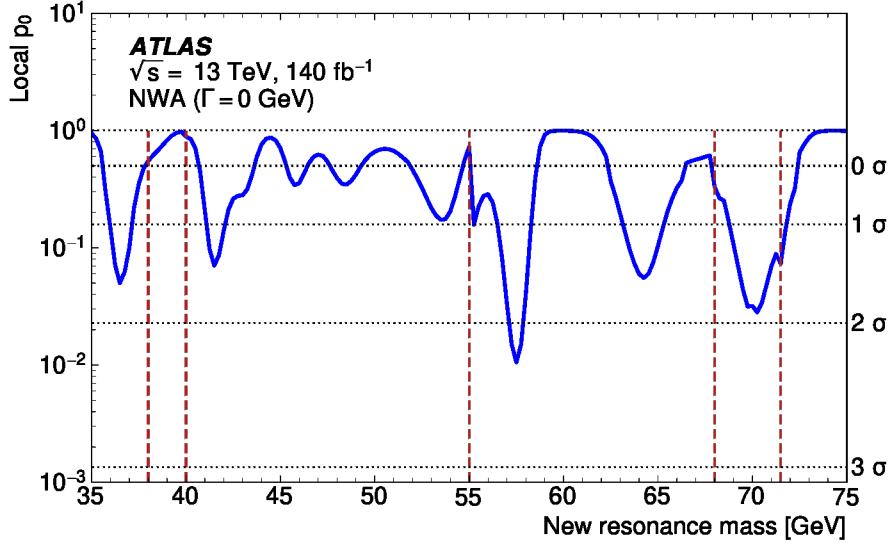


Figure 7: Scan of the p_0 values as a function of the new resonance mass. Discontinuities correspond to the boundaries between different Gaussian process hyper-parameter regions. The vertical dashed lines indicate the mass points where the hyper-parameters are changed.

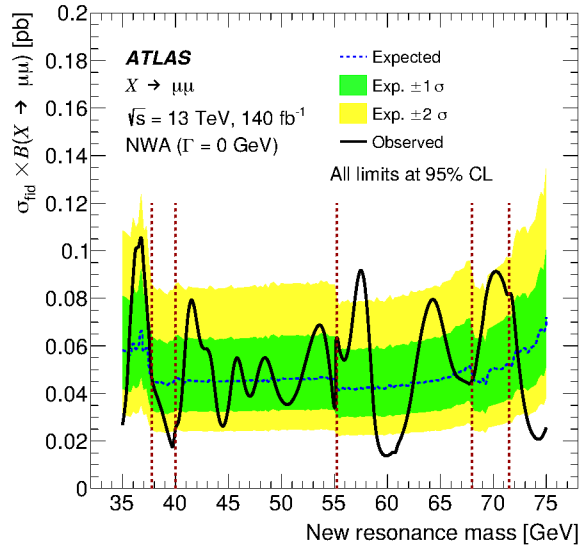
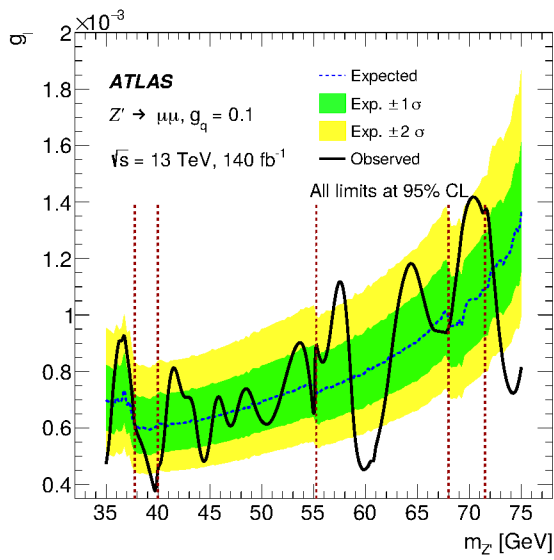
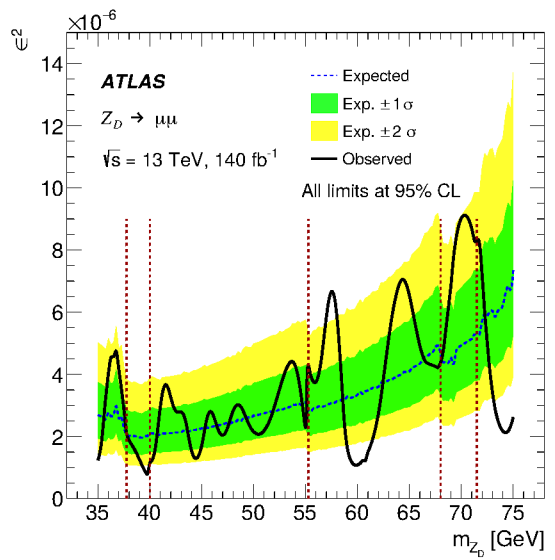


Figure 8: Observed and expected 95% CL upper limits on the production fiducial cross-section times branching ratio of a narrow-width ($\Gamma = 0$ GeV) resonance, as a function of the new resonance mass. Discontinuities correspond to the boundaries between different GP hyper-parameter regions. The vertical dashed lines indicate the mass points where the hyper-parameters are changed.



(a)



(b)

Figure 9: (a) Observed and expected 95% CL upper limits on the coupling between the Z' boson and leptons as a function of $m_{Z'}$, assuming $g_q = 0.1$. (b) Observed and expected 95% CL upper limits on the kinematic mixing parameter (ϵ^2 in the dark photon model) as a function of m_{Z_D} . Discontinuities correspond to the boundaries between different GP hyper-parameter regions. Vertical dashed lines indicate the mass points where the hyper-parameters are changed.

10 Conclusions

A search for new resonances in the dimuon invariant mass spectrum between 35 GeV and 75 GeV is performed using 140 fb^{-1} of Run-2 proton–proton collision data at $\sqrt{s} = 13 \text{ TeV}$, collected with the ATLAS detector at the LHC. This study constitutes the first ATLAS search targeting this mass region, extending the sensitivity of previous dimuon resonance analyses to lower masses.

A novel background-modelling technique based on Gaussian process regression is employed, providing a flexible and accurate description of the rapidly varying Drell–Yan continuum and enhancing sensitivity to narrow resonances. The largest excess occurs near 57.5 GeV, with a local significance of 2.3 standard deviations, while the corresponding global significance is negligible.

Upper limits are set on the fiducial production cross-section times branching ratio, defined within a fiducial region closely matching the detector-level selection. The observed limits range from 20 fb to 110 fb, depending on statistical fluctuations and variations in the background modelling configurations. The results are additionally interpreted in terms of constraints on theoretical parameters in both a simplified dark-matter mediator model and a dark-photon model.

Acknowledgements

We thank CERN for the very successful operation of the LHC and its injectors, as well as the support staff at CERN and at our institutions worldwide without whom ATLAS could not be operated efficiently.

The crucial computing support from all WLCG partners is acknowledged gratefully, in particular from CERN, the ATLAS Tier-1 facilities at TRIUMF/SFU (Canada), NDGF (Denmark, Norway, Sweden), CC-IN2P3 (France), KIT/GridKA (Germany), INFN-CNAF (Italy), NL-T1 (Netherlands), PIC (Spain), RAL (UK) and BNL (USA), the Tier-2 facilities worldwide and large non-WLCG resource providers. Major contributors of computing resources are listed in Ref. [67].

We gratefully acknowledge the support of ANPCyT, Argentina; YerPhI, Armenia; ARC, Australia; BMWFW and FWF, Austria; ANAS, Azerbaijan; CNPq and FAPESP, Brazil; NSERC, NRC and CFI, Canada; CERN; ANID, Chile; CAS, MOST and NSFC, China; Minciencias, Colombia; MEYS CR, Czech Republic; DNRF and DNSRC, Denmark; IN2P3-CNRS and CEA-DRF/IRFU, France; SRNSFG, Georgia; BMFTR, HGF and MPG, Germany; GSRI, Greece; RGC and Hong Kong SAR, China; ICHEP and Academy of Sciences and Humanities, Israel; INFN, Italy; MEXT and JSPS, Japan; CNRST, Morocco; NWO, Netherlands; RCN, Norway; MNiSW, Poland; FCT, Portugal; MNE/IFA, Romania; MSTDI, Serbia; MSSR, Slovakia; ARIS and MVZI, Slovenia; DSI/NRF, South Africa; MICIU/AEI, Spain; SRC and Wallenberg Foundation, Sweden; SERI, SNSF and Cantons of Bern and Geneva, Switzerland; NSTC, Taipei; TENMAK, Türkiye; STFC/UKRI, United Kingdom; DOE and NSF, United States of America.

Individual groups and members have received support from BCKDF, CANARIE, CRC and DRAC, Canada; CERN-CZ, FORTE and PRIMUS, Czech Republic; COST, ERC, ERDF, Horizon 2020 and Marie Skłodowska-Curie Actions, European Union; Investissements d’Avenir Labex, Investissements d’Avenir Idex and ANR, France; DFG and AvH Foundation, Germany; Herakleitos, Thales and Aristeia programmes co-financed by EU-ESF and the Greek NSRF, Greece; BSF-NSF and MINERVA, Israel; NCN and NAWA, Poland; La Caixa Banking Foundation, CERCA Programme Generalitat de Catalunya and PROMETEO and GenT Programmes Generalitat Valenciana, Spain; Göran Gustafssons Stiftelse, Sweden; The Royal Society and Leverhulme Trust, United Kingdom; Schmidt Foundation, United States of America.

In addition, individual members wish to acknowledge support from Chile: Agencia Nacional de Investigación y Desarrollo (FONDECYT 1230812, FONDECYT 1240864, Fondecyt 3240661, Fondecyt Regular 1240721); China: Chinese Ministry of Science and Technology (MOST-2023YFA1605700, MOST-2023YFA1609300), National Natural Science Foundation of China (NSFC - 12175119, NSFC 12275265); Czech Republic: Czech Science Foundation (GACR - 24-11373S), Ministry of Education Youth and Sports (ERC-CZ-LL2327, FORTE CZ.02.01.01/00/22_008/0004632), PRIMUS Research Programme (PRIMUS/21/SCI/017); EU: H2020 European Research Council (ERC - 101002463); European Union: European Research Council (BARD No. 101116429, ERC - 948254, ERC 101089007), European Regional Development Fund (HE COFUND GA No.101081355, ERDF), European Union, Future Artificial Intelligence Research (FAIR-NextGenerationEU PE00000013); France: Agence Nationale de la Recherche (ANR-21-CE31-0013, ANR-21-CE31-0022, ANR-22-EDIR-0002, ANR-24-CE31-0504-01); Germany: Deutsche Forschungsgemeinschaft (DFG - 469666862); China: Research Grants Council (GRF); Italy: Ministero dell’Università e della Ricerca (NextGenEU 153D23001490006 M4C2.1.1, NextGenEU I53D23000820006 M4C2.1.1, NextGenEU I53D23001490006 M4C2.1.1, SOE2024_0000023); Japan: Japan Society for the Promotion of Science (JSPS KAKENHI JP22H01227, JSPS KAKENHI JP22H04944, JSPS KAKENHI JP22KK0227, JSPS KAKENHI JP24K23939, JSPS KAKENHI JP24KK0251, JSPS KAKENHI JP25H00650, JSPS KAKENHI JP25H01291, JSPS KAKENHI JP25K01023); Norway: Research Council

of Norway (RCN-314472); Poland: Ministry of Science and Higher Education (IDUB AGH, POB8, D4 no 9722), Polish National Science Centre (NCN 2021/42/E/ST2/00350, NCN OPUS 2023/51/B/ST2/02507, NCN OPUS nr 2022/47/B/ST2/03059, NCN UMO-2019/34/E/ST2/00393, UMO-2022/47/O/ST2/00148, UMO-2023/49/B/ST2/04085, UMO-2023/51/B/ST2/00920, UMO-2024/53/N/ST2/00869); Portugal: Foundation for Science and Technology (FCT); Spain: CERCA Programme Generalitat de Catalunya (AGAUR - 2023 BP 00141), Generalitat Valenciana (ASFAE/2022/008), Ministry of Science and Innovation (RYC2019-028510-I, RYC2020-030254-I, RYC2021-031273-I, RYC2022-038164-I), Ministerio de Ciencia, Innovación y Universidades/Agencia Estatal de Investigación (PID2022-142604OB-C22); Sweden: Carl Trygger Foundation (Carl Trygger Foundation CTS 22:2312), Swedish Research Council (Swedish Research Council 2023-04654, VR 2021-03651, VR 2022-03845, VR 2022-04683, VR 2023-03403, VR 2024-05451), Knut and Alice Wallenberg Foundation (KAW 2018.0458, KAW 2022.0358, KAW 2023.0366); Switzerland: Swiss National Science Foundation (SNSF - PCEFP2_194658); United Kingdom: The Binks Trust, Royal Society (NIF-R1-231091); United States of America: U.S. Department of Energy (ECA DE-AC02-76SF00515), John Templeton Foundation (John Templeton Foundation 63206), Neubauer Family Foundation.

References

- [1] G. Bertone, D. Hooper and J. Silk, *Particle dark matter: evidence, candidates and constraints*, *Phys. Rept.* **405** (2005) 279, arXiv: [hep-ph/0404175](#).
- [2] J. L. Feng, *Dark Matter Candidates from Particle Physics and Methods of Detection*, *Ann. Rev. Astron. Astrophys.* **48** (2010) 495, arXiv: [1003.0904 \[astro-ph.CO\]](#).
- [3] T. A. Porter, R. P. Johnson and P. W. Graham, *Dark Matter Searches with Astroparticle Data*, *Ann. Rev. Astron. Astrophys.* **49** (2011) 155, arXiv: [1104.2836 \[astro-ph.HE\]](#).
- [4] Planck Collaboration, *Planck 2018 results - I. Overview and the cosmological legacy of Planck*, *Astron. Astrophys.* **641** (2020) A1, arXiv: [1807.06205 \[astro-ph.CO\]](#).
- [5] ATLAS Collaboration, *Constraints on mediator-based dark matter and scalar dark energy models using $\sqrt{s} = 13$ TeV pp collision data collected by the ATLAS detector*, *JHEP* **05** (2019) 142, arXiv: [1903.01400 \[hep-ex\]](#).
- [6] L. Evans and P. Bryant, *LHC Machine*, *JINST* **3** (2008) S08001.
- [7] D. Abercrombie et al., *Dark Matter benchmark models for early LHC Run-2 Searches: Report of the ATLAS/CMS Dark Matter Forum*, *Phys. Dark Univ.* **27** (2020) 100371, arXiv: [1507.00966 \[hep-ex\]](#).
- [8] D. Curtin, R. Essig, S. Gori and J. Shelton, *Illuminating Dark Photons with High-Energy Colliders*, *JHEP* **02** (2015) 157, arXiv: [1412.0018 \[hep-ph\]](#).
- [9] CMS Collaboration, *Search for a Narrow Resonance Lighter than 200 GeV Decaying to a Pair of Muons in Proton-Proton Collisions at $\sqrt{s} = 13$ TeV*, *Phys. Rev. Lett.* **124** (2020) 131802, arXiv: [1912.04776 \[hep-ex\]](#).
- [10] CMS Collaboration, *Search for direct production of GeV-scale resonances decaying to a pair of muons in proton-proton collisions at $\sqrt{s} = 13$ TeV*, *JHEP* **12** (2023) 070, arXiv: [2309.16003 \[hep-ex\]](#).
- [11] LHCb Collaboration, *Search for $A' \rightarrow \mu^+ \mu^-$ Decays*, *Phys. Rev. Lett.* **124** (2020) 041801, arXiv: [1910.06926 \[hep-ex\]](#).

- [12] ATLAS Collaboration, *The ATLAS Experiment at the CERN Large Hadron Collider*, [JINST 3 \(2008\) S08003](#).
- [13] C. E. Rasmussen and C. K. I. Williams, *Gaussian processes for machine learning*, Adaptive computation and machine learning, MIT Press, 2006 I, 1, ISBN: 026218253X.
- [14] M. Frate, K. Cranmer, S. Kalia, A. Vandenberg-Rodes and D. Whiteson, *Modeling Smooth Backgrounds and Generic Localized Signals with Gaussian Processes*, 2017, arXiv: [1709.05681 \[physics.data-an\]](#).
- [15] A. Gandrakota, A. Lath, A. V. Morozov and S. Murthy, *Model selection and signal extraction using Gaussian Process regression*, [JHEP 02 \(2023\) 230](#), arXiv: [2202.05856 \[hep-ex\]](#).
- [16] ATLAS Collaboration, *Search for boosted diphoton resonances in the 10 to 70 GeV mass range using 138fb^{-1} of 13 TeV pp collisions with the ATLAS detector*, [JHEP 07 \(2023\) 155](#), arXiv: [2211.04172 \[hep-ex\]](#).
- [17] ATLAS Collaboration, *Search for low-mass resonances decaying into two jets and produced in association with a photon or a jet at $\sqrt{s} = 13\text{ TeV}$ with the ATLAS detector*, [Phys. Rev. D 110 \(2024\) 032002](#), arXiv: [2403.08547 \[hep-ex\]](#).
- [18] ATLAS Collaboration, *Search for high-mass dilepton resonances using 139fb^{-1} of pp collision data collected at $\sqrt{s} = 13\text{ TeV}$ with the ATLAS detector*, [Phys. Lett. B 796 \(2019\) 68](#), arXiv: [1903.06248 \[hep-ex\]](#).
- [19] ATLAS Collaboration, *ATLAS Insertable B-Layer: Technical Design Report*, ATLAS-TDR-19; CERN-LHCC-2010-013, 2010, URL: <https://cds.cern.ch/record/1291633>, Addendum: ATLAS-TDR-19-ADD-1; CERN-LHCC-2012-009, 2012, URL: <https://cds.cern.ch/record/1451888>.
- [20] B. Abbott et al., *Production and integration of the ATLAS Insertable B-Layer*, [JINST 13 \(2018\) T05008](#), arXiv: [1803.00844 \[physics.ins-det\]](#).
- [21] ATLAS Collaboration, *Performance of the ATLAS trigger system in 2015*, [Eur. Phys. J. C 77 \(2017\) 317](#), arXiv: [1611.09661 \[hep-ex\]](#).
- [22] ATLAS Collaboration, *Software and computing for Run 3 of the ATLAS experiment at the LHC*, [Eur. Phys. J. C 85 \(2025\) 234](#), arXiv: [2404.06335 \[hep-ex\]](#), Erratum: [Eur. Phys. J. C 85 \(2025\) 907](#).
- [23] ATLAS Collaboration, *ATLAS data quality operations and performance for 2015–2018 data-taking*, [JINST 15 \(2020\) P04003](#), arXiv: [1911.04632 \[physics.ins-det\]](#).
- [24] ATLAS Collaboration, *Luminosity determination in pp collisions at $\sqrt{s} = 13\text{ TeV}$ using the ATLAS detector at the LHC*, [Eur. Phys. J. C 83 \(2023\) 982](#), arXiv: [2212.09379 \[hep-ex\]](#).
- [25] G. Avoni et al., *The new LUCID-2 detector for luminosity measurement and monitoring in ATLAS*, [JINST 13 \(2018\) P07017](#).
- [26] ATLAS Collaboration, *Performance of the ATLAS muon triggers in Run 2*, [JINST 15 \(2020\) P09015](#), arXiv: [2004.13447 \[physics.ins-det\]](#).
- [27] ATLAS Collaboration, *Muon reconstruction and identification efficiency in ATLAS using the full Run 2 pp collision data set at $\sqrt{s} = 13\text{ TeV}$* , [Eur. Phys. J. C 81 \(2021\) 578](#), arXiv: [2012.00578 \[hep-ex\]](#).

- [28] C. Degrande et al., *UFO – The Universal FeynRules Output*, *Comput. Phys. Commun.* **183** (2012) 1201, arXiv: [1108.2040 \[hep-ph\]](#).
- [29] A. Alloul, N. D. Christensen, C. Degrande, C. Duhr and B. Fuks, *FeynRules 2.0 - A complete toolbox for tree-level phenomenology*, *Comput. Phys. Commun.* **185** (2014) 2250, arXiv: [1310.1921 \[hep-ph\]](#).
- [30] M. Backović et al., *Higher-order QCD predictions for dark matter production at the LHC in simplified models with s-channel mediators*, *Eur. Phys. J. C* **75** (2015) 482, arXiv: [1508.05327 \[hep-ph\]](#).
- [31] A. Albert et al., *Recommendations of the LHC Dark Matter Working Group: Comparing LHC searches for dark matter mediators in visible and invisible decay channels and calculations of the thermal relic density*, *Phys. Dark Univ.* **26** (2019) 100377, arXiv: [1703.05703 \[hep-ex\]](#).
- [32] ATLAS Collaboration, *ATLAS Pythia 8 tunes to 7 TeV data*, ATL-PHYS-PUB-2014-021, 2014, URL: <https://cds.cern.ch/record/1966419>.
- [33] G. Watt and R. Thorne, *Study of Monte Carlo approach to experimental uncertainty propagation with MSTW 2008 PDFs*, *JHEP* **08** (2012) 052, arXiv: [1205.4024 \[hep-ph\]](#).
- [34] T. Sjöstrand et al., *An introduction to PYTHIA 8.2*, *Comput. Phys. Commun.* **191** (2015) 159, arXiv: [1410.3012 \[hep-ph\]](#).
- [35] T. Sjöstrand, S. Mrenna and P. Skands, *A brief introduction to PYTHIA 8.1*, *Comput. Phys. Commun.* **178** (2008) 852, arXiv: [0710.3820 \[hep-ph\]](#).
- [36] NNPDF Collaboration, R. D. Ball et al., *Parton distributions with LHC data*, *Nucl. Phys. B* **867** (2013) 244, arXiv: [1207.1303 \[hep-ph\]](#).
- [37] ATLAS Collaboration, *The ATLAS Simulation Infrastructure*, *Eur. Phys. J. C* **70** (2010) 823, arXiv: [1005.4568 \[physics.ins-det\]](#).
- [38] A.H. Ajjath et al., *Resummed Drell-Yan cross-section at N^3LL* , *JHEP* **10** (2020) 153, arXiv: [2001.11377 \[hep-ph\]](#).
- [39] ATLAS Collaboration, *The Pythia 8 A3 tune description of ATLAS minimum bias and inelastic measurements incorporating the Donnachie–Landshoff diffractive model*, ATL-PHYS-PUB-2016-017, 2016, URL: <https://cds.cern.ch/record/2206965>.
- [40] E. Bothmann et al., *Event generation with Sherpa 2.2*, *SciPost Phys.* **7** (2019) 034, arXiv: [1905.09127 \[hep-ph\]](#).
- [41] T. Gleisberg and S. Höche, *Comix, a new matrix element generator*, *JHEP* **12** (2008) 039, arXiv: [0808.3674 \[hep-ph\]](#).
- [42] F. Cascioli, P. Maierhöfer and S. Pozzorini, *Scattering Amplitudes with Open Loops*, *Phys. Rev. Lett.* **108** (2012) 111601, arXiv: [1111.5206 \[hep-ph\]](#).
- [43] A. Denner, S. Dittmaier and L. Hofer, *COLLIER: A fortran-based complex one-loop library in extended regularizations*, *Comput. Phys. Commun.* **212** (2017) 220, arXiv: [1604.06792 \[hep-ph\]](#).
- [44] NNPDF Collaboration, R. D. Ball et al., *Parton distributions for the LHC run II*, *JHEP* **04** (2015) 040, arXiv: [1410.8849 \[hep-ph\]](#).

- [45] S. Schumann and F. Krauss, *A parton shower algorithm based on Catani–Seymour dipole factorisation*, *JHEP* **03** (2008) 038, arXiv: [0709.1027 \[hep-ph\]](#).
- [46] S. Höche, F. Krauss, M. Schönherr and F. Siegert, *A critical appraisal of NLO+PS matching methods*, *JHEP* **09** (2012) 049, arXiv: [1111.1220 \[hep-ph\]](#).
- [47] S. Höche, F. Krauss, M. Schönherr and F. Siegert, *QCD matrix elements + parton showers. The NLO case*, *JHEP* **04** (2013) 027, arXiv: [1207.5030 \[hep-ph\]](#).
- [48] S. Catani, F. Krauss, B. R. Webber and R. Kuhn, *QCD Matrix Elements + Parton Showers*, *JHEP* **11** (2001) 063, arXiv: [hep-ph/0109231](#).
- [49] S. Höche, F. Krauss, S. Schumann and F. Siegert, *QCD matrix elements and truncated showers*, *JHEP* **05** (2009) 053, arXiv: [0903.1219 \[hep-ph\]](#).
- [50] S. Frixione, G. Ridolfi and P. Nason, *A positive-weight next-to-leading-order Monte Carlo for heavy flavour hadroproduction*, *JHEP* **09** (2007) 126, arXiv: [0707.3088 \[hep-ph\]](#).
- [51] E. Re, *Single-top Wt -channel production matched with parton showers using the POWHEG method*, *Eur. Phys. J. C* **71** (2011) 1547, arXiv: [1009.2450 \[hep-ph\]](#).
- [52] S. Agostinelli et al., *GEANT4 – a simulation toolkit*, *Nucl. Instrum. Meth. A* **506** (2003) 250.
- [53] ATLAS Collaboration, *A search for the dimuon decay of the Standard Model Higgs boson with the ATLAS detector*, *Phys. Lett. B* **812** (2021) 135980, arXiv: [2007.07830 \[hep-ex\]](#).
- [54] ATLAS Collaboration, *Performance of the ATLAS track reconstruction algorithms in dense environments in LHC Run 2*, *Eur. Phys. J. C* **77** (2017) 673, arXiv: [1704.07983 \[hep-ex\]](#).
- [55] ATLAS Collaboration, *Studies of the muon momentum calibration and performance of the ATLAS detector with pp collisions at $\sqrt{s} = 13$ TeV*, *Eur. Phys. J. C* **83** (2023) 686, arXiv: [2212.07338 \[hep-ex\]](#).
- [56] ATLAS Collaboration, *Jet reconstruction and performance using particle flow with the ATLAS Detector*, *Eur. Phys. J. C* **77** (2017) 466, arXiv: [1703.10485 \[hep-ex\]](#).
- [57] M. Oreglia, *A Study of the Reactions $\psi' \rightarrow \gamma\gamma\psi$* , SLAC-R-0236 (1980), URL: www.slac.stanford.edu/cgi-wrap/getdoc/slac-r-236.pdf.
- [58] ATLAS Collaboration, *Search for Scalar Diphoton Resonances in the Mass Range 65–600 GeV with the ATLAS Detector in pp Collision Data at $\sqrt{s} = 8$ TeV*, *Phys. Rev. Lett.* **113** (2014) 171801, arXiv: [1407.6583 \[hep-ex\]](#).
- [59] ATLAS Collaboration, *Search for resonances in diphoton events at $\sqrt{s} = 13$ TeV with the ATLAS detector*, *JHEP* **09** (2016) 001, arXiv: [1606.03833 \[hep-ex\]](#).
- [60] J. Butterworth et al., *PDF4LHC recommendations for LHC Run II*, *J. Phys. G* **43** (2016) 023001, arXiv: [1510.03865 \[hep-ph\]](#).

- [61] ATLAS Collaboration, *Muon reconstruction performance of the ATLAS detector in proton–proton collision data at $\sqrt{s} = 13$ TeV*, *Eur. Phys. J. C* **76** (2016) 292, arXiv: [1603.05598 \[hep-ex\]](#).
- [62] ATLAS Collaboration, *Observation of a new particle in the search for the Standard Model Higgs boson with the ATLAS detector at the LHC*, *Phys. Lett. B* **716** (2012) 1, arXiv: [1207.7214 \[hep-ex\]](#).
- [63] ATLAS Collaboration, *Recommendations for the Modeling of Smooth Backgrounds*, ATL-PHYS-PUB-2020-028, 2020, URL: <https://cds.cern.ch/record/2743717>.
- [64] R. W. S. Alan V. Oppenheim, *Discrete-Time Signal Processing, Third Edition*, 2009, ISBN: 978-1292-02572-8.
- [65] G. Cowan, K. Cranmer, E. Gross and O. Vitells, *Asymptotic formulae for likelihood-based tests of new physics*, *Eur. Phys. J. C* **71** (2011) 1554, arXiv: [1007.1727 \[physics.data-an\]](#), Erratum: *Eur. Phys. J. C* **73** (2013) 2501.
- [66] A. L. Read, *Presentation of search results: the CL_s technique*, *J. Phys. G* **28** (2002) 2693.
- [67] ATLAS Collaboration, *ATLAS Computing Acknowledgements*, ATL-SOFT-PUB-2025-001, 2025, URL: <https://cds.cern.ch/record/2922210>.

The ATLAS Collaboration

G. Aad ¹⁰³, E. Aakvaag ¹⁷, B. Abbott ¹²³, S. Abdelhameed ^{119a}, K. Abeling ⁵⁵, N.J. Abicht ⁴⁹, S.H. Abidi ³⁰, M. Aboeela ⁴⁵, A. Abouhorma ^{36e}, H. Abramowicz ¹⁵⁶, B.S. Acharya ^{69a,69b,m}, A. Ackermann ^{63a}, C. Adam Bourdarios ⁴, L. Adamczyk ^{86a}, S.V. Addepalli ¹⁴⁸, M.J. Addison ¹⁰², J. Adelman ¹¹⁸, A. Adiguzel ^{22c}, T. Adye ¹³⁷, A.A. Affolder ¹³⁹, Y. Afik ⁴⁰, M.N. Agaras ¹³, A. Aggarwal ¹⁰¹, C. Agheorghiesei ^{28c}, F. Ahmadov ^{39,ad}, S. Ahuja ⁹⁶, S. Ahuja ¹⁶⁸, X. Ai ^{114c}, G. Aielli ^{76a,76b}, A. Aikot ¹⁶⁸, M. Ait Tamlihat ^{36e}, B. Aitbenchikh ^{36a}, T.P.A. Åkesson ⁹⁹, D. Akiyama ¹⁷³, N.N. Akolkar ²⁵, S. Aktas ¹⁷¹, G.L. Alberghi ^{24b}, J. Albert ¹⁷⁰, U. Alberti ²⁰, P. Albicocco ⁵³, G.L. Albouy ⁶⁰, S. Alderweireldt ⁵², Z.L. Alegria ¹²⁴, M. Aleksa ³⁷, I.N. Aleksandrov ³⁹, C. Alexa ^{28b}, T. Alexopoulos ¹⁰, F. Alfonsi ^{24b}, M. Algren ⁵⁶, M. Alhroob ¹⁷², B. Ali ¹³⁵, H.M.J. Ali ^{92,v}, S. Ali ³², S.W. Alibocus ⁹³, M. Aliev ^{34c}, G. Alimonti ^{71a}, C. Allaire ⁶⁶, B.M.M. Allbrooke ¹⁵¹, D.R. Allen ¹²⁴, J.S. Allen ¹⁰², J.F. Allen ⁵², C.S. Alley ¹, A. Aloisio ^{72a,72b}, F. Alonso ⁹¹, C. Alpigiani ¹⁴², Z.M.K. Alsolami ⁹², A. Alvarez Fernandez ¹⁰¹, M. Alves Cardoso ⁵⁶, M.G. Alviggi ^{72a,72b}, M. Aly ¹⁰², Y. Amaral Coutinho ^{82b}, A. Ambler ¹⁰⁵, C. Amelung ³⁷, M. Amerl ¹⁰², T. Amezza ¹³⁰, B. Amini ⁵⁴, K. Amirie ¹⁶⁰, A. Amirkhanov ³⁹, S.P. Amor Dos Santos ^{133a}, D. Amperiadou ¹⁵⁷, S. An ⁸³, C. Anastopoulos ¹⁴⁴, T. Andeen ¹¹, J.K. Anders ⁹³, A.C. Anderson ⁵⁹, A. Andreazza ^{71a,71b}, S. Angelidakis ⁹, A. Angerami ⁴², A.V. Anisenkov ³⁹, A. Annovi ^{74a}, C. Antel ³⁷, E. Antipov ¹⁵⁰, M. Antonelli ⁵³, F. Anulli ^{75a}, M. Aoki ⁸³, T. Aoki ¹⁵⁸, M.A. Aparo ¹³, L. Aperio Bella ⁴⁸, M. Apicella ³¹, C. Appelt ¹⁵⁶, A. Apyan ²⁷, M. Arampatzis ¹⁰, S.J. Arbiol Val ⁸⁷, C. Arcangeletti ⁵³, A.T.H. Arce ⁵¹, J-F. Arguin ¹⁰⁹, S. Argyropoulos ¹⁵⁷, J.-H. Arling ⁴⁸, O. Arnaez ⁴, H. Arnold ¹⁵⁰, G. Artoni ^{75a,75b}, H. Asada ¹¹², S. Asatryan ¹⁷⁸, N.A. Asbah ³⁷, R.A. Ashby Pickering ¹⁷², A.M. Aslam ⁹⁶, K. Assamagan ³⁰, R. Astalos ^{29a}, K.S.V. Astrand ⁹⁹, S. Atashi ¹⁶⁴, R.J. Atkin ^{34a}, H. Atmani ^{36f}, P.A. Atlasiddha ¹³¹, K. Augsten ¹³⁵, A.D. Auriol ⁴¹, V.A. Austrup ¹⁰², A.S. Avad ⁹⁵, G. Avolio ³⁷, K. Axiotis ⁵⁶, A. Azzam ¹³, D. Babal ^{29b}, H. Bachacou ¹³⁸, K. Bachas ^{157,p}, A. Bachiu ³⁵, E. Bachmann ⁵⁰, M.J. Backes ^{63a}, A. Badea ⁴⁰, T.M. Baer ¹⁰⁷, M. Bahmani ¹⁹, D. Bahner ⁵⁴, K. Bai ¹²⁶, L. Baines ⁹⁵, O.K. Baker ¹⁷⁷, D. Bakshi Gupta ⁸, L.E. Balabram Filho ^{82b}, V. Balakrishnan ¹²³, R. Balasubramanian ⁴, E.M. Baldin ³⁸, P. Balek ^{86a}, E. Ballabene ^{24b,24a}, F. Balli ¹³⁸, L.M. Baltes ^{63a}, W.K. Balunas ¹²⁹, J. Balz ¹⁰¹, I. Bamwidhi ^{119b}, E. Banas ⁸⁷, M. Bandieramonte ¹³², A. Bandyopadhyay ²⁵, S. Bansal ²⁵, L. Barak ¹⁵⁶, M. Barakat ⁴⁸, E.L. Barberio ¹⁰⁶, D. Barberis ^{18b}, M. Barbero ¹⁰³, M.Z. Barel ¹¹⁷, T. Barillari ¹¹¹, M-S. Barisits ³⁷, T. Barklow ¹⁴⁸, P. Baron ¹³⁶, D.A. Baron Moreno ¹⁰², A. Baroncelli ⁶², A.J. Barr ¹²⁹, J.D. Barr ⁹⁷, F. Barreiro ¹⁰⁰, J. Barreiro Guimarães da Costa ¹⁴, M.G. Barros Teixeira ^{133a}, S. Barsov ³⁸, F. Bartels ^{63a}, R. Bartoldus ¹⁴⁸, A.E. Barton ⁹², P. Bartos ^{29a}, M. Baselga ⁴⁹, S. Bashiri ⁸⁷, A. Bassalat ^{66,b}, M.J. Basso ^{161a}, S. Bataju ⁴⁵, R. Bate ¹⁶⁹, R.L. Bates ⁵⁹, S. Batlamous ¹⁰⁰, M. Battaglia ¹³⁹, D. Battulga ¹⁹, M. Bauce ^{75a,75b}, L. Bauckhage ⁴⁸, P. Bauer ²⁵, L.T. Bayer ⁴⁸, L.T. Bazzano Hurrell ³¹, J.B. Beacham ¹¹¹, T. Beau ¹³⁰, J.Y. Beaucamp ⁹¹, P.H. Beauchemin ¹⁶³, P. Bechtel ²⁵, H.P. Beck ^{20,o}, K. Becker ¹⁷², A.J. Beddall ⁸¹, V.A. Bednyakov ³⁹, C.P. Bee ¹⁵⁰, L.J. Beemster ¹⁶, M. Begalli ^{82d}, M. Begel ³⁰, J.K. Behr ⁴⁸, J.F. Beirer ³⁷, F. Beisiegel ²⁵, M. Belfkir ^{119b}, G. Bella ¹⁵⁶, L. Bellagamba ^{24b}, A. Bellerive ³⁵, C.D. Bellgraph ⁶⁸, P. Bellos ²¹, K. Beloborodov ³⁸, I. Benaoumeur ²¹, D. Bencheikroun ^{36a}, F. Bendebba ^{36a}, Y. Benhammou ¹⁵⁶, K.C. Benkendorfer ⁶¹, L. Beresford ⁴⁸, M. Beretta ⁵³, E. Bergeaas Kuutmann ¹⁶⁶, N. Berger ⁴, B. Bergmann ¹³⁵, J. Beringer ^{18a}, G. Bernardi ⁵,

C. Bernius ¹⁴⁸, F.U. Bernlochner ²⁵, A. Berrocal Guardia ¹³, T. Berry ⁹⁶, P. Berta ¹³⁶,
 A. Berti ^{133a}, R. Bertrand ¹⁰³, S. Bethke ¹¹¹, A. Betti ^{75a,75b}, A.J. Bevan ⁹⁵, L. Bezio ⁵⁶,
 N.K. Bhalla ⁵⁴, S. Bharthuar ¹¹¹, S. Bhatta ¹⁵⁰, P. Bhattacharai ¹⁴⁸, Z.M. Bhatti ¹²⁰, K.D. Bhide ⁵⁴,
 V.S. Bhopatkar ¹²⁴, R.M. Bianchi ¹³², G. Bianco ^{24b,24a}, O. Biebel ¹¹⁰, M. Biglietti ^{77a}, P. Bijl ⁵⁴,
 C.S. Billingsley ⁴⁵, Y. Bimgdi ^{36f}, M. Bindi ⁵⁵, A. Bingham ¹⁷⁶, A. Bingul ^{22b}, C. Bini ^{75a,75b},
 G.A. Bird ³³, M. Birman ¹⁷⁴, M. Biroš ¹³⁶, S. Biryukov ¹⁵¹, T. Bisanz ⁴⁹, E. Bisceglie ^{24b,24a},
 J.P. Biswal ¹³⁷, D. Biswas ¹⁴⁶, I. Bloch ⁴⁸, A. Blue ⁵⁹, U. Blumenschein ⁹⁵,
 V.S. Bobrovnikov ³⁹, L. Boccardo ^{57b,57a}, M. Boehler ⁵⁴, B. Boehm ¹⁷¹, D. Bogavac ¹³,
 A.G. Bogdanchikov ³⁸, L.S. Boggia ¹³⁰, V. Boisvert ⁹⁶, P. Bokan ¹⁶⁶, T. Bold ^{86a}, M. Bomben ⁵,
 M. Bona ⁹⁵, M. Boonekamp ¹³⁸, A.G. Borbély ⁵⁹, I.S. Bordulev ³⁸, G. Borissov ⁹²,
 D. Bortoletto ¹²⁹, D. Boscherini ^{24b}, M. Bosman ¹³, K. Bouaouda ^{36a}, L. Boudet ⁴,
 J. Boudreau ¹³², E.V. Bouhova-Thacker ⁹², D. Boumediene ⁴¹, R. Bouquet ^{57b,57a}, A. Boveia ¹²²,
 J. Boyd ³⁷, D. Boye ³⁰, I.R. Boyko ³⁹, L. Bozianu ⁵⁶, J. Bracinek ²¹, N. Brahimi ⁴,
 G. Brandt ¹⁷⁶, O. Brandt ³³, B. Brau ¹⁰⁴, R. Brener ¹⁷⁴, L. Brenner ¹¹⁷, R. Brenner ¹⁶⁶,
 S. Bressler ¹⁷⁴, G. Brianti ¹¹⁷, D. Britton ⁵⁹, D. Britzger ¹¹¹, I. Brock ²⁵, R. Brock ¹⁰⁸,
 H. Bronson ¹³¹, G. Brooijmans ⁴², A.J. Brooks ⁶⁸, E.M. Brooks ^{161b}, E. Brost ³⁰,
 L.M. Brown ^{170,161a}, L.E. Bruce ⁶¹, T.L. Bruckler ¹²⁹, P.A. Bruckman de Renstrom ⁸⁷,
 B. Brüers ⁴⁸, A. Bruni ^{24b}, G. Bruni ^{24b}, D. Brunner ^{47a,47b}, M. Bruschi ^{24b}, N. Brusino ^{75a,75b},
 T. Buanes ¹⁷, Q. Buat ¹⁴², D. Buchin ¹¹¹, A.G. Buckley ⁵⁹, J. Bucko ¹³⁶, M. Bühring ⁵⁰,
 O. Bulekov ⁸¹, B.A. Bullard ¹⁴⁸, T.O. Buratovich ⁹¹, S. Burdin ⁹³, C.D. Burgard ⁴⁹,
 A.M. Burger ⁹⁰, B. Burghgrave ⁸, O. Burlayenko ⁵⁴, J. Burleson ¹⁶⁷, J.C. Burzynski ¹⁴⁷,
 V. Büscher ¹⁰¹, P.J. Bussey ⁵⁹, O. But ²⁵, J.M. Butler ²⁶, C.M. Buttar ⁵⁹, J.M. Butterworth ⁹⁷,
 P. Butti ³⁷, W. Buttinger ¹³⁷, C.J. Buxo Vazquez ¹⁰⁸, A.R. Buzykaev ³⁹, S. Cabrera Urbán ¹⁶⁸,
 L. Cadamuro ⁶⁶, H. Cai ³⁷, Y. Cai ^{24b,113c,24a}, Y. Cai ^{113a}, V.M.M. Cairo ³⁷, O. Cakir ^{3a},
 N. Calace ³⁷, P. Calafiura ^{18a}, G. Calderini ¹³⁰, P. Calfayan ³⁵, L. Calic ⁹⁹, G. Callea ⁵⁹,
 L.P. Caloba ^{82b}, D. Calvet ⁴¹, S. Calvet ⁴¹, R. Camacho Toro ¹³⁰, S. Camarda ³⁷,
 D. Camarero Munoz ²⁷, P. Camarri ^{76a,76b}, C. Camincher ³⁷, M. Campanelli ⁹⁷, A. Camplani ⁴³,
 V. Canale ^{72a,72b}, A.C. Canbay ^{3a}, E. Canonero ⁹⁶, J. Cantero ¹⁶⁸, Y. Cao ¹⁶⁷, F. Capocasa ²⁷,
 M. Capua ^{44b,44a}, A. Carbone ^{71a,71b}, R. Cardarelli ^{76a}, J.C.J. Cardenas ⁸, M.P. Cardiff ²⁷,
 G. Carducci ^{44b,44a}, T. Carli ³⁷, G. Carlino ^{72a}, J.I. Carlotto ¹³, B.T. Carlson ^{132,q},
 E.M. Carlson ¹⁷⁰, L. Carminati ^{71a,71b}, A. Carnelli ⁴, M. Carnesale ³⁷, S. Caron ¹¹⁶,
 E. Carquin ^{140g}, I.B. Carr ¹⁰⁶, S. Carrá ^{73a,73b}, G. Carratta ^{24b,24a}, C. Carrion Martinez ¹⁶⁸,
 A.M. Carroll ¹²⁶, M.P. Casado ^{13,h}, P. Casolaro ^{72a,72b}, M. Caspar ⁴⁸, W.R. Castiglioni ⁴⁰,
 F.L. Castillo ⁴, L. Castillo Garcia ¹³, V. Castillo Gimenez ¹⁶⁸, N.F. Castro ^{133a,133e},
 A. Catinaccio ³⁷, J.R. Catmore ¹²⁸, T. Cavaliere ⁴, V. Cavaliere ³⁰, L.J. Caviedes Betancourt ^{23b},
 E. Celebi ⁸¹, S. Cella ¹⁵⁶, V. Cepaitis ⁵⁶, K. Cerny ¹²⁵, A.S. Cerqueira ^{82a}, A. Cerri ^{74a,am},
 L. Cerrito ^{76a,76b}, F. Cerutti ^{18a}, B. Cervato ^{71a,71b}, A. Cervelli ^{24b}, G. Cesarini ⁵³, S.A. Cetin ⁸¹,
 P.M. Chabrilat ¹³⁰, R. Chakkappai ⁵⁶, S. Chakraborty ¹⁷², A. Chambers ⁶¹, J. Chan ^{18a},
 W.Y. Chan ¹⁵⁸, J.D. Chapman ³³, E. Chapon ¹³⁸, B. Chargeishvili ^{154b}, D.G. Charlton ²¹,
 C. Chauhan ¹³⁴, Y. Che ^{113a}, S. Chekanov ⁶, G.A. Chelkov ^{39,a}, B. Chen ¹⁷⁰, H. Chen ³⁰,
 J. Chen ^{143a}, J. Chen ¹⁴⁷, M. Chen ¹²⁹, S. Chen ⁸⁸, S.J. Chen ^{113a}, X. Chen ^{143a}, X. Chen ^{15,ah},
 Z. Chen ⁶², C.L. Cheng ¹⁷⁵, H.C. Cheng ^{64a}, S. Cheong ¹⁴⁸, A. Cheplakov ³⁹,
 E. Cherepanova ¹¹⁷, E. Cheu ⁷, K. Cheung ⁶⁵, L. Chevalier ¹³⁸, G. Chiarelli ^{74a}, G. Chiodini ^{70a},
 A.S. Chisholm ²¹, A. Chitan ^{28b}, M. Chitishvili ¹⁶⁸, M.V. Chizhov ^{39,r}, K. Choi ¹¹, Y. Chou ¹⁴²,
 E.Y.S. Chow ¹¹⁶, K.L. Chu ¹⁷⁴, M.C. Chu ^{64a}, Z. Chubinidze ⁵³, J. Chudoba ¹³⁴,
 J.J. Chwastowski ⁸⁷, D. Cieri ¹¹¹, K.M. Ciesla ^{86a}, V. Cindro ⁹⁴, A. Ciocio ^{18a}, F. Ciroto ^{72a,72b},
 Z.H. Citron ¹⁷⁴, M. Citterio ^{71a}, D.A. Ciubotaru ^{28b}, A. Clark ⁵⁶, P.J. Clark ⁵², N. Clarke Hall ⁹⁷,

C. Clarry [id](#)¹⁶⁰, S.E. Clawson [id](#)⁴⁸, C. Clement [id](#)^{47a,47b}, L. Clissa [id](#)^{24b,24a}, Y. Coadou [id](#)¹⁰³,
 M. Cobal [id](#)^{69a,69c}, A. Coccaro [id](#)^{57b}, M.G. Cochran Branson [id](#)¹⁴², R.F. Coelho Barrue [id](#)^{133a},
 R. Coelho Lopes De Sa [id](#)¹⁰⁴, S. Coelli [id](#)^{71a}, M.M. Cohen [id](#)¹³¹, L.S. Colangeli [id](#)¹⁶⁰, B. Cole [id](#)⁴²,
 P. Collado Soto [id](#)¹⁰⁰, J. Collot [id](#)⁶⁰, R. Coluccia [id](#)^{70a,70b}, P. Conde Muiño [id](#)^{133a,133g}, M.P. Connell [id](#)^{34c},
 S.H. Connell [id](#)^{34c}, E.I. Conroy [id](#)¹²⁹, M. Contreras Cossio [id](#)¹¹, F. Conventi [id](#)^{72a,aj},
 A.M. Cooper-Sarkar [id](#)¹²⁹, L. Corazzina [id](#)^{75a,75b}, F.A. Corchia [id](#)^{24b,24a}, A. Cordeiro Oudot Choi [id](#)¹⁴²,
 L.D. Corpe [id](#)⁴¹, M. Corradi [id](#)^{75a,75b}, F. Corriveau [id](#)^{105,ab}, A. Cortes-Gonzalez [id](#)¹⁵⁸, M.J. Costa [id](#)¹⁶⁸,
 F. Costanza [id](#)⁴, D. Costanzo [id](#)¹⁴⁴, J. Couthures [id](#)⁴, G. Cowan [id](#)⁹⁶, K. Cranmer [id](#)¹⁷⁵, L. Cremer [id](#)⁴⁹,
 D. Cremonini [id](#)^{24b,24a}, S. Crépe-Renaudin [id](#)⁶⁰, F. Crescioli [id](#)¹³⁰, T. Cresta [id](#)^{73a,73b}, M. Cristinziani [id](#)¹⁴⁶,
 M. Cristoforetti [id](#)^{78a,78b}, E. Critelli [id](#)⁹⁷, A. Cueto [id](#)¹⁰⁰, H. Cui [id](#)⁹⁷, Z. Cui [id](#)⁷, B.M. Cunnett [id](#)¹⁵¹,
 W.R. Cunningham [id](#)⁵⁹, F. Curcio [id](#)¹⁶⁸, J.R. Curran [id](#)⁵², M.J. Da Cunha Sargedas De Sousa [id](#)^{57b,57a},
 J.V. Da Fonseca Pinto [id](#)^{82b}, C. Da Via [id](#)¹⁰², W. Dabrowski [id](#)^{86a}, T. Dado [id](#)³⁷, S. Dahbi [id](#)¹⁵³,
 T. Dai [id](#)¹⁰⁷, D. Dal Santo [id](#)²⁰, C. Dallapiccola [id](#)¹⁰⁴, M. Dam [id](#)⁴³, G. D'amen [id](#)³⁰, V. D'Amico [id](#)¹¹⁰,
 J.R. Dandoy [id](#)³⁵, M. D'Andrea [id](#)^{57b,57a}, D. Dannheim [id](#)³⁷, G. D'anniballe [id](#)^{74a,74b}, M. Danninger [id](#)¹⁴⁷,
 V. Dao [id](#)¹⁵⁰, G. Darbo [id](#)^{57b}, S.J. Das [id](#)³⁰, F. Dattola [id](#)⁴⁸, S. D'Auria [id](#)^{71a,71b}, A. D'Avanzo [id](#)^{72a,72b},
 T. Davidek [id](#)¹³⁶, J. Davidson [id](#)¹⁷², I. Dawson [id](#)⁹⁵, K. De [id](#)⁸, C. De Almeida Rossi [id](#)¹⁶⁰,
 R. De Asmundis [id](#)^{72a}, N. De Biase [id](#)⁴⁸, S. De Castro [id](#)^{24b,24a}, N. De Groot [id](#)¹¹⁶, P. de Jong [id](#)¹¹⁷,
 H. De la Torre [id](#)¹¹⁸, A. De Maria [id](#)^{113a}, A. De Salvo [id](#)^{75a}, U. De Sanctis [id](#)^{76a,76b}, F. De Santis [id](#)^{70a,70b},
 A. De Santo [id](#)¹⁵¹, J.B. De Vivie De Regie [id](#)⁶⁰, J. Debevc [id](#)⁹⁴, D.V. Dedovich [id](#)³⁹, J. Degens [id](#)⁹³,
 A.M. Deiana [id](#)⁴⁵, J. Del Peso [id](#)¹⁰⁰, L. Delagrangé [id](#)²⁷, F. Deliot [id](#)¹³⁸, C.M. Delitzsch [id](#)⁴⁹,
 M. Della Pietra [id](#)^{72a,72b}, D. Della Volpe [id](#)⁵⁶, A. Dell'Acqua [id](#)³⁷, L. Dell'Asta [id](#)^{71a,71b}, M. Delmastro [id](#)⁴,
 C.C. Delogu [id](#)^{57b,57a}, P.A. Delsart [id](#)⁶⁰, S. Demers [id](#)¹⁷⁷, M. Demichev [id](#)³⁹, S.P. Denisov [id](#)³⁸,
 H. Denizli [id](#)^{22a,1}, M.G. Depala [id](#)⁹³, L. D'Eramo [id](#)⁴¹, D. Derendarz [id](#)⁸⁷, L. Derin [id](#)^{57b,57a}, F. Derue [id](#)¹³⁰,
 P. Dervan [id](#)^{93,*}, A.M. Desai [id](#)¹, K. Desch [id](#)²⁵, F.A. Di Bello [id](#)^{74a,74b}, A. Di Ciaccio [id](#)^{76a,76b},
 L. Di Ciaccio [id](#)⁴, C. Di Donato [id](#)^{72a,72b}, A. Di Girolamo [id](#)³⁷, G. Di Gregorio [id](#)⁶⁶, A. Di Luca [id](#)^{78a,78b},
 B. Di Micco [id](#)^{77a,77b}, R. Di Nardo [id](#)^{77a,77b}, K.F. Di Petrillo [id](#)⁴⁰, M. Diamantopoulou [id](#)³⁵, F.A. Dias [id](#)¹¹⁷,
 M.A. Diaz [id](#)^{140a,140b}, A.R. Didenko [id](#)³⁹, M. Didenko [id](#)¹⁶⁸, S.D. Diefenbacher [id](#)^{18a}, E.B. Diehl [id](#)¹⁰⁷,
 S. Díez Cornell [id](#)⁴⁸, C. Díez Pardos [id](#)¹⁴⁶, C. Dimitriadi [id](#)¹⁴⁹, A. Dimitrievska [id](#)²¹, A. Dimri [id](#)¹⁵⁰,
 Y. Ding [id](#)⁶², J. Dingfelder [id](#)²⁵, T. Dingley [id](#)¹²⁹, I-M. Dinu [id](#)^{28b}, S.J. Dittmeier [id](#)^{63b}, F. Dittus [id](#)³⁷,
 M. Divisek [id](#)¹³⁶, B. Dixit [id](#)⁹³, F. Djama [id](#)¹⁰³, T. Djobava [id](#)^{154b}, C. Doglioni [id](#)^{102,99}, A. Dohmalova [id](#)^{29a},
 Z. Dolezal [id](#)¹³⁶, K. Domijan [id](#)^{86a}, K.M. Dona [id](#)⁴⁰, M. Donadelli [id](#)^{82d}, B. Dong [id](#)¹⁰⁸, J. Donini [id](#)⁴¹,
 A. D'Onofrio [id](#)^{72a,72b}, M. D'Onofrio [id](#)⁹³, J. Dopke [id](#)¹³⁷, A. Doria [id](#)^{72a}, N. Dos Santos Fernandes [id](#)^{133a},
 I.A. Dos Santos Luz [id](#)^{82e}, P. Dougan [id](#)⁴⁵, M.T. Dova [id](#)⁹¹, A.T. Doyle [id](#)⁵⁹, M.P. Drescher [id](#)⁵⁵,
 E. Dreyer [id](#)¹⁷⁴, I. Drivas-koulouris [id](#)¹⁰, M. Drnevich [id](#)¹²⁰, D. Du [id](#)⁶², T.A. du Pree [id](#)¹¹⁷, Z. Duan [id](#)^{113a},
 M. Dubau [id](#)⁴, F. Dubinin [id](#)³⁹, M. Dubovsky [id](#)^{29a}, E. Duchovni [id](#)¹⁷⁴, G. Duckeck [id](#)¹¹⁰, P.K. Duckett [id](#)⁹⁷,
 O.A. Ducu [id](#)^{28b}, D. Duda [id](#)⁵², A. Dudarev [id](#)³⁷, M.M. Dudek [id](#)⁸⁷, E.R. Duden [id](#)²⁷, M. D'uffizi [id](#)¹⁰²,
 L. Duflot [id](#)⁶⁶, M. Dührssen [id](#)³⁷, I. Duminica [id](#)^{28g}, A.E. Dumitriu [id](#)^{28b}, M. Dunford [id](#)^{63a},
 A. Duperrin [id](#)¹⁰³, H. Duran Yildiz [id](#)^{3a}, A. Durglishvili [id](#)^{154b}, G.I. Dyckes [id](#)^{18a}, M. Dyndal [id](#)^{86a},
 B.S. Dziedzic [id](#)³⁷, Z.O. Earnshaw [id](#)¹⁵¹, G.H. Eberwein [id](#)¹²⁹, B. Eckerova [id](#)^{29a}, S. Eggebrecht [id](#)⁵⁵,
 E. Egidio Purcino De Souza [id](#)^{82e}, G. Eigen [id](#)¹⁷, K. Einsweiler [id](#)^{18a}, T. Ekelof [id](#)¹⁶⁶, P.A. Ekman [id](#)⁹⁹,
 S. El Farkh [id](#)^{36b}, Y. El Ghazali [id](#)⁶², H. El Jarrari [id](#)¹⁰⁵, A. El Moussaouy [id](#)^{36a}, I. Elbaz [id](#)¹⁵⁶,
 D. Elitez [id](#)³⁷, M. Ellert [id](#)¹⁶⁶, F. Ellinghaus [id](#)¹⁷⁶, T.A. Elliot [id](#)⁹⁶, J. Elmsheuser [id](#)³⁰, M. Elsayy [id](#)^{119a},
 M. Elsing [id](#)³⁷, D. Emeliyanov [id](#)¹³⁷, Y. Enari [id](#)⁸³, S. Epari [id](#)¹⁰⁹, D. Ernani Martins Neto [id](#)⁸⁷, F. Ernst [id](#)³⁷,
 M. Escalier [id](#)⁶⁶, C. Escobar [id](#)¹⁶⁸, R. Estevam De Paula [id](#)^{82c}, E. Etzion [id](#)¹⁵⁶, G. Evans [id](#)^{133a,133b},
 H. Evans [id](#)⁶⁸, L.S. Evans [id](#)⁴⁸, A. Ezhilov [id](#)³⁸, S. Ezzarqtouni [id](#)^{36a}, F. Fabbri [id](#)^{24b,24a}, L. Fabbri [id](#)^{24b,24a},
 G. Facini [id](#)⁹⁷, V. Fadeyev [id](#)¹³⁹, R.M. Fakhruddinov [id](#)³⁸, D. Fakoudis [id](#)¹⁰¹, S. Falciano [id](#)^{75a},
 L.F. Falda Ulhoa Coelho [id](#)²⁷, F. Fallavollita [id](#)¹¹¹, G. Falsetti [id](#)^{44b,44a}, J. Faltova [id](#)¹³⁶, C. Fan [id](#)¹⁶⁷,

K.Y. Fan ^{64b}, Y. Fan ¹⁴, Y. Fang ^{14,113c}, M. Fanti ^{71a,71b}, M. Faraj ^{69a,69c}, Z. Farazpay ⁹⁸,
 A. Farbin ⁸, A. Farilla ^{77a}, K. Farman ¹⁵³, J.N. Farr ¹⁷⁷, M.S. Farrington ⁶¹,
 S.M. Farrington ^{137,52}, F. Fassi ^{36e}, D. Fassouliotis ⁹, L. Fayard ⁶⁶, P. Federic ¹³⁶,
 P. Federicova ¹³⁴, O.L. Fedin ^{38,a}, M. Feickert ¹⁷⁵, L. Feligioni ¹⁰³, D.E. Fellers ^{18a},
 C. Feng ^{114b}, Y. Feng ¹⁴, Z. Feng ⁶⁶, B. Fernandez Barbadillo ⁹², P. Fernandez Martinez ⁶⁷,
 M.J.V. Fernoux ¹⁰³, J. Ferrando ⁹², A. Ferrari ¹⁶⁶, P. Ferrari ^{117,116}, R. Ferrari ^{73a}, D. Ferrere ⁵⁶,
 C. Ferretti ¹⁰⁷, M.P. Fewell ¹, D. Fiacco ^{75a,75b}, F. Fiedler ¹⁰¹, P. Fiedler ¹³⁵, S. Filimonov ³⁹,
 M.S. Filip ^{28b,s}, A. Filipčič ⁹⁴, E.K. Filmer ^{161a}, F. Filthaut ¹¹⁶, M.C.N. Fiolhais ^{133a,133c,c},
 L. Fiorini ¹⁶⁸, W.C. Fisher ¹⁰⁸, T. Fitschen ¹⁰², I. Fleck ¹⁴⁶, P. Fleischmann ¹⁰⁷, T. Flick ¹⁷⁶,
 M. Flores ^{34d,ag}, L.R. Flores Castillo ^{64a}, M. Foll ¹²⁸, F.M. Follega ^{78a,78b}, N. Fomin ³³,
 J.H. Foo ¹⁶⁰, A. Formica ¹³⁸, A.C. Forti ¹⁰², E. Fortin ¹⁵⁰, A.W. Fortman ^{18a}, L. Foster ^{18a},
 L. Fountas ⁹, H. Fox ⁹², P. Francavilla ^{74a,74b}, S. Francescato ⁶¹, S. Franchellucci ⁵⁶,
 M. Franchini ^{24b,24a}, S. Franchino ^{63a}, D. Francis ³⁷, L. Franco ⁴⁸, L. Franconi ⁴⁸, M. Franklin ⁶¹,
 G. Frattari ²⁷, Y.Y. Frid ¹⁵⁶, J. Friend ⁵⁹, N. Fritzsche ³⁷, A. Froch ⁵⁶, D. Froidevaux ³⁷,
 J.A. Frost ¹³⁷, Y. Fu ¹⁰⁸, S. Fuenzalida Garrido ^{140g}, M. Fujimoto ¹⁵⁰, K.Y. Fung ^{64a},
 E. Furtado De Simas Filho ^{82e}, M. Furukawa ¹⁵⁸, M. Fuste Costa ⁴⁸, J. Fuster ¹⁶⁸, A. Gaa ⁵⁵,
 A. Gabrielli ^{24b,24a}, A. Gabrielli ¹⁶⁰, P. Gadow ³⁷, G. Gagliardi ^{57b,57a}, L.G. Gagnon ^{18a},
 S. Gaid ^{84b}, S. Galantzan ¹⁵⁶, J. Gallagher ¹, E.J. Gallas ¹²⁹, A.L. Gallen ¹⁶⁶, B.J. Gallop ¹³⁷,
 K.K. Gan ¹²², Y. Gao ⁵², Z. Gao ^{113a}, A. Garabaglu ¹⁴², F.M. Garay Walls ^{140a,140b},
 C. García ¹⁶⁸, A. Garcia Alonso ¹¹⁷, A.G. Garcia Caffaro ¹⁷⁷, J.E. García Navarro ¹⁶⁸,
 M.A. Garcia Ruiz ^{23b}, M. Garcia-Sciveres ^{18a}, G.L. Gardner ¹³¹, R.W. Gardner ⁴⁰, N. Garelli ¹⁶³,
 R.B. Garg ¹⁴⁸, J.M. Gargan ³³, C.A. Garner ¹⁶⁰, C.M. Garvey ^{34a}, V.K. Gassmann ¹⁶³, G. Gaudio ^{73a},
 V. Gautam ¹³, J. Gavranovic ⁹⁴, I.L. Gavrilenko ^{133a}, A. Gavrilyuk ³⁸, C. Gay ¹⁶⁹, G. Gaycken ¹²⁶,
 A. Gekow ¹²², C. Gemme ^{57b}, M.H. Genest ⁶⁰, A.D. Gentry ¹¹⁵, S. George ⁹⁶, T. Geralis ⁴⁶,
 A.A. Gerwin ¹²³, P. Gessinger-Befurt ³⁷, M. Ghani ¹⁷², K. Ghorbanian ⁹⁵, A. Ghosal ¹⁴⁶,
 A. Ghosh ¹⁶⁴, A. Ghosh ⁷, B. Giacobbe ^{24b}, S. Giagu ^{75a,75b}, A. Giannini ⁶², S.M. Gibson ⁹⁶,
 D.T. Gil ^{86b}, A.K. Gilbert ^{86a}, B.J. Gilbert ⁴², D. Gillberg ³⁵, G. Gilles ¹¹⁷, D.M. Gingrich ^{2,ai},
 M.P. Giordani ^{69a,69c}, P.F. Giraud ¹³⁸, G. Giugliarelli ^{69a,69c}, D. Giugni ^{71a}, F. Giuli ^{76a,76b},
 I. Gkialas ^{9,i}, L.K. Gladilin ³⁸, C. Glasman ¹⁰⁰, M. Glazewska ²⁰, R.M. Gleason ¹⁶⁴,
 G. Glemža ⁴⁸, M. Glisic ¹²⁶, I. Gnesi ^{44b}, Y. Go ³⁰, M. Goblirsch-Kolb ³⁷, B. Gocke ⁴⁹,
 D. Godin ¹⁰⁹, B. Gokturk ^{22a}, S. Goldfarb ¹⁰⁶, T. Golling ⁵⁶, M.G.D. Gololo ^{34c}, A. Golub ¹⁴²,
 D. Golubkov ³⁸, J.P. Gombas ¹⁰⁸, A. Gomes ^{133a,133b}, G. Gomes Da Silva ¹⁴⁶,
 A.J. Gomez Delegido ³⁷, R. Gonçalves ^{133a}, A. Gongadze ^{154c}, F. Gonnella ²¹, J.L. Gonski ¹⁴⁸,
 R.Y. González Andana ⁵², S. González de la Hoz ¹⁶⁸, M.V. Gonzalez Rodrigues ⁴⁸,
 R. Gonzalez Suarez ¹⁶⁶, S. Gonzalez-Sevilla ⁵⁶, L. Goossens ³⁷, B. Gorini ³⁷, E. Gorini ^{70a,70b},
 A. Gorišek ⁹⁴, T.C. Gosart ¹³¹, A.T. Goshaw ⁵¹, M.I. Gostkin ³⁹, S. Goswami ¹²⁴,
 C.A. Gottardo ³⁷, S.A. Gotz ¹¹⁰, M. Goughri ^{36b}, A.G. Goussiou ¹⁴², N. Govender ^{34c},
 R.P. Grabarczyk ¹²⁹, I. Grabowska-Bold ^{86a}, K. Graham ³⁵, E. Gramstad ¹²⁸,
 S. Grancagnolo ^{70a,70b}, C.M. Grant ¹, P.M. Gravila ^{28f}, F.G. Gravili ^{70a,70b}, H.M. Gray ^{18a},
 M. Greco ¹¹¹, M.J. Green ¹, C. Grefe ²⁵, A.S. Grefsrud ¹⁷, I.M. Gregor ⁴⁸, K.T. Greif ¹⁶⁴,
 P. Grenier ¹⁴⁸, S.G. Grewe ¹¹¹, K. Grimm ³², S. Grinstein ^{13,x}, E. Gross ¹⁷⁴, J. Grosse-Knetter ⁵⁵,
 L.H. Grossman ^{18b}, L. Guan ¹⁰⁷, G. Guerrieri ³⁷, R. Guevara ¹²⁸, R. Gugel ¹⁰¹,
 J.A.M. Guhit ¹⁰⁷, A. Guida ¹⁹, E. Guilloton ¹⁷², S. Guindon ³⁷, F. Guo ^{14,113c}, J. Guo ^{143a},
 L. Guo ⁴⁸, L. Guo ^{113b,u}, Y. Guo ¹⁰⁷, Y. Guo ⁴², A. Gupta ⁴⁹, R. Gupta ¹³², S. Gupta ²⁷,
 S. Gurbuz ²⁵, S.S. Gurdasani ⁴⁸, G. Gustavino ^{75a,75b}, P. Gutierrez ¹²³,
 L.F. Gutierrez Zagazeta ¹³¹, M. Gutsche ⁵⁰, C. Gutschow ⁹⁷, C. Gwenlan ¹²⁹, C.B. Gwilliam ⁹³,
 E.S. Haaland ¹²⁸, A. Haas ¹²⁰, M. Habedank ⁵⁹, C. Haber ^{18a}, H.K. Hadavand ⁸, A. Haddad ⁴¹,

A. Hadeef ⁵⁰, A.I. Hagan ⁹², J.J. Hahn ¹⁴⁶, M. Haleem ¹⁷¹, J. Haley ¹²⁴, G.D. Hallewell ¹⁰³,
 J.A. Hallford ⁴⁸, K. Hamano ¹⁷⁰, H. Hamdaoui ¹⁶⁶, M. Hamer ²⁵, S.E.D. Hammoud ⁶⁶,
 E.J. Hampshire ⁹⁶, L. Han ^{113a}, L. Han ⁶², S. Han ¹⁴, K. Hanagaki ⁸³, M. Hance ¹³⁹,
 D.A. Hangal ⁴², H. Hanif ¹⁴⁷, M.D. Hank ¹³¹, J.B. Hansen ⁴³, P.H. Hansen ⁴³, T. Harenberg ¹⁷⁶,
 S. Harkusha ¹⁷⁸, M.L. Harris ¹⁰⁴, Y.T. Harris ²⁵, J. Harrison ¹³, P.F. Harrison ¹⁷², M.L.E. Hart ⁹⁷,
 N.M. Hartman ¹¹¹, N.M. Hartmann ¹¹⁰, R.Z. Hasan ^{96,137}, Y. Hasegawa ¹⁴⁵, D. Hashimoto ¹¹²,
 F. Haslbeck ³⁷, S. Hassan ¹⁷, R. Hauser ¹⁰⁸, M. Haviernik ¹³⁶, C.M. Hawkes ²¹,
 R.J. Hawkings ³⁷, Y. Hayashi ¹⁵⁸, D. Hayden ¹⁰⁸, R.L. Hayes ¹¹⁷, C.P. Hays ¹²⁹, J.M. Hays ⁹⁵,
 H.S. Hayward ⁹³, M. He ^{14,113c}, Y. He ⁴⁸, Y. He ⁹⁷, N.B. Heatley ⁹⁵, V. Hedberg ⁹⁹,
 J. Heilman ³⁵, S. Heim ⁴⁸, T. Heim ^{18a}, J.J. Heinrich ¹²⁶, L. Heinrich ¹¹¹, J. Hejbal ¹³⁴,
 M. Helbig ⁵⁰, A. Held ¹⁷⁵, S. Hellesund ¹⁷, C.M. Helling ¹⁶⁹, H. Herde ⁹⁹,
 Y. Hernández Jiménez ¹⁵⁰, L.M. Herrmann ²⁵, G. Herten ⁵⁴, R. Hertenberger ¹¹⁰, L. Hervas ³⁷,
 M.E. Hesping ¹⁰¹, N.P. Hessey ^{161a}, J. Hessler ¹¹¹, R. Hicks ¹³¹, M. Hidaoui ^{36b}, N. Hidic ¹³⁶,
 E. Hill ¹⁶⁰, T.S. Hillersoy ¹⁷, S.J. Hillier ²¹, J.R. Hinds ¹⁰⁸, F. Hinterkeuser ²⁵, M. Hirose ¹²⁷,
 S. Hirose ¹⁶², D. Hirschbuehl ¹⁷⁶, T.G. Hitchings ¹⁰², B. Hiti ⁹⁴, J. Hobbs ¹⁵⁰, R. Hobincu ^{28e},
 N. Hod ¹⁷⁴, A.M. Hodges ¹⁶⁷, M.C. Hodgkinson ¹⁴⁴, B.H. Hodgkinson ¹²⁹, A. Hoecker ³⁷,
 D.D. Hofer ¹⁰⁷, J. Hofer ¹⁶⁸, J. Hofner ¹⁰¹, M. Holzbock ³⁷, L.B.A.H. Hommels ³³,
 V. Homsak ¹²⁹, J.J. Hong ⁶⁸, T.M. Hong ¹³², B.H. Hooberman ¹⁶⁷, W.H. Hopkins ⁶,
 M.C. Hoppesch ¹⁶⁷, Y. Horii ¹¹², M.E. Horstmann ¹¹¹, S. Hou ¹⁵³, M.R. Housenga ¹⁶⁷,
 J. Howarth ⁵⁹, J. Hoya ⁶, M. Hrabovsky ¹²⁵, T. Hryn'ova ⁴, P.J. Hsu ⁶⁵, S.-C. Hsu ¹⁴²,
 T. Hsu ⁶⁶, M. Hu ^{18a}, Q. Hu ⁶², S. Huang ³³, X. Huang ^{14,113c}, Y. Huang ¹³⁶, Y. Huang ^{113b},
 Y. Huang ¹⁴, Z. Huang ⁶⁶, Z. Hubacek ¹³⁵, F. Huegging ²⁵, T.B. Huffman ¹²⁹,
 M. Hufnagel Maranha De Faria ^{82a}, C.A. Hugli ⁴⁸, M. Huhtinen ³⁷, S.K. Huiberts ¹²⁸,
 R. Hulsken ¹⁰⁵, C.E. Hultquist ^{18a}, D.L. Humphreys ¹⁰⁴, N. Huseynov ¹², J. Huston ¹⁰⁸,
 B. Huth ³⁷, J. Huth ⁶¹, L. Huth ⁴⁸, R. Hyneman ⁷, G. Iacobucci ⁵⁶, G. Iakovidis ³⁰,
 L. Iconomidou-Fayard ⁶⁶, J.P. Iddon ³⁷, P. Iengo ^{72a,72b}, Y. Iiyama ¹⁵⁸, T. Iizawa ¹⁵⁸,
 Y. Ikegami ⁸³, D. Iliadis ¹⁵⁷, N. Ilic ¹⁶⁰, H. Imam ^{36a}, G. Inacio Goncalves ^{82d},
 S.A. Infante Cabanas ^{140c}, T. Ingebretsen Carlson ^{47a,47b}, J.M. Inglis ⁹⁵, G. Introzzi ^{73a,73b},
 M. Iodice ^{77a}, V. Ippolito ^{75a,75b}, R.K. Irwin ⁹³, M. Ishino ¹⁵⁸, W. Islam ¹⁷⁵, C. Issever ¹⁹,
 S. Istin ^{22a,ao}, K. Itabashi ¹²⁷, H. Ito ¹⁷³, R. Iuppa ^{78a,78b}, A. Ivina ¹⁷⁴, S. Izumiyama ¹¹²,
 V. Izzo ^{72a}, P. Jacka ¹³⁵, P. Jackson ¹, P.R. Jacobson ⁵¹, P. Jain ⁴⁸, K. Jakobs ⁵⁴,
 T. Jakoubek ¹⁷⁴, J. Jamieson ⁵⁹, W. Jang ¹⁵⁸, S. Jankovych ¹¹⁷, M. Javurkova ¹⁰⁴, P. Jawahar ¹⁰²,
 L. Jeanty ¹²⁶, J. Jejelava ^{154a,ae}, P. Jenni ^{54,f}, L. Jerala ⁹⁴, C.E. Jessiman ³⁵, H. Jia ¹⁶⁹,
 J. Jia ¹⁵⁰, X. Jia ^{111,113c}, Z. Jia ^{113a}, C. Jiang ⁵², Q. Jiang ^{64b}, S. Jiggins ⁴⁸,
 M. Jimenez Ortega ¹⁶⁸, J. Jimenez Pena ¹³, S. Jin ^{113a}, A. Jinaru ^{28b}, O. Jinnouchi ¹⁴¹,
 P. Johansson ¹⁴⁴, K.A. Johns ⁷, J.W. Johnson ¹³⁹, F.A. Jolly ⁴⁸, D.M. Jones ¹⁵¹, E. Jones ⁴⁸,
 K.S. Jones⁸, P. Jones ³³, R.W.L. Jones ⁹², T.J. Jones ⁹³, H.L. Joos ⁵⁵, R. Joshi ¹²²,
 J. Jovicevic ¹⁶, X. Ju ^{18a}, J.J. Junggeburth ³⁷, T. Junkermann ^{63a}, A. Juste Rozas ^{13,x},
 M.K. Juzek ⁸⁷, S. Kabana ^{140f}, A. Kaczmaraska ⁸⁷, S.A. Kadir ¹⁴⁸, M. Kado ¹¹¹, H. Kagan ¹²²,
 M. Kagan ¹⁴⁸, A. Kahn ¹³¹, C. Kahra ¹⁰¹, T. Kaji ¹⁵⁸, E. Kajomovitz ¹⁵⁵, N. Kakati ¹⁷⁴,
 N. Kakoty ¹³, S. Kandel ⁸, N. Kanellos ¹⁰, N.J. Kang ¹³⁹, D. Kar ^{34j,*}, E. Karentzos ²⁵,
 K. Karki ⁸, O. Karkout ¹¹⁷, S.N. Karpov ³⁹, Z.M. Karpova ³⁹, V. Kartvelishvili ^{92,154b},
 A.N. Karyukhin ³⁸, E. Kasimi ¹⁵⁷, J. Katzy ⁴⁸, S. Kaur ³⁵, K. Kawade ¹⁴⁵, M.P. Kawale ¹²³,
 C. Kawamoto ⁸⁸, E.F. Kay ³⁷, S. Kazakos ¹⁰⁸, K. Kazakova ¹⁰³, V.F. Kazanin ³⁸,
 J.M. Keaveney ^{34a}, R. Keeler ¹⁷⁰, G.V. Kehris ⁶¹, J.S. Keller ³⁵, J.M. Kelly ¹⁷⁰,
 J.J. Kempster ¹⁵¹, O. Kepka ¹³⁴, J. Kerr ^{161b}, B.P. Kerridge ¹³⁷, B.P. Kerševan ⁹⁴,
 L. Keszeghova ^{29a}, R.A. Khan ¹³², A. Khanov ¹²⁴, A.G. Kharlamov ³⁸, T. Kharlamova ³⁸,

M. Kholodenko ^{133a}, T.J. Khoo ¹⁹, G. Khoriauli ¹⁷¹, Y. Khoulaki ^{36a}, Y.A.R. Khwaira ¹³⁰,
D. Kim ⁶, D.W. Kim ^{18b}, Y.K. Kim ⁴⁰, N. Kimura ⁹⁷, M.K. Kingston ⁵⁵, C. Kirfel ²⁵,
F. Kirfel ²⁵, J. Kirk ¹³⁷, A.E. Kiryunin ¹¹¹, S. Kita ¹⁶², O. Kivernyk ²⁵, M. Klassen ¹⁶³,
C. Klein ³⁵, L. Klein ¹⁷¹, M.H. Klein ⁴⁵, S.B. Klein ⁵⁶, U. Klein ⁹³, A. Klimentov ³⁰,
P. Kluit ¹¹⁷, S. Kluth ¹¹¹, E. Kneringer ⁷⁹, T.M. Knight ¹⁶⁰, A. Knue ⁴⁹, M. Kobel ⁵⁰,
D. Kobylanskii ¹⁷⁴, S.F. Koch ³⁷, M. Kocian ¹⁴⁸, P. Kodyš ¹³⁶, D.M. Koeck ¹²⁶, T. Koffas ³⁵,
K. Kojima ⁸³, O. Kolay ⁵⁰, I. Koletsou ⁴, T. Komarek ⁸⁷, K. Köneke ⁵⁵, A.X.Y. Kong ¹,
T. Kono ¹²¹, N. Konstantinidis ⁹⁷, P. Kontaxakis ⁵⁶, B. Konya ⁹⁹, R. Kopeliansky ⁴²,
S. Koperny ^{86a}, R. Koppenhofer ⁵⁴, K. Korcyl ⁸⁷, K. Kordas ^{157,d}, A. Korn ⁹⁷, S. Korn ⁵⁵,
I. Korolkov ¹³, N. Korotkova ³⁸, B. Kortman ¹¹⁷, O. Kortner ¹¹¹, S. Kortner ¹¹¹,
W.H. Kostecka ¹¹⁸, M. Kostov ^{29a}, V.V. Kostyukhin ¹⁴⁶, A. Kotsokechagia ³⁷, A. Kotwal ⁵¹,
A. Koulouris ³⁷, A. Kourkoumeli-Charalampidi ^{73a,73b}, E. Kourlitis ¹¹¹, O. Kovanda ¹²⁶,
R. Kowalewski ¹⁷⁰, W. Kozanecki ¹²⁶, A.S. Kozhin ³⁸, V.A. Kramarenko ³⁸, G. Kramberger ⁹⁴,
P. Kramer ²⁵, A. Krasznahorkay ¹⁰⁴, A.C. Kraus ¹¹⁸, J.W. Kraus ¹⁷⁶, J.A. Kremer ⁴⁸,
N.B. Kregel ¹⁴⁶, T. Kresse ⁵⁰, L. Kretschmann ¹⁷⁶, J. Kretschmar ⁹³, P. Krieger ¹⁶⁰,
K. Krizka ²¹, K. Kroeninger ⁴⁹, H. Kroha ¹¹¹, J. Kroll ¹³⁴, J. Kroll ¹³¹, K.S. Krowpman ¹⁰⁸,
U. Kruchonak ³⁹, H. Krüger ²⁵, N. Krumnack ⁸⁰, M.C. Kruse ⁵¹, O. Kuchinskaja ³⁹, S. Kuday ^{3a},
S. Kuehn ³⁷, R. Kuesters ⁵⁴, T. Kuhl ⁴⁸, V. Kukhtin ³⁹, Y. Kulchitsky ³⁹, S. Kuleshov ^{140d,140b},
J. Kull ¹, E.V. Kumar ¹¹⁰, M. Kumar ^{34j}, N. Kumari ⁴⁸, P. Kumari ^{161b}, A. Kupco ¹³⁴,
A. Kupich ³⁸, O. Kuprash ⁵⁴, H. Kurashige ⁸⁵, L.L. Kurchaninov ^{161a}, O. Kurdysh ⁴,
A. Kurova ³⁸, M. Kuze ¹⁴¹, A.K. Kvam ¹⁰⁴, J. Kvita ¹²⁵, N.G. Kyriacou ¹⁴², M. Laassiri ³⁰,
C. Lacasta ¹⁶⁸, H. Lacker ¹⁹, D. Lacour ¹³⁰, E. Ladygin ³⁹, A. Lafarge ⁴¹, B. Laforge ¹³⁰,
T. Lagouri ¹⁷⁷, F.Z. Lahbabi ^{36a}, S. Lai ⁵⁵, W.S. Lai ⁹⁷, I.K. Lakomicc ⁵⁵, J.E. Lambert ¹⁷⁰,
S. Lammers ⁶⁸, W. Lampl ⁷, C. Lampoudis ¹⁵⁷, G. Lamprinoudis ¹⁷¹, A.N. Lancaster ¹¹⁸,
U. Landgraf ⁵⁴, M.P.J. Landon ⁹⁵, V.S. Lang ⁵⁴, A.J. Lankford ¹⁶⁴, F. Lanni ³⁷, C.S. Lantz ¹⁶⁷,
K. Lantzsck ²⁵, A. Lanza ^{73a}, M. Lanzac Berrocal ¹⁶⁸, T. Lari ^{71a}, D. Larsen ¹⁷, L. Larson ¹¹,
F. Lasagni Manghi ^{24b}, M. Lassnig ³⁷, S.D. Lawlor ¹⁴⁴, R. Lazaridou ¹⁶⁴, M. Lazzaroni ^{71a,71b},
E.T.T. Le ¹⁶⁴, H.D.M. Le ¹⁰⁸, E.M. Le Boulicaut ¹⁷⁷, L.T. Le Pottier ^{18a}, B. Leban ^{24b,24a},
F. Ledroit-Guillon ⁶⁰, T.F. Lee ^{161b}, L.L. Leeuw ^{34h}, M. Lefebvre ¹⁷⁰, C. Leggett ^{18a},
G. Lehmann Miotto ³⁷, M. Leigh ⁵⁶, W.A. Leight ¹⁰⁴, W. Leinonen ¹¹⁶, A. Leisos ^{157,t},
M.A.L. Leite ^{82c}, C.E. Leitgeb ¹⁹, R. Leitner ¹³⁶, K.J.C. Leney ⁴⁵, T. Lenz ²⁵, S. Leone ^{74a},
C. Leonidopoulos ⁵², A. Leopold ¹⁴⁹, J. LePage-Bourbonnais ³⁵, R. Les ¹⁰⁸, C.G. Lester ³³,
M. Levchenko ³⁸, J. Levêque ⁴, L.J. Levinson ¹⁷⁴, G. Levrini ^{24b,24a}, M.P. Lewicki ⁸⁷,
C. Lewis ¹⁴², D.J. Lewis ⁴, L. Lewitt ¹⁴⁴, A. Li ³⁰, B. Li ^{114b}, C. Li ¹⁰⁷, C-Q. Li ¹¹¹, H. Li ^{114b},
H. Li ¹⁰², H. Li ¹⁵, H. Li ⁶², H. Li ^{114b}, J. Li ^{143a}, L. Li ^{143a}, R. Li ¹⁷⁷, S. Li ^{143b,143a}, T. Li ⁵,
Y. Li ¹⁴, Z. Li ^{14,113c}, Z. Li ⁶², S. Liang ^{14,113c}, Z. Liang ¹⁴, M. Liberatore ¹³⁸, B. Liberti ^{76a},
G.B. Libotte ^{82d}, K. Lie ^{64c}, J. Lieber Marin ^{82e}, H. Lien ⁶⁸, H. Lin ¹⁰⁷, S.F. Lin ¹⁵⁰,
L. Linden ¹¹⁰, R.E. Lindley ⁷, J.H. Lindon ³⁷, J. Ling ⁶¹, E. Lipeles ¹³¹, A. Lipniacka ¹⁷,
A. Lister ¹⁶⁹, J.D. Little ⁶⁸, B. Liu ¹⁴, B.X. Liu ^{113b}, D. Liu ¹⁵⁵, D. Liu ¹³⁹, E.H.L. Liu ²¹,
H. Liu ^{113b}, J.K.K. Liu ¹²⁰, K. Liu ^{143b}, K. Liu ^{143b}, M. Liu ⁶², M.Y. Liu ⁶², P. Liu ^{114b},
Q. Liu ¹⁴⁸, S. Liu ¹⁵⁰, X. Liu ^{114b}, Y. Liu ^{113b,113c}, Y. Liu ¹⁶⁷, Y.L. Liu ^{114b}, Y.W. Liu ⁶²,
Z. Liu ^{66j}, S.L. Lloyd ⁹⁵, E.M. Lobodzinska ⁴⁸, P. Loch ⁷, E. Lodhi ¹⁶⁰, K. Lohwasser ¹⁴⁴,
E. Loiacono ⁴⁸, J.D. Lomas ²¹, I. Longarini ¹⁶⁴, R. Longo ^{24b,24a}, A. Lopez Solis ¹³,
N.A. Lopez-canelas ⁷, N. Lorenzo Martinez ⁴, A.M. Lory ¹¹⁰, M. Losada ^{119a},
G. Lösckce Centeno ⁴, X. Lou ^{14,113c}, P.A. Love ⁹², M. Lu ⁶⁶, S. Lu ¹³¹, Y.J. Lu ¹⁵³,
H.J. Lubatti ¹⁴², C. Luci ^{75a,75b}, F.L. Lucio Alves ^{113a}, F. Luehring ⁶⁸, B.S. Lunday ¹³¹,
O. Lundberg ¹⁴⁹, J. Lunde ³⁷, N.A. Luongo ⁶, M.S. Lutz ¹⁷⁰, A.B. Lux ²⁶, D. Lynn ³⁰,

R. Lysak ¹³⁴, V. Lysenko ¹³⁵, E. Lytken ⁹⁹, V. Lyubushkin ³⁹, T. Lyubushkina ³⁹, M.M. Lyukova ¹⁵⁰, H. Ma ³⁰, K. Ma ⁶², L.L. Ma ^{114b}, W. Ma ⁶², Y. Ma ¹²⁴, J.C. MacDonald ¹⁰¹, P.C. Machado De Abreu Farias ^{82e}, D. Macina ³⁷, R. Madar ⁴¹, T. Madula ⁹⁷, J. Maeda ⁸⁵, T. Maeno ³⁰, P.T. Mafa ^{34f}, H. Maguire ¹⁴⁴, M. Maheshwari ³³, V. Maiboroda ⁶⁶, A. Maio ^{133a,133b,133d}, K. Maj ^{86a}, O. Majersky ⁴⁸, S. Majewski ¹²⁶, R. Makhmanazarov ³⁸, N. Makovec ⁶⁶, V. Maksimovic ¹⁶, B. Malaescu ¹³⁰, J. Malamant ¹²⁸, Pa. Malecki ⁸⁷, V.P. Maleev ³⁸, F. Malek ^{60,n}, M. Mali ⁹⁴, D. Malito ⁹⁶, A. Maloizel ⁵, A. Malvezzi Lopes ^{82d}, S. Malyukov ³⁹, J. Mamuzic ⁹⁴, G. Mancini ⁵³, M.N. Mancini ²⁷, G. Manco ^{73a,73b}, S.S. Mandarry ¹⁵¹, I. Mandić ⁹⁴, L. Manhaes de Andrade Filho ^{82a}, I.M. Maniatis ¹⁷⁴, J. Manjarres Ramos ⁹⁰, D.C. Mankad ¹⁷⁴, A. Mann ¹¹⁰, T. Manoussos ³⁷, M.N. Mantinan ⁴⁰, S. Manzoni ³⁷, L. Mao ^{143a}, X. Mapekula ^{34c}, A. Marantis ¹⁵⁷, R.R. Marcelo Gregorio ¹, G. Marchiori ⁵, C. Marcon ^{71a}, E. Maricic ¹⁶, M. Marinescu ⁴⁸, S. Marium ⁴⁸, M. Marjanovic ¹²³, A. Markhoos ⁵⁴, M. Markovitch ⁶⁶, M.K. Maroun ¹⁰⁴, M.C. Marr ¹⁴⁷, G.T. Marsden ¹⁰², E.J. Marshall ⁹², Z. Marshall ^{18a}, S. Marti-Garcia ¹⁶⁸, J. Martin ⁹⁷, T.A. Martin ¹³⁷, V.J. Martin ⁵², B. Martin dit Latour ¹⁷, L. Martinelli ^{75a,75b}, P. Martinez Agullo ¹⁶⁸, V.I. Martinez Outschoorn ¹⁰⁴, P. Martinez Suarez ³⁷, S. Martin-Haugh ¹³⁷, G. Martinovicova ¹³⁶, V.S. Martoiu ^{28b}, A.C. Martyniuk ⁹⁷, A. Marzin ³⁷, D. Mascione ^{78a,78b}, L. Masetti ¹⁰¹, J. Masik ¹⁰², A.L. Maslennikov ³⁹, S.L. Mason ⁴², P. Massarotti ^{72a,72b}, P. Mastrandrea ^{74a,74b}, A. Mastroberardino ^{44b,44a}, T. Masubuchi ¹²⁷, T.T. Mathew ¹²⁶, J. Matousek ¹³⁶, D.M. Mattern ⁴⁹, K. Mauer ⁴⁸, J. Maurer ^{28b}, T. Maurin ⁵⁹, A.J. Maury ⁶⁶, B. Maček ⁹⁴, C. Mavungu Tsava ¹⁰³, D.A. Maximov ³⁸, A.E. May ¹⁰², E. Mayer ⁴¹, R. Mazini ^{34j}, S.M. Mazza ¹³⁹, E. Mazzeo ³⁷, J.P. Mc Gowan ¹⁷⁰, S.P. Mc Kee ¹⁰⁷, C.C. McCracken ¹⁶⁹, E.F. McDonald ¹⁰⁶, L.F. Mcelhinney ⁹², J.A. Mcfayden ¹⁵¹, R.P. McGovern ¹³¹, R.P. Mckenzie ^{34j}, D.J. Mclaughlin ⁹⁷, S.J. McMahan ¹³⁷, C.M. Mcpartland ⁹³, R.A. McPherson ^{170,ab}, S. Mehlhase ¹¹⁰, A. Mehta ⁹³, D. Melini ¹⁶⁸, B.R. Mellado Garcia ^{34j}, A.H. Melo ⁵⁵, F. Meloni ⁴⁸, A.M. Mendes Jacques Da Costa ¹⁰², L. Meng ⁹², S. Menke ¹¹¹, M. Mentink ³⁷, E. Meoni ^{44b,44a}, G. Mercado ¹¹⁸, S. Merianos ¹⁵⁷, C. Merlassino ^{69a,69c}, C. Meroni ^{71a,71b}, J. Metcalfe ⁶, A.S. Mete ⁶, E. Meuser ¹⁰¹, C. Meyer ⁶⁸, J-P. Meyer ¹³⁸, Y. Miao ^{113a}, R.P. Middleton ¹³⁷, M. Mihovilovic ⁶⁶, L. Mijović ⁵², G. Mikenberg ¹⁷⁴, M. Mikestikova ¹³⁴, M. Mikuž ⁹⁴, H. Mildner ¹⁰¹, A. Milic ³⁷, D.W. Miller ⁴⁰, E.H. Miller ¹⁴⁸, A. Milov ¹⁷⁴, D.A. Milstead ^{47a,47b}, T. Min ^{113a}, A.A. Minaenko ³⁸, I.A. Minashvili ^{154b}, A.I. Mincer ¹²⁰, B. Mindur ^{86a}, M. Mineev ³⁹, Y. Mino ⁸⁸, L.M. Mir ¹³, M. Miralles Lopez ⁵⁹, M. Mironova ^{18a}, M. Missio ⁴¹, A. Mitra ¹⁷², V.A. Mitsou ¹⁶⁸, Y. Mitsumori ¹¹², P.S. Miyagawa ⁹⁵, T. Mkrtchyan ³⁷, M. Mlinarevic ⁹⁷, T. Mlinarevic ⁹⁷, M. Mlynarikova ¹³⁶, L. Mlynarska ^{86a}, C. Mo ^{143a}, S. Mobius ²⁰, M.H. Mohamed Farook ¹¹⁵, S. Mohapatra ⁴², M.F. Mohd Soberi ⁵², S. Mohiuddin ¹²⁴, G. Mokgatitswane ^{34j}, L. Moleri ¹⁷⁴, U. Molinatti ¹²⁹, L.G. Mollier ²⁰, B. Mondal ¹³⁴, S. Mondal ¹³⁶, K. Mönig ⁴⁸, E. Monnier ¹⁰³, L. Monsonis Romero ¹⁶⁸, A. Montella ^{47a,47b}, M. Montella ¹²², F. Montekali ^{77a,77b}, F. Monticelli ⁹¹, S. Monzani ^{69a,69c}, A. Morancho Tarda ⁴³, N. Morange ⁶⁶, M. Moreno Llácer ¹⁶⁸, C. Moreno Martinez ⁵⁶, J.M. Moreno Perez ^{23b}, P. Morettini ^{57b}, S. Morgenstern ^{63a}, M. Morii ⁶¹, M. Morinaga ¹⁵⁸, F. Morodei ^{75a,75b}, P. Moschovakos ³⁷, B. Moser ⁵⁴, M. Mosidze ^{154b}, T. Moskalets ⁴⁵, P. Moskvitina ¹¹⁶, J. Moss ³², T. Motta Quirino ^{82d}, A. Moussa ^{36d}, Y. Moyal ^{174,k}, H. Moyano Gomez ¹³, E.J.W. Moyses ¹⁰⁴, T.G. Mroz ⁸⁷, S. Muanza ¹⁰³, M. Mucha ²⁵, J. Mueller ¹³², G.A. Mullier ¹⁶⁶, A.J. Mullin ³³, J.J. Mullin ⁵¹, A.C. Mullins ⁴⁵, A.E. Mulski ⁶¹, D.P. Mungo ¹⁶⁰, D. Munoz Perez ¹⁶⁸, F.J. Munoz Sanchez ¹⁰², W.J. Murray ^{172,137}, E. Musajan ⁶², M. Muškinja ⁹⁴, C. Mwewa ⁴⁸, A.G. Myagkov ^{38,a}, A.J. Myers ⁸, G. Myers ¹⁰⁷, M. Myska ¹³⁵, B.P. Nachman ¹⁴⁸, K. Nagai ¹²⁹,

K. Nagano ⁸³, R. Nagasaka ¹⁵⁸, J.L. Nagle ^{30,al}, E. Nagy ¹⁰³, A.M. Nairz ³⁷, Y. Nakahama ⁸³,
 K. Nakamura ⁸³, K. Nakkalil ⁵, A. Nandi ^{63b}, H. Nanjo ¹²⁷, E.A. Narayanan ⁴⁵,
 Y. Narukawa ¹⁵⁸, I. Naryshkin ³⁸, L. Nasella ^{71a,71b}, S. Nasri ^{119b}, C. Nass ²⁵, G. Navarro ^{23a},
 A. Nayaz ¹⁹, P.Y. Nechaeva ³⁸, S. Nechaeva ^{24b,24a}, F. Nechansky ¹³⁴, L. Nedic ¹²⁹,
 A. Negri ^{73a,73b}, M. Negrini ^{24b}, C. Nellist ¹¹⁷, C. Nelson ¹⁰⁵, K. Nelson ¹⁰⁷, S. Nemecek ¹³⁴,
 M. Nessi ^{37,g}, M.S. Neubauer ¹⁶⁷, J. Newell ⁹³, P.R. Newman ²¹, Y.W.Y. Ng ¹⁶⁷, B. Ngair ^{119a},
 H.D.N. Nguyen ¹⁰⁹, J.D. Nichols ¹²³, R. Nicolaidou ¹³⁸, J. Nielsen ¹³⁹, M. Niemeyer ⁵⁵,
 J. Niermann ³⁷, N. Nikiforou ³⁷, V. Nikolaenko ^{38,a}, I. Nikolic-Audit ¹³⁰, P. Nilsson ³⁰,
 G. Ninio ¹⁵⁶, A. Nisati ^{75a}, R. Nisius ¹¹¹, N. Nitika ¹⁷⁴, E.K. Nkadimeng ^{34b}, T. Nobe ¹⁵⁸,
 D. Noll ¹⁴⁸, T. Nommensen ¹⁵², M.B. Norfolk ¹⁴⁴, B.J. Norman ³⁵, L.C. Nosler ^{18a}, M. Noury ^{36a},
 J. Novak ⁹⁴, T. Novak ⁹⁴, P. Novotny ¹⁷⁴, R. Novotny ¹³⁵, L. Nozka ¹²⁵, K. Ntekas ³⁷,
 D. Ntounis ¹⁴⁸, N.M.J. Nunes De Moura Junior ^{82b}, J. Ocariz ¹³⁰, I. Ochoa ^{133a},
 A. Odella Rodriguez ¹³, S. Oerdek ^{48,y}, J.T. Offermann ⁴⁰, A. Ogrodnik ⁸⁷, A. Oh ¹⁰²,
 C.C. Ohm ¹⁴⁹, H. Oide ⁸³, M.L. Ojeda ³⁷, Y. Okumura ¹⁵⁸, L.F. Oleiro Seabra ^{133a},
 I. Oleksiyuk ⁵⁶, G. Oliveira Correa ¹³, D. Oliveira Damazio ³⁰, J.L. Oliver ¹, R. Omar ⁶⁸,
 A.P. O'Neill ²⁰, Y. Onoda ¹⁴¹, A. Onofre ^{133a,133e,e}, P.U.E. Onyisi ¹¹, M.J. Oreglia ⁴⁰,
 D. Orestano ^{77a,77b}, R. Orlandini ^{77a,77b}, R.S. Orr ¹⁶⁰, L.M. Osojnak ⁴², Y. Osumi ¹¹²,
 G. Otero y Garzon ³¹, H. Otono ⁸⁹, M. Ouchrif ^{36d}, F. Ould-Saada ¹²⁸, T. Ovsiannikova ¹⁴²,
 M. Owen ⁵⁹, R.E. Owen ¹³⁷, V.E. Ozcan ^{22a}, F. Ozturk ⁸⁷, N. Ozturk ⁸, S. Ozturk ⁸¹,
 H.A. Pacey ¹²⁹, K. Pachal ^{161a}, A. Pacheco Pages ¹³, C. Padilla Aranda ¹³, G. Padovano ^{75a,75b},
 S. Pagan Griso ^{18a}, L. Pagani ^{76a,76b}, J. Pampel ²⁵, J. Pan ¹⁷⁷, D.K. Panchal ¹¹, C.E. Pandini ⁶⁰,
 J.G. Panduro Vazquez ¹³⁷, H.D. Pandya ¹, H. Pang ¹³⁸, P. Pani ⁴⁸, G. Panizzo ^{69a,69c},
 L. Panwar ^{130,w}, L. Paolozzi ⁵⁶, S. Parajuli ¹⁶⁷, A. Paramonov ⁶, C. Paraskevopoulos ⁵³,
 D. Paredes Hernandez ^{64b}, S.R. Paredes Saenz ⁵², A. Pareti ^{73a,73b}, K.R. Park ⁴², T.H. Park ¹¹¹,
 F. Parodi ^{57b,57a}, J.A. Parsons ⁴², U. Parzefall ⁵⁴, B. Pascual Dias ⁴¹, L. Pascual Dominguez ¹⁰⁰,
 E. Pasqualucci ^{75a}, S. Passaggio ^{57b}, F. Pastore ⁹⁶, P. Patel ⁸⁷, U.M. Patel ⁵¹, J.R. Pater ¹⁰²,
 T. Pauly ³⁷, F. Pauwels ¹³⁶, C.I. Pazos ¹⁶³, M. Pedersen ¹²⁸, R. Pedro ^{133a}, S.V. Peleganchuk ³⁸,
 O. Penc ¹³⁴, S. Peng ¹⁵, G.D. Penn ¹⁷⁷, K.E. Pensi ¹¹⁰, M. Penzin ³⁸, B.S. Peralva ^{82d},
 A.P. Pereira Peixoto ¹⁴², L. Pereira Sanchez ¹⁴⁸, D.V. Perepelitsa ^{30,al}, G. Perera ¹⁰⁴,
 E. Perez Codina ³⁷, M. Perganti ¹⁰, H. Pernegger ³⁷, S. Perrella ^{75a,75b}, K. Peters ⁴⁸,
 R.F.Y. Peters ¹⁰², B.A. Petersen ³⁷, T.C. Petersen ⁴³, E. Petit ¹⁰³, V. Petousis ¹³⁵,
 A.R. Petri ^{71a,71b}, T. Petru ¹³⁶, M. Pettee ^{18a}, A. Petukhov ⁸¹, K. Petukhova ³⁷, R. Pezoa ^{140g},
 L. Pezzotti ^{24b,24a}, G. Pezzullo ¹⁷⁷, L. Pfaffenbichler ³⁷, A.J. Pflieger ⁷⁹, T.M. Pham ¹⁷⁵,
 T. Pham ¹⁰⁶, P.W. Phillips ¹³⁷, G. Piacquadio ¹⁵⁰, E. Pianori ^{18a}, F. Piazza ¹²⁶, R. Piegai ³¹,
 D. Pietreanu ^{28b}, A.D. Pilkington ¹⁰², M. Pinamonti ^{69a,69c}, J.L. Pinfeld ², G. Pinheiro Matos ⁴²,
 B.C. Pinheiro Pereira ^{133a}, J. Pinol Bel ¹³, A.E. Pinto Pinoargote ¹³⁰, L. Pintucci ^{69a,69c},
 A. Pirttikoski ⁵⁶, D.A. Pizzi ³⁵, L. Pizzimento ^{64b}, A. Plebani ³³, M.-A. Pleier ³⁰, V. Pleskot ¹³⁶,
 E. Plotnikova ³⁹, G. Poddar ⁹⁵, R. Poettgen ⁹⁹, L. Poggioli ¹³⁰, S. Polacek ¹³⁶, G. Polesello ^{73a},
 A. Poley ¹⁴⁷, A. Polini ^{24b}, C.S. Pollard ¹⁷², Z.B. Pollock ¹²², E. Pompa Pacchi ¹²³, N.I. Pond ⁹⁷,
 D. Ponomarenko ⁶⁸, L. Pontecorvo ³⁷, S. Popa ^{28a}, G.A. Popeneciu ^{28d}, A. Poreba ^{63a},
 D.M. Portillo Quintero ^{161a}, S. Pospisil ¹³⁵, M.A. Postill ¹⁴⁴, P. Postolache ^{28c}, K. Potamianos ¹⁷²,
 P.A. Potepa ^{86a}, I.N. Potrap ³⁹, C.J. Potter ³³, H. Potti ¹⁵², J. Poveda ¹⁶⁸,
 M.E. Pozo Astigarraga ³⁷, R. Pozzi ³⁷, A. Prades Ibanez ^{76a,76b}, S.R. Pradhan ¹⁴⁴, J. Pretel ¹⁷⁰,
 D. Price ¹⁰², M. Primavera ^{70a}, L. Primomo ^{69a,69c}, M.A. Principe Martin ¹⁰⁰, R. Privara ¹²⁵,
 T. Procter ^{86b}, M.L. Proffitt ¹⁴², N. Proklova ¹³¹, K. Prokofiev ^{64c}, G. Proto ¹¹¹, J. Proudfoot ⁶,
 M. Przybycien ^{86a}, W.W. Przygoda ^{86b}, A. Psallidas ⁴⁶, J.E. Puddefoot ¹⁴⁴, D. Pudzha ⁵³,
 P. Puhl ⁵⁸, H.I. Purnell ¹, D. Pyatiizbyantseva ¹¹⁶, J. Qian ¹⁰⁷, R. Qian ¹⁰⁸, D. Qichen ¹²⁹,

Y. Qin ¹³, T. Qiu ⁵², A. Quadt ⁵⁵, M. Queitsch-Maitland ¹⁰², G. Quetant ⁵⁶, R.P. Quinn ¹⁶⁹,
 G. Rabanal Bolanos ⁶¹, D. Rafanoharana ¹¹¹, F. Raffaelli ^{76a,76b}, J.L. Rainbolt ⁴⁰,
 S. Rajagopalan ³⁰, E. Ramakoti ³⁹, L. Rambelli ^{57b,57a}, I.A. Ramirez-Berend ³⁵, K. Ran ^{107,113c},
 D.S. Rankin ¹³¹, N.P. Rapheeha ^{34j}, H. Rasheed ^{28b}, A. Rastogi ^{18a}, S. Rave ¹⁰¹,
 S. Ravera ^{57b,57a}, B. Ravina ³⁷, I. Ravinovich ¹⁷⁴, M. Raymond ³⁷, A.L. Read ¹²⁸,
 N.P. Readioff ¹⁴⁴, D.M. Rebuzzi ^{73a,73b}, A.S. Reed ⁵⁹, K. Reeves ²⁷, D. Reikher ³⁷, A. Rej ⁴⁹,
 C. Rembser ³⁷, H. Ren ⁶², M. Renda ^{28b}, F. Renner ⁴⁸, A.G. Rennie ⁵⁹, M. Repik ⁵⁶,
 A.L. Rescia ^{57b,57a}, S. Resconi ^{71a}, M. Ressegotti ^{57b}, S. Rettie ¹¹⁷, W.F. Rettie ³⁵,
 M.M. Revering ³³, O.L. Rezanova ³⁹, P. Reznicek ¹³⁶, H. Riani ^{36d}, N. Ribaric ⁵¹,
 B. Ricci ^{69a,69c}, E. Ricci ^{78a,78b}, R. Richter ¹¹¹, E. Richter-Was ^{86b}, M. Ridel ¹³⁰,
 S. Ridouani ^{36d}, P. Rieck ¹²⁰, P. Riedler ³⁷, E.M. Riefel ^{47a,47b}, J.O. Rieger ¹¹⁷, M. Rimoldi ^{34c},
 L. Rinaldi ^{24b,24a}, P. Rincke ^{166,55}, G. Ripellino ¹⁶⁶, I. Riu ¹³, J.C. Rivera Vergara ¹⁷⁰,
 F. Rizatdinova ¹²⁴, E. Rizvi ⁹⁵, B.R. Roberts ⁴⁰, S.S. Roberts ¹³⁹, D. Robinson ³³, A. Robson ⁵⁹,
 A. Rocchi ^{76a,76b}, C. Roda ^{74a,74b}, F.A. Rodriguez ¹¹⁸, S. Rodriguez Bosca ³⁷,
 Y. Rodriguez Garcia ^{23a}, A.M. Rodríguez Vera ¹¹⁸, S. Roe ³⁷, J.T. Roemer ³⁷, O. Røhne ¹²⁸,
 R.A. Rojas ³⁷, C.P.A. Roland ¹³⁰, A. Romaniouk ⁷⁹, E. Romano ^{73a,73b}, M. Romano ^{24b},
 N. Rompotis ⁹³, L. Roos ¹³⁰, S. Rosati ^{75a}, B.J. Rosser ⁴⁰, E. Rossi ¹²⁹, E. Rossi ^{72a,72b},
 L.P. Rossi ⁶¹, L. Rossini ⁵⁴, R. Rosten ¹²², M. Rotaru ^{28b}, R. Roth ³⁷, D. Rousseau ⁶⁶,
 D. Rousso ⁴⁸, S. Roy-Garand ¹⁶⁰, A. Rozanov ¹⁰³, Z.M.A. Rozario ⁵⁹, Y. Rozen ¹⁵⁵,
 A. Rubio Jimenez ¹⁶⁸, V.H. Ruelas Rivera ¹⁹, T.A. Ruggeri ¹, A. Ruggiero ¹²⁹,
 A. Ruiz-Martinez ¹⁶⁸, A. Rummler ³⁷, G.B. Rupnik Boero ³⁷, Z. Rurikova ⁵⁴, N.A. Rusakovich ³⁹,
 S. Ruscelli ⁴⁹, H.L. Russell ¹⁷⁰, G. Russo ¹³⁹, J.P. Rutherford ⁷, S. Rutherford Colmenares ¹²⁰,
 M. Rybar ¹³⁶, P. Rybczynski ^{86a}, A. Ryzhov ⁴⁵, F. Safai Tehrani ^{75a}, S. Saha ¹, B. Sahoo ¹⁷⁴,
 A. Saibel ¹⁶⁸, B.T. Saifuddin ¹²³, M. Saimpert ¹³⁸, G.T. Saito ^{82c}, M. Saito ¹⁵⁸, T. Saito ¹⁵⁸,
 A. Sala ^{71a,71b}, O.T. Salin ⁶⁶, A. Salnikov ¹⁴⁸, J. Salt ¹⁶⁸, A. Salvador Salas ¹⁵⁶, F. Salvatore ¹⁵¹,
 A. Salzburger ³⁷, D. Sammel ⁵⁴, E. Sampson ⁹², D. Sampsonidis ^{157,d}, D. Sampsonidou ¹²⁶,
 M.A.A. Samy ⁵⁹, J. Sánchez ¹⁶⁸, V. Sanchez Sebastian ¹⁶⁸, H. Sandaker ¹²⁸, C.O. Sander ⁴⁸,
 J.A. Sandesara ¹⁷⁵, M. Sandhoff ¹⁷⁶, C. Sandoval ^{23b}, L. Sanfilippo ^{63a}, D.P.C. Sankey ¹³⁷,
 T. Sano ⁸⁸, A. Sansoni ⁵³, M. Santana Queiroz ^{18b}, L. Santi ³⁷, C. Santoni ⁴¹,
 H. Santos ^{133a,133b}, L. Santos Pereira Trigo ⁴⁸, E. Sanzani ^{24b,24a}, K.A. Saoucha ^{84b},
 J.G. Saraiva ^{133a,133d}, J. Sardain ⁷, O. Sasaki ⁸³, K. Sato ¹⁶², C. Sauer ³⁷, E. Sauvan ⁴,
 P. Savard ^{160,ai}, R. Sawada ¹⁵⁸, C. Sawyer ¹³⁷, L. Sawyer ⁹⁸, A.M. Sayed ²⁷, C. Sbarra ^{24b},
 A. Sbrizzi ^{24b,24a}, T. Scanlon ⁹⁷, J. Schaarschmidt ¹⁴², U. Schäfer ¹⁰¹, A.C. Schaffer ^{66,45},
 D. Schaile ¹¹⁰, R.D. Schamberger ¹⁵⁰, C. Scharf ¹⁹, M.M. Schefer ²⁰, V.A. Schegelsky ³⁸,
 D. Scheirich ¹³⁶, M. Schernau ^{140f}, C. Scheulen ⁵⁶, C. Schiavi ^{57b,57a}, M. Schioppa ^{44b,44a},
 S. Schlenker ³⁷, J. Schmeing ¹⁷⁶, E. Schmidt ¹¹¹, M.A. Schmidt ¹⁷⁶, K. Schmieden ²⁵,
 C. Schmitt ¹⁰¹, N. Schmitt ¹⁰¹, S. Schmitt ⁴⁸, N.A. Schneider ¹¹⁰, L. Schoeffel ¹³⁸,
 A. Schoening ^{63b}, P.G. Scholer ³⁵, E. Schopf ¹⁴⁶, M. Schott ²⁵, S. Schramm ⁵⁶, T. Schroer ⁵⁶,
 H-C. Schultz-Coulon ^{63a}, M. Schumacher ⁵⁴, B.A. Schumm ¹³⁹, Ph. Schune ¹³⁸, H.R. Schwartz ⁷,
 A. Schwartzman ¹⁴⁸, T.A. Schwarz ¹⁰⁷, Ph. Schwemling ¹³⁸, R. Schwienhorst ¹⁰⁸,
 F.G. Sciacca ²⁰, A. Sciandra ³⁰, G. Sciolla ²⁷, S.A. Scoville ¹³², F. Scuri ^{74a}, C.D. Sebastiani ³⁷,
 K. Sedlaczek ¹¹⁸, S.C. Seidel ¹¹⁵, B.D. Seidlitz ⁴², C. Seitz ⁴⁸, J.M. Seixas ^{82b},
 G. Sekhniaidze ^{72a}, L. Selem ¹³⁰, N. Semprini-Cesari ^{24b,24a}, A. Semushin ¹⁷⁸, D. Sengupta ⁵⁶,
 V. Senthilkumar ¹¹⁷, L. Serin ⁶⁶, M. Sessa ^{72a,72b}, H. Severini ¹²³, F. Sforza ^{57b,57a}, A. Sfyrla ⁵⁶,
 Q. Sha ¹⁴, H. Shaddix ¹¹⁸, A.H. Shah ³³, R. Shaheen ¹⁴⁹, J.D. Shahinian ¹³¹, M. Shamim ³⁷,
 L.Y. Shan ¹⁴, M. Shapiro ^{18a}, A. Sharma ³⁷, A.S. Sharma ¹⁶⁹, P. Sharma ³⁰, P.B. Shatalov ³⁸,
 K. Shaw ¹⁵¹, S.M. Shaw ¹⁰², Q. Shen ¹⁴, D.J. Sheppard ¹⁴⁷, P. Sherwood ⁹⁷, L. Shi ^{113b},

X. Shi ¹⁴, S. Shimizu ⁸³, S. Shirabe ⁸⁹, M. Shiyakova ^{39,z}, M.J. Shochet ⁴⁰, D.R. Shope ¹²⁸, B. Shrestha ¹²³, S. Shrestha ^{122,an}, I. Shreyber ³⁹, M.J. Shroff ¹⁰⁵, P. Sicho ¹³⁴, A.M. Sickles ¹⁶⁷, E. Sideras Haddad ^{34j,165}, A.C. Sidley ¹¹⁷, A. Sidoti ^{24b}, F. Siegert ⁵⁰, Dj. Sijacki ¹⁶, F. Sili ⁶², J.M. Silva ⁵², I. Silva Ferreira ^{82b}, M.V. Silva Oliveira ³⁰, S.B. Silverstein ^{47a}, S. Simion ⁶⁶, R. Simoniello ³⁷, E.L. Simpson ¹⁰², H. Simpson ¹⁵¹, L.R. Simpson ⁶, S. Simsek ⁸¹, S. Sindhu ⁵⁵, S.N. Singh ²⁷, S. Singh ³⁰, S. Sinha ⁴⁸, S. Sinha ¹⁰², M. Sioli ^{24b,24a}, K. Sioulas ⁹, I. Siral ³⁷, E. Sitnikova ⁴⁸, J. Sjölin ^{47a,47b}, A. Skaf ⁵⁵, E. Skorda ²¹, P. Skubic ¹²³, M. Slawinska ⁸⁷, I. Slazyk ¹⁷, I. Sliusar ¹²⁸, V. Smakhtin ¹⁷⁴, B.H. Smart ¹³⁷, S.Yu. Smirnov ^{140b}, Y. Smirnov ^{34c}, L.N. Smirnova ^{38,a}, O. Smirnova ⁹⁹, A.C. Smith ⁴², J.L. Smith ¹⁰², M.B. Smith ³⁵, R. Smith ¹⁴⁸, H. Smitmanns ¹⁰¹, M. Smizanska ⁹², K. Smolek ¹³⁵, P. Smolyanskiy ¹³⁵, A.A. Snesarev ³⁹, H.L. Snoek ¹¹⁷, R.M. Snyder ⁵¹, S. Snyder ³⁰, R. Sobie ^{170,ab}, A. Soffer ¹⁵⁶, C.A. Solans Sanchez ³⁷, E.Yu. Soldatov ³⁹, U. Soldevila ¹⁶⁸, A.A. Solodkov ^{34j}, S. Solomon ²⁷, A. Soloshenko ³⁹, K. Solovieva ⁵⁴, O.V. Solovyanov ⁴¹, P. Sommer ⁵⁰, A. Sonay ¹³, A. Sopcza ¹³⁵, A.L. Sopio ⁵², F. Sopkova ^{29b}, J.D. Sorenson ¹¹⁵, I.R. Sotarriva Alvarez ¹⁴¹, V. Sothilingam ^{63a}, O.J. Soto Sandoval ^{140c,140b}, S. Sottocornola ⁶⁸, R. Soualah ^{84a}, Z. Soumami ^{36e}, D. South ⁴⁸, N. Soybelman ¹⁷⁴, S. Spagnolo ^{70a,70b}, A.S. Spellman ¹²⁶, D. Sperlich ⁵⁴, B. Spisso ^{72a,72b}, L. Splendori ¹⁰³, M. Spousta ¹³⁶, E.J. Staats ³⁵, R. Stamen ^{63a}, E. Stanecka ⁸⁷, W. Stanek-Maslouska ⁴⁸, M.V. Stange ⁵⁰, B. Stanislaus ^{18a}, M.M. Stanitzki ⁴⁸, E.A. Starchenko ³⁸, G.H. Stark ¹³⁹, J. Stark ⁹⁰, P. Staroba ¹³⁴, P. Starovoitov ^{84b}, R. Staszewski ⁸⁷, C. Stauch ¹¹⁰, G. Stavropoulos ⁴⁶, A. Stefl ³⁷, A. Stein ¹⁰¹, P. Steinberg ³⁰, B. Stelzer ^{147,161a}, H.J. Stelzer ¹³², O. Stelzer ^{161a}, H. Stenzel ⁵⁸, T.J. Stevenson ¹⁵¹, G.A. Stewart ⁴⁸, G. Stoicea ^{28b}, M. Stolarski ^{133a}, S. Stonjek ¹¹¹, A. Straessner ⁵⁰, J. Strandberg ¹⁴⁹, S. Strandberg ^{47a,47b}, M. Stratmann ¹⁷⁶, M. Strauss ¹²³, T. Streblor ¹⁰³, P. Strizenc ^{29b}, R. Ströhmer ¹⁷¹, D.M. Strom ¹²⁶, R. Stroynowski ⁴⁵, A. Strubig ^{47a,47b}, S.A. Stucci ³⁰, B. Stugu ¹⁷, J. Stupak ¹²³, N.A. Styles ⁴⁸, D. Su ¹⁴⁸, S. Su ⁶², X. Su ⁶², D. Suchy ^{29a}, A.D. Sudhakar Ponnu ⁵⁵, L. Sudit ¹⁷⁴, Y. Sue ⁸³, K. Sugizaki ¹³¹, V.V. Sulin ³⁸, D.M.S. Sultan ¹²⁹, L. Sultanaliev ²⁵, S. Sultansoy ^{3b}, S. Sun ¹⁷⁵, W. Sun ¹⁴, S. Sundar Raman ¹⁶⁹, N. Sur ⁹⁹, J.P. Surdutovich ¹²², N. Suri Jr ¹⁷⁷, M.R. Sutton ¹⁵¹, M. Svatos ¹³⁴, P.N. Swallow ³³, M. Swiatlowski ^{161a}, A. Swoboda ³⁷, I. Sykora ^{29a}, M. Sykora ¹³⁶, T. Sykora ¹³⁶, D. Ta ¹⁰¹, K. Tackmann ^{48,y}, A. Taffard ¹⁶⁴, R. Tafirout ^{161a}, Y. Takubo ⁸³, M. Talby ¹⁰³, A.A. Talyshv ³⁸, N.M. Tamir ¹⁵⁶, A. Tanaka ¹⁵⁸, J. Tanaka ¹⁵⁸, R. Tanaka ⁶⁶, M. Tanasini ¹⁵⁰, Z. Tao ¹⁶⁹, S. Tapia Araya ^{140g}, S. Tapprogge ¹⁰¹, A. Tarek Abouelfadl Mohamed ³⁷, S. Tarem ¹⁵⁵, K. Tariq ¹⁴, G. Tarna ³⁷, G.F. Tartarelli ^{71a}, M.J. Tartarin ⁹⁰, P. Tas ¹³⁶, M. Tasevsky ¹³⁴, E. Tassi ^{44b,44a}, A.C. Tate ¹⁶⁷, Y. Tayalati ^{36e,aa}, G.N. Taylor ¹⁰⁶, W. Taylor ^{161b}, R.J. Taylor Vara ¹⁶⁸, A.S. Tegetmeier ⁹⁰, P. Teixeira-Dias ⁹⁶, J.J. Teoh ¹⁶⁰, K. Terashi ¹⁵⁸, J. Terron ¹⁰⁰, S. Terzo ¹³, M. Testa ⁵³, R.J. Teuscher ^{160,ab}, A. Thaler ⁷⁹, O. Theiner ⁵⁶, T. Thevenaux-Pelzer ¹⁰³, J.P. Thomas ²¹, E.A. Thompson ^{18a}, P.D. Thompson ²¹, E. Thomson ¹³¹, R.E. Thornberry ⁴⁵, T.M. Thory-Rao ²¹, C. Tian ⁶², Y. Tian ⁵⁶, V. Tikhomirov ⁸¹, Yu.A. Tikhonov ³⁹, S. Timoshenko ³⁸, D. Timoshyn ¹³⁶, E.X.L. Ting ¹, P. Tipton ¹⁷⁷, A. Tishelman-Charny ³⁰, K. Todome ¹⁴¹, S. Todorova-Nova ¹³⁶, L. Toffolin ^{69a,69c}, M. Togawa ⁸³, J. Tojo ⁸⁹, S. Tokár ^{29a}, O. Toldaiev ⁶⁸, G. Tolkachev ¹⁰³, M. Tomoto ⁸³, L. Tompkins ¹⁴⁸, E. Torrence ¹²⁶, H. Torres ⁹⁰, D.I. Torres Arza ^{140g}, E. Torró Pastor ¹⁶⁸, M. Toscani ³¹, C. Tosciri ⁴⁰, M. Tost ¹¹, D.R. Tovey ¹⁴⁴, T. Trefzger ¹⁷¹, P.M. Tricarico ¹³, A. Tricoli ³⁰, I.M. Trigger ^{161a}, S. Trincas-Duvoid ¹³⁰, D.A. Trischuk ¹⁷⁰, A. Tropina ³⁹, D. Truncali ^{76a,76b}, L. Truong ^{34c}, M. Trzebinski ⁸⁷, A. Trzupek ⁸⁷, F. Tsai ¹⁵⁰, M. Tsai ¹⁰⁷, A. Tsiamis ¹⁵⁷, P.V. Tsiarehshka ³⁹, S. Tsigaridas ^{161a}, A. Tsigotis ^{157,t}, V. Tsiskaridze ^{154a}, E.G. Tskhadadze ^{154a}, Y. Tsujikawa ⁸⁸, I.I. Tsukerman ³⁸, V. Tsulaia ^{18a},

K. Tsuru [ID121](#), D. Tsybychev [ID150](#), Y. Tu [ID64b](#), A. Tudorache [ID28b](#), V. Tudorache [ID28b](#), S.B. Tuncay [ID129](#),
 S. Turchikhin [ID57b,57a](#), I. Turk Cakir [ID3a](#), R. Turra [ID71a](#), T. Turtuvshin [ID39,ac](#), P.M. Tuts [ID42](#),
 Y. Uematsu [ID83](#), F. Ukegawa [ID162](#), P.A. Ulloa Poblete [ID140c,140b](#), G. Unal [ID37](#), A. Undrus [ID30](#),
 J. Urban [ID29b](#), P. Urrejola [ID140e](#), G. Usai [ID8](#), R. Ushioda [ID159](#), M. Usman [ID109](#), F. Ustuner [ID52](#),
 Z. Uysal [ID81](#), V. Vacek [ID135](#), B. Vachon [ID105](#), T. Vafeiadis [ID37](#), A. Vaitkus [ID97](#), C. Valderanis [ID110](#),
 E. Valdes Santurio [ID47a,47b](#), M. Valente [ID37](#), S. Valentinetti [ID24b,24a](#), A. Valero [ID168](#),
 E. Valiente Moreno [ID168](#), A. Vallier [ID90](#), J.A. Valls Ferrer [ID168](#), D.R. Van Arneman [ID117](#),
 R. Van Den Broucke [ID130](#), A. Van Der Graaf [ID49](#), H.Z. Van Der Schyf [ID34j](#), P. Van Gemmeren [ID6](#),
 M. Van Rijnbach [ID37](#), S. Van Stroud [ID97](#), I. Van Vulpen [ID117](#), P. Vana [ID136](#), M. Vanadia [ID76a,76b](#),
 U.M. Vande Voorde [ID149](#), W. Vandelli [ID37](#), E.R. Vandewall [ID148](#), D. Vannicola [ID156](#), L. Vannoli [ID53](#),
 R. Vari [ID75a](#), M. Varma [ID177](#), E.W. Varnes [ID7](#), C. Varni [ID79](#), D. Varouchas [ID66](#), L. Varriale [ID168](#),
 K.E. Varvell [ID152](#), M.E. Vasile [ID28b](#), L. Vaslin [ID83](#), M.D. Vassilev [ID148](#), A. Vasyukov [ID39](#),
 L.M. Vaughan [ID124](#), R. Vavricka [ID136](#), T. Vazquez Schroeder [ID13](#), J. Veatch [ID32](#), V. Vecchio [ID102](#),
 M.J. Veen [ID104](#), I. Veliscek [ID30](#), I. Velkovska [ID94](#), L.M. Veloce [ID160](#), F. Veloso [ID133a,133c](#),
 A.G. Veltman [ID52](#), S.H. Venetianer [ID163](#), S. Veneziano [ID75a](#), A. Ventura [ID70a,70b](#), A. Verbytskyi [ID111](#),
 M. Verducci [ID74a,74b](#), C. Vergis [ID95](#), M. Verissimo De Araujo [ID82b](#), W. Verkerke [ID117](#),
 J.C. Vermeulen [ID117](#), C. Vernieri [ID148](#), M. Vessella [ID164](#), M.C. Vetterli [ID147,ai](#), A. Vgenopoulos [ID101](#),
 N. Viaux Maira [ID140g,af](#), T. Vickey [ID144](#), O.E. Vickey Boeriu [ID144](#), G.H.A. Viehhauser [ID129](#),
 L. Vigani [ID63b](#), M. Vigi [ID111](#), M. Villa [ID24b,24a](#), M. Villaplana Perez [ID168](#), E.M. Villhauer [ID40](#),
 E. Vilucchi [ID53](#), M. Vincent [ID168](#), M.G. Vincter [ID35](#), A. Visibile [ID117](#), A. Visive [ID117](#), C. Vittori [ID37](#),
 I. Vivarelli [ID24b,24a](#), M.I. Vivas Albornoz [ID48](#), E. Voevodina [ID111](#), F. Vogel [ID110](#), J.C. Voigt [ID50](#),
 P. Vokac [ID135](#), Yu. Volkotrub [ID86b](#), L. Vomberg [ID25](#), E. Von Toerne [ID25](#), B. Vormwald [ID37](#),
 K. Vorobev [ID51](#), M. Vos [ID168](#), K. Voss [ID146](#), M. Vozak [ID37](#), L. Vozdecky [ID123](#), N. Vranjes [ID16](#),
 M. Vranjes Milosavljevic [ID16](#), M. Vreeswijk [ID117](#), N.K. Vu [ID143b,143a](#), R. Vuillermet [ID37](#),
 O. Vujinovic [ID101](#), I. Vukotic [ID40](#), I.K. Vyas [ID35](#), J.F. Wack [ID33](#), A. Wada [ID112](#), S. Wada [ID162](#),
 C. Wagner [ID148](#), J.M. Wagner [ID18a](#), W. Wagner [ID176](#), S. Wahdan [ID176](#), H. Wahlberg [ID91](#), C.H. Waits [ID123](#),
 J. Walder [ID137](#), R. Walker [ID110](#), K. Walkingshaw Pass [ID59](#), W. Walkowiak [ID146](#), A. Wall [ID131](#),
 E.J. Wallin [ID99](#), T. Wamorkar [ID148](#), K. Wandall-Christensen [ID168](#), A. Wang [ID62](#), A.Z. Wang [ID139](#),
 C. Wang [ID48](#), C. Wang [ID11](#), H. Wang [ID18a](#), J. Wang [ID64c](#), P. Wang [ID102](#), P. Wang [ID97](#), R. Wang [ID61](#),
 R. Wang [ID107](#), R. Wang [ID6](#), S.M. Wang [ID153](#), S. Wang [ID14](#), T. Wang [ID116](#), T. Wang [ID62](#),
 W.T. Wang [ID129](#), X. Wang [ID167](#), X. Wang [ID143a](#), X. Wang [ID48](#), Y. Wang [ID150](#), Y. Wang [ID115](#),
 Z. Wang [ID107](#), Z. Wang [ID143b](#), Z. Wang [ID107](#), Z. Wang [ID64b](#), C. Wanotayaroj [ID83](#), A. Warburton [ID105](#),
 A.L. Warnerbring [ID146](#), S. Waterhouse [ID96](#), A.T. Watson [ID21](#), H. Watson [ID52](#), M.F. Watson [ID21](#),
 E. Watton [ID37](#), G. Watts [ID142](#), B.M. Waugh [ID97](#), J.M. Webb [ID54](#), C. Weber [ID30](#), M.S. Weber [ID20](#),
 C. Wei [ID62](#), Y. Wei [ID54](#), A.R. Weidberg [ID129](#), E.J. Weik [ID120](#), J. Weingarten [ID49](#), C. Weiser [ID54](#),
 C.J. Wells [ID48](#), T. Wenaus [ID30](#), T. Wengler [ID37](#), N.S. Wenke [ID111](#), N. Wermes [ID25](#), M. Wessels [ID63a](#),
 A.M. Wharton [ID92](#), A.S. White [ID37](#), A. White [ID8](#), M.J. White [ID1](#), D. Whiteson [ID164](#),
 L. Wickremasinghe [ID127](#), W. Wiedenmann [ID175](#), M. Wielers [ID137](#), R. Wierda [ID149](#), C. Wiglesworth [ID43](#),
 H.G. Wilkens [ID37](#), J.J.H. Wilkinson [ID33](#), S. Williams [ID33](#), S. Willocq [ID104](#), D.J. Wilson [ID102](#),
 P.J. Windischhofer [ID40](#), F.I. Winkel [ID31](#), F. Winklmeier [ID126](#), B.T. Winter [ID54](#), M. Wittgen [ID148](#),
 M. Wobisch [ID98](#), T. Wojtkowski [ID60](#), Z. Wolffs [ID117](#), J. Wollrath [ID37](#), M.W. Wolter [ID87](#), H. Wolters [ID133a,133c](#),
 M.C. Wong [ID139](#), E.L. Woodward [ID42](#), S.D. Worm [ID48](#), B.K. Wosiek [ID87](#), K.W. Woźniak [ID87](#),
 S. Wozniowski [ID55](#), K. Wraight [ID59](#), C. Wu [ID160](#), C. Wu [ID21](#), J. Wu [ID158](#), M. Wu [ID113b](#), M. Wu [ID116](#),
 S.L. Wu [ID175](#), S. Wu [ID14,ak](#), X. Wu [ID62](#), Y.Q. Wu [ID160](#), Y. Wu [ID62](#), Z. Wu [ID4](#), Z. Wu [ID113a](#),
 J. Wuerzinger [ID111](#), T.R. Wyatt [ID102](#), B.M. Wynne [ID52](#), S. Xella [ID43](#), L. Xia [ID113a](#), M. Xie [ID62](#),
 A. Xiong [ID126](#), D. Xu [ID14](#), H. Xu [ID62](#), L. Xu [ID62](#), R. Xu [ID131](#), T. Xu [ID107](#), W. Xu [ID113a](#), Y. Xu [ID142](#),
 Z. Xu [ID52](#), R. Xue [ID132](#), B. Yabsley [ID152](#), S. Yacoob [ID11](#), Y. Yamaguchi [ID83](#), E. Yamashita [ID158](#),

H. Yamauchi ¹⁶², T. Yamazaki ^{18a}, Y. Yamazaki ⁸⁵, S. Yan ⁵⁹, Z. Yan ¹⁰⁴, H.J. Yang ^{143a}, H.T. Yang ⁶², S. Yang ⁶², X. Yang ³⁷, X. Yang ¹⁴, Y. Yang ¹⁵⁸, Y. Yang ⁶², W-M. Yao ^{18a}, C.L. Yardley ¹⁵¹, J. Ye ¹⁴, S. Ye ³⁰, X. Ye ⁶², Y. Yeh ⁹⁷, I. Yeletsikh ³⁹, B. Yeo ^{18b}, M.R. Yexley ⁹⁷, T.P. Yildirim ¹²⁹, K. Yorita ¹⁷³, C.J.S. Young ³⁷, C. Young ¹⁴⁸, I.N.L. Young ⁵⁹, N.D. Young ¹²⁶, Y. Yu ⁶², J. Yuan ^{14,113c,ak}, M. Yuan ¹⁰⁷, R. Yuan ^{143b}, L. Yue ⁹⁷, M. Zaazoua ⁶², B. Zabinski ⁸⁷, I. Zahir ^{36a}, A. Zaio ^{57b,57a}, Z.K. Zak ⁸⁷, T. Zakareishvili ¹⁶⁸, S. Zambito ⁵⁶, J.A. Zamora Saa ^{140d}, J. Zang ¹⁵⁸, R. Zanzottera ^{71a,71b}, O. Zaplatilek ¹³⁵, C. Zeitnitz ¹⁷⁶, H. Zeng ¹⁴, D.T. Zenger Jr ²⁷, O. Zenin ³⁸, T. Ženiš ^{29a}, S. Zenz ⁹⁵, D. Zerwas ⁶⁶, B. Zhang ¹⁷², D.F. Zhang ¹⁴⁴, G. Zhang ^{14,ak}, J. Zhang ^{114b}, J. Zhang ⁶, L. Zhang ⁶², L. Zhang ^{113a}, P. Zhang ^{14,113c}, R. Zhang ^{113a}, S. Zhang ⁹⁰, Y. Zhang ¹⁴², Y. Zhang ⁹⁷, Y. Zhang ⁶², Y. Zhang ^{113a}, Z. Zhang ^{18a}, Z. Zhang ^{114b}, Z. Zhang ⁶⁶, H. Zhao ¹⁴², T. Zhao ^{114b}, Y. Zhao ³⁵, Z. Zhao ⁶², Z. Zhao ⁶², A. Zhemchugov ³⁹, J. Zheng ^{113a}, K. Zheng ¹⁶⁷, L. Zheng ^{114b}, X. Zheng ⁶², Z. Zheng ¹⁴⁸, D. Zhong ¹⁶⁷, B. Zhou ¹⁰⁷, B. Zhou ^{143b,143a}, H. Zhou ⁷, N. Zhou ^{143a}, Y. Zhou ¹⁵, Y. Zhou ^{113a}, Y. Zhou ⁷, J. Zhu ¹⁰⁷, X. Zhu ^{143b}, Y. Zhu ^{143a}, X. Zhuang ¹⁴, K. Zhukov ⁶⁸, N.I. Zimine ³⁹, J. Zinsser ^{63b}, M. Ziolkowski ¹⁴⁶, L. Živković ¹⁶, A. Zoccoli ^{24b,24a}, K. Zoch ⁶¹, A. Zografos ³⁷, T.G. Zorbas ¹⁴⁴, O. Zormpa ⁴⁶, L. Zwalinski ³⁷.

¹Department of Physics, University of Adelaide, Adelaide; Australia.

²Department of Physics, University of Alberta, Edmonton AB; Canada.

^{3(a)}Department of Physics, Ankara University, Ankara; ^(b)Division of Physics, TOBB University of Economics and Technology, Ankara; Türkiye.

⁴LAPP, Université Savoie Mont Blanc, CNRS/IN2P3, Annecy; France.

⁵APC, Université Paris Cité, CNRS/IN2P3, Paris; France.

⁶High Energy Physics Division, Argonne National Laboratory, Argonne IL; United States of America.

⁷Department of Physics, University of Arizona, Tucson AZ; United States of America.

⁸Department of Physics, University of Texas at Arlington, Arlington TX; United States of America.

⁹Physics Department, National and Kapodistrian University of Athens, Athens; Greece.

¹⁰Physics Department, National Technical University of Athens, Zografou; Greece.

¹¹Department of Physics, University of Texas at Austin, Austin TX; United States of America.

¹²Institute of Physics, Azerbaijan Academy of Sciences, Baku; Azerbaijan.

¹³Institut de Física d'Altes Energies (IFAE), Barcelona Institute of Science and Technology, Barcelona; Spain.

¹⁴Institute of High Energy Physics, Chinese Academy of Sciences, Beijing; China.

¹⁵Physics Department, Tsinghua University, Beijing; China.

¹⁶Institute of Physics, University of Belgrade, Belgrade; Serbia.

¹⁷Department for Physics and Technology, University of Bergen, Bergen; Norway.

^{18(a)}Physics Division, Lawrence Berkeley National Laboratory, Berkeley CA; ^(b)University of California, Berkeley CA; United States of America.

¹⁹Institut für Physik, Humboldt Universität zu Berlin, Berlin; Germany.

²⁰Albert Einstein Center for Fundamental Physics and Laboratory for High Energy Physics, University of Bern, Bern; Switzerland.

²¹School of Physics and Astronomy, University of Birmingham, Birmingham; United Kingdom.

^{22(a)}Department of Physics, Bogazici University, Istanbul; ^(b)Department of Physics Engineering, Gaziantep University, Gaziantep; ^(c)Department of Physics, Istanbul University, Istanbul; Türkiye.

^{23(a)}Facultad de Ciencias y Centro de Investigaciones, Universidad Antonio Nariño, Bogotá; ^(b)Departamento de Física, Universidad Nacional de Colombia, Bogotá; Colombia.

- ^{24(a)}Dipartimento di Fisica e Astronomia A. Righi, Università di Bologna, Bologna; ^(b)INFN Sezione di Bologna; Italy.
- ²⁵Physikalisches Institut, Universität Bonn, Bonn; Germany.
- ²⁶Department of Physics, Boston University, Boston MA; United States of America.
- ²⁷Department of Physics, Brandeis University, Waltham MA; United States of America.
- ^{28(a)}Transilvania University of Brasov, Brasov; ^(b)Horia Hulubei National Institute of Physics and Nuclear Engineering, Bucharest; ^(c)Department of Physics, Alexandru Ioan Cuza University of Iasi, Iasi; ^(d)National Institute for Research and Development of Isotopic and Molecular Technologies, Physics Department, Cluj-Napoca; ^(e)National University of Science and Technology Politehnica, Bucharest; ^(f)West University in Timisoara, Timisoara; ^(g)Faculty of Physics, University of Bucharest, Bucharest; Romania.
- ^{29(a)}Faculty of Mathematics, Physics and Informatics, Comenius University, Bratislava; ^(b)Department of Subnuclear Physics, Institute of Experimental Physics of the Slovak Academy of Sciences, Kosice; Slovak Republic.
- ³⁰Physics Department, Brookhaven National Laboratory, Upton NY; United States of America.
- ³¹Universidad de Buenos Aires, Facultad de Ciencias Exactas y Naturales, Departamento de Física, y CONICET, Instituto de Física de Buenos Aires (IFIBA), Buenos Aires; Argentina.
- ³²California State University, CA; United States of America.
- ³³Cavendish Laboratory, University of Cambridge, Cambridge; United Kingdom.
- ^{34(a)}Department of Physics, University of Cape Town, Cape Town; ^(b)iThemba Labs, Western Cape; ^(c)Department of Mechanical Engineering Science, University of Johannesburg, Johannesburg; ^(d)National Institute of Physics, University of the Philippines Diliman (Philippines); ^(e)Department of Physics, Stellenbosch University, Matieland; ^(f)University of KwaZulu-Natal, School of Agriculture and Science, Mathematics, Westville; ^(g)University of South Africa, Department of Physics, Pretoria; ^(h)University of Pretoria, Department of Mechanical and Aeronautical Engineering, Pretoria; ⁽ⁱ⁾University of Zululand, KwaDlangezwa; ^(j)School of Physics, University of the Witwatersrand, Johannesburg; South Africa.
- ³⁵Department of Physics, Carleton University, Ottawa ON; Canada.
- ^{36(a)}Faculté des Sciences Ain Chock, Université Hassan II de Casablanca; ^(b)Faculté des Sciences, Université Ibn-Tofail, Kénitra; ^(c)Faculté des Sciences Semlalia, Université Cadi Ayyad, LPHEA-Marrakech; ^(d)LPMR, Faculté des Sciences, Université Mohamed Premier, Oujda; ^(e)Faculté des sciences, Université Mohammed V, Rabat; ^(f)Institute of Applied Physics, Mohammed VI Polytechnic University, Ben Guerir; Morocco.
- ³⁷CERN, Geneva; Switzerland.
- ³⁸Affiliated with an institute formerly covered by a cooperation agreement with CERN.
- ³⁹Affiliated with an international laboratory covered by a cooperation agreement with CERN.
- ⁴⁰Enrico Fermi Institute, University of Chicago, Chicago IL; United States of America.
- ⁴¹LPC, Université Clermont Auvergne, CNRS/IN2P3, Clermont-Ferrand; France.
- ⁴²Nevis Laboratory, Columbia University, Irvington NY; United States of America.
- ⁴³Niels Bohr Institute, University of Copenhagen, Copenhagen; Denmark.
- ^{44(a)}Dipartimento di Fisica, Università della Calabria, Rende; ^(b)INFN Gruppo Collegato di Cosenza, Laboratori Nazionali di Frascati; Italy.
- ⁴⁵Physics Department, Southern Methodist University, Dallas TX; United States of America.
- ⁴⁶National Centre for Scientific Research "Demokritos", Agia Paraskevi; Greece.
- ^{47(a)}Department of Physics, Stockholm University; ^(b)Oskar Klein Centre, Stockholm; Sweden.
- ⁴⁸Deutsches Elektronen-Synchrotron DESY, Hamburg and Zeuthen; Germany.
- ⁴⁹Fakultät Physik, Technische Universität Dortmund, Dortmund; Germany.
- ⁵⁰Institut für Kern- und Teilchenphysik, Technische Universität Dresden, Dresden; Germany.

- ⁵¹Department of Physics, Duke University, Durham NC; United States of America.
- ⁵²SUPA - School of Physics and Astronomy, University of Edinburgh, Edinburgh; United Kingdom.
- ⁵³INFN e Laboratori Nazionali di Frascati, Frascati; Italy.
- ⁵⁴Physikalisches Institut, Albert-Ludwigs-Universität Freiburg, Freiburg; Germany.
- ⁵⁵II. Physikalisches Institut, Georg-August-Universität Göttingen, Göttingen; Germany.
- ⁵⁶Département de Physique Nucléaire et Corpusculaire, Université de Genève, Genève; Switzerland.
- ⁵⁷(^a) Dipartimento di Fisica, Università di Genova, Genova; (^b) INFN Sezione di Genova; Italy.
- ⁵⁸II. Physikalisches Institut, Justus-Liebig-Universität Giessen, Giessen; Germany.
- ⁵⁹SUPA - School of Physics and Astronomy, University of Glasgow, Glasgow; United Kingdom.
- ⁶⁰LPSC, Université Grenoble Alpes, CNRS/IN2P3, Grenoble INP, Grenoble; France.
- ⁶¹Laboratory for Particle Physics and Cosmology, Harvard University, Cambridge MA; United States of America.
- ⁶²Department of Modern Physics and State Key Laboratory of Particle Detection and Electronics, University of Science and Technology of China, Hefei; China.
- ⁶³(^a) Kirchhoff-Institut für Physik, Ruprecht-Karls-Universität Heidelberg, Heidelberg; (^b) Physikalisches Institut, Ruprecht-Karls-Universität Heidelberg, Heidelberg; Germany.
- ⁶⁴(^a) Department of Physics, Chinese University of Hong Kong, Shatin, N.T., Hong Kong; (^b) Department of Physics, University of Hong Kong, Hong Kong; (^c) Department of Physics and Institute for Advanced Study, Hong Kong University of Science and Technology, Clear Water Bay, Kowloon, Hong Kong; China.
- ⁶⁵Department of Physics, National Tsing Hua University, Hsinchu; Taiwan.
- ⁶⁶IJCLab, Université Paris-Saclay, CNRS/IN2P3, 91405, Orsay; France.
- ⁶⁷Centro Nacional de Microelectrónica (IMB-CNM-CSIC), Barcelona; Spain.
- ⁶⁸Department of Physics, Indiana University, Bloomington IN; United States of America.
- ⁶⁹(^a) INFN Gruppo Collegato di Udine, Sezione di Trieste, Udine; (^b) ICTP, Trieste; (^c) Dipartimento Politecnico di Ingegneria e Architettura, Università di Udine, Udine; Italy.
- ⁷⁰(^a) INFN Sezione di Lecce; (^b) Dipartimento di Matematica e Fisica, Università del Salento, Lecce; Italy.
- ⁷¹(^a) INFN Sezione di Milano; (^b) Dipartimento di Fisica, Università di Milano, Milano; Italy.
- ⁷²(^a) INFN Sezione di Napoli; (^b) Dipartimento di Fisica, Università di Napoli, Napoli; Italy.
- ⁷³(^a) INFN Sezione di Pavia; (^b) Dipartimento di Fisica, Università di Pavia, Pavia; Italy.
- ⁷⁴(^a) INFN Sezione di Pisa; (^b) Dipartimento di Fisica E. Fermi, Università di Pisa, Pisa; Italy.
- ⁷⁵(^a) INFN Sezione di Roma; (^b) Dipartimento di Fisica, Sapienza Università di Roma, Roma; Italy.
- ⁷⁶(^a) INFN Sezione di Roma Tor Vergata; (^b) Dipartimento di Fisica, Università di Roma Tor Vergata, Roma; Italy.
- ⁷⁷(^a) INFN Sezione di Roma Tre; (^b) Dipartimento di Matematica e Fisica, Università Roma Tre, Roma; Italy.
- ⁷⁸(^a) INFN-TIFPA; (^b) Università degli Studi di Trento, Trento; Italy.
- ⁷⁹Universität Innsbruck, Department of Astro and Particle Physics, Innsbruck; Austria.
- ⁸⁰Department of Physics and Astronomy, Iowa State University, Ames IA; United States of America.
- ⁸¹Istinye University, Sariyer, Istanbul; Türkiye.
- ⁸²(^a) Departamento de Engenharia Elétrica, Universidade Federal de Juiz de Fora (UFJF), Juiz de Fora; (^b) Universidade Federal do Rio De Janeiro COPPE/EE/IF, Rio de Janeiro; (^c) Instituto de Física, Universidade de São Paulo, São Paulo; (^d) Rio de Janeiro State University, Rio de Janeiro; (^e) Federal University of Bahia, Bahia; Brazil.
- ⁸³KEK, High Energy Accelerator Research Organization, Tsukuba; Japan.
- ⁸⁴(^a) Khalifa University of Science and Technology, Abu Dhabi; (^b) University of Sharjah, Sharjah; United Arab Emirates.
- ⁸⁵Graduate School of Science, Kobe University, Kobe; Japan.

- ⁸⁶(^a) AGH University of Krakow, Faculty of Physics and Applied Computer Science, Krakow; (^b) Marian Smoluchowski Institute of Physics, Jagiellonian University, Krakow; Poland.
- ⁸⁷Institute of Nuclear Physics Polish Academy of Sciences, Krakow; Poland.
- ⁸⁸Faculty of Science, Kyoto University, Kyoto; Japan.
- ⁸⁹Research Center for Advanced Particle Physics and Department of Physics, Kyushu University, Fukuoka ; Japan.
- ⁹⁰L2IT, Université de Toulouse, CNRS/IN2P3, UPS, Toulouse; France.
- ⁹¹Instituto de Física La Plata, Universidad Nacional de La Plata and CONICET, La Plata; Argentina.
- ⁹²Physics Department, Lancaster University, Lancaster; United Kingdom.
- ⁹³Oliver Lodge Laboratory, University of Liverpool, Liverpool; United Kingdom.
- ⁹⁴Department of Experimental Particle Physics, Jožef Stefan Institute and Department of Physics, University of Ljubljana, Ljubljana; Slovenia.
- ⁹⁵Department of Physics and Astronomy, Queen Mary University of London, London; United Kingdom.
- ⁹⁶Department of Physics, Royal Holloway University of London, Egham; United Kingdom.
- ⁹⁷Department of Physics and Astronomy, University College London, London; United Kingdom.
- ⁹⁸Louisiana Tech University, Ruston LA; United States of America.
- ⁹⁹Fysiska institutionen, Lunds universitet, Lund; Sweden.
- ¹⁰⁰Departamento de Física Teórica C-15 and CIAFF, Universidad Autónoma de Madrid, Madrid; Spain.
- ¹⁰¹Institut für Physik, Universität Mainz, Mainz; Germany.
- ¹⁰²School of Physics and Astronomy, University of Manchester, Manchester; United Kingdom.
- ¹⁰³CPPM, Aix-Marseille Université, CNRS/IN2P3, Marseille; France.
- ¹⁰⁴Department of Physics, University of Massachusetts, Amherst MA; United States of America.
- ¹⁰⁵Department of Physics, McGill University, Montreal QC; Canada.
- ¹⁰⁶School of Physics, University of Melbourne, Victoria; Australia.
- ¹⁰⁷Department of Physics, University of Michigan, Ann Arbor MI; United States of America.
- ¹⁰⁸Department of Physics and Astronomy, Michigan State University, East Lansing MI; United States of America.
- ¹⁰⁹Group of Particle Physics, University of Montreal, Montreal QC; Canada.
- ¹¹⁰Fakultät für Physik, Ludwig-Maximilians-Universität München, München; Germany.
- ¹¹¹Max-Planck-Institut für Physik (Werner-Heisenberg-Institut), München; Germany.
- ¹¹²Graduate School of Science and Kobayashi-Maskawa Institute, Nagoya University, Nagoya; Japan.
- ¹¹³(^a) Department of Physics, Nanjing University, Nanjing; (^b) School of Science, Shenzhen Campus of Sun Yat-sen University; (^c) University of Chinese Academy of Science (UCAS), Beijing; China.
- ¹¹⁴(^a) School of Physics, Nankai University, Tianjin; (^b) Institute of Frontier and Interdisciplinary Science and Key Laboratory of Particle Physics and Particle Irradiation (MOE), Shandong University, Qingdao; (^c) School of Physics, Zhengzhou University; China.
- ¹¹⁵Department of Physics and Astronomy, University of New Mexico, Albuquerque NM; United States of America.
- ¹¹⁶Institute for Mathematics, Astrophysics and Particle Physics, Radboud University/Nikhef, Nijmegen; Netherlands.
- ¹¹⁷Nikhef National Institute for Subatomic Physics and University of Amsterdam, Amsterdam; Netherlands.
- ¹¹⁸Department of Physics, Northern Illinois University, DeKalb IL; United States of America.
- ¹¹⁹(^a) New York University Abu Dhabi, Abu Dhabi; (^b) United Arab Emirates University, Al Ain; United Arab Emirates.
- ¹²⁰Department of Physics, New York University, New York NY; United States of America.
- ¹²¹Ochanomizu University, Otsuka, Bunkyo-ku, Tokyo; Japan.

- ¹²²Ohio State University, Columbus OH; United States of America.
- ¹²³Homer L. Dodge Department of Physics and Astronomy, University of Oklahoma, Norman OK; United States of America.
- ¹²⁴Department of Physics, Oklahoma State University, Stillwater OK; United States of America.
- ¹²⁵Palacký University, Joint Laboratory of Optics, Olomouc; Czech Republic.
- ¹²⁶Institute for Fundamental Science, University of Oregon, Eugene, OR; United States of America.
- ¹²⁷Graduate School of Science, University of Osaka, Osaka; Japan.
- ¹²⁸Department of Physics, University of Oslo, Oslo; Norway.
- ¹²⁹Department of Physics, Oxford University, Oxford; United Kingdom.
- ¹³⁰LPNHE, Sorbonne Université, Université Paris Cité, CNRS/IN2P3, Paris; France.
- ¹³¹Department of Physics, University of Pennsylvania, Philadelphia PA; United States of America.
- ¹³²Department of Physics and Astronomy, University of Pittsburgh, Pittsburgh PA; United States of America.
- ¹³³(^a) Laboratório de Instrumentação e Física Experimental de Partículas - LIP, Lisboa; (^b) Departamento de Física, Faculdade de Ciências, Universidade de Lisboa, Lisboa; (^c) Departamento de Física, Universidade de Coimbra, Coimbra; (^d) Centro de Física Nuclear da Universidade de Lisboa, Lisboa; (^e) Departamento de Física, Escola de Ciências, Universidade do Minho, Braga; (^f) Departamento de Física Teórica y del Cosmos, Universidad de Granada, Granada (Spain); (^g) Departamento de Física, Instituto Superior Técnico, Universidade de Lisboa, Lisboa; Portugal.
- ¹³⁴Institute of Physics of the Czech Academy of Sciences, Prague; Czech Republic.
- ¹³⁵Czech Technical University in Prague, Prague; Czech Republic.
- ¹³⁶Charles University, Faculty of Mathematics and Physics, Prague; Czech Republic.
- ¹³⁷Particle Physics Department, Rutherford Appleton Laboratory, Didcot; United Kingdom.
- ¹³⁸IRFU, CEA, Université Paris-Saclay, Gif-sur-Yvette; France.
- ¹³⁹Santa Cruz Institute for Particle Physics, University of California Santa Cruz, Santa Cruz CA; United States of America.
- ¹⁴⁰(^a) Departamento de Física, Pontificia Universidad Católica de Chile, Santiago; (^b) Millennium Institute for Subatomic physics at high energy frontier (SAPHIR), Santiago; (^c) Instituto de Investigación Multidisciplinario en Ciencia y Tecnología, y Departamento de Física, Universidad de La Serena; (^d) Universidad Andres Bello, Department of Physics, Santiago; (^e) Universidad San Sebastian, Recoleta; (^f) Instituto de Alta Investigación, Universidad de Tarapacá, Arica; (^g) Departamento de Física, Universidad Técnica Federico Santa María, Valparaíso; Chile.
- ¹⁴¹Department of Physics, Institute of Science, Tokyo; Japan.
- ¹⁴²Department of Physics, University of Washington, Seattle WA; United States of America.
- ¹⁴³(^a) State Key Laboratory of Dark Matter Physics, School of Physics and Astronomy, Shanghai Jiao Tong University, Key Laboratory for Particle Astrophysics and Cosmology (MOE), SKLPPC, Shanghai; (^b) State Key Laboratory of Dark Matter Physics, Tsung-Dao Lee Institute, Shanghai Jiao Tong University, Shanghai; China.
- ¹⁴⁴Department of Physics and Astronomy, University of Sheffield, Sheffield; United Kingdom.
- ¹⁴⁵Department of Physics, Shinshu University, Nagano; Japan.
- ¹⁴⁶Department Physik, Universität Siegen, Siegen; Germany.
- ¹⁴⁷Department of Physics, Simon Fraser University, Burnaby BC; Canada.
- ¹⁴⁸SLAC National Accelerator Laboratory, Stanford CA; United States of America.
- ¹⁴⁹Department of Physics, Royal Institute of Technology, Stockholm; Sweden.
- ¹⁵⁰Departments of Physics and Astronomy, Stony Brook University, Stony Brook NY; United States of America.
- ¹⁵¹Department of Physics and Astronomy, University of Sussex, Brighton; United Kingdom.

- ¹⁵²School of Physics, University of Sydney, Sydney; Australia.
- ¹⁵³Institute of Physics, Academia Sinica, Taipei; Taiwan.
- ¹⁵⁴(^a) E. Andronikashvili Institute of Physics, Iv. Javakhishvili Tbilisi State University, Tbilisi; (^b) High Energy Physics Institute, Tbilisi State University, Tbilisi; (^c) University of Georgia, Tbilisi; Georgia.
- ¹⁵⁵Department of Physics, Technion, Israel Institute of Technology, Haifa; Israel.
- ¹⁵⁶Raymond and Beverly Sackler School of Physics and Astronomy, Tel Aviv University, Tel Aviv; Israel.
- ¹⁵⁷Department of Physics, Aristotle University of Thessaloniki, Thessaloniki; Greece.
- ¹⁵⁸International Center for Elementary Particle Physics and Department of Physics, University of Tokyo, Tokyo; Japan.
- ¹⁵⁹Graduate School of Science and Technology, Tokyo Metropolitan University, Tokyo; Japan.
- ¹⁶⁰Department of Physics, University of Toronto, Toronto ON; Canada.
- ¹⁶¹(^a) TRIUMF, Vancouver BC; (^b) Department of Physics and Astronomy, York University, Toronto ON; Canada.
- ¹⁶²Division of Physics and Tomonaga Center for the History of the Universe, Faculty of Pure and Applied Sciences, University of Tsukuba, Tsukuba; Japan.
- ¹⁶³Department of Physics and Astronomy, Tufts University, Medford MA; United States of America.
- ¹⁶⁴Department of Physics and Astronomy, University of California Irvine, Irvine CA; United States of America.
- ¹⁶⁵University of West Attica, Athens; Greece.
- ¹⁶⁶Department of Physics and Astronomy, University of Uppsala, Uppsala; Sweden.
- ¹⁶⁷Department of Physics, University of Illinois, Urbana IL; United States of America.
- ¹⁶⁸Instituto de Física Corpuscular (IFIC), Centro Mixto Universidad de Valencia - CSIC, Valencia; Spain.
- ¹⁶⁹Department of Physics, University of British Columbia, Vancouver BC; Canada.
- ¹⁷⁰Department of Physics and Astronomy, University of Victoria, Victoria BC; Canada.
- ¹⁷¹Fakultät für Physik und Astronomie, Julius-Maximilians-Universität Würzburg, Würzburg; Germany.
- ¹⁷²Department of Physics, University of Warwick, Coventry; United Kingdom.
- ¹⁷³Waseda University, Tokyo; Japan.
- ¹⁷⁴Department of Particle Physics and Astrophysics, Weizmann Institute of Science, Rehovot; Israel.
- ¹⁷⁵Department of Physics, University of Wisconsin, Madison WI; United States of America.
- ¹⁷⁶Fakultät für Mathematik und Naturwissenschaften, Fachgruppe Physik, Bergische Universität Wuppertal, Wuppertal; Germany.
- ¹⁷⁷Department of Physics, Yale University, New Haven CT; United States of America.
- ¹⁷⁸Yerevan Physics Institute, Yerevan; Armenia.
- ^a Also at Affiliated with an institute formerly covered by a cooperation agreement with CERN.
- ^b Also at An-Najah National University, Nablus; Palestine.
- ^c Also at Borough of Manhattan Community College, City University of New York, New York NY; United States of America.
- ^d Also at Center for Interdisciplinary Research and Innovation (CIRI-AUTH), Thessaloniki; Greece.
- ^e Also at Centre of Physics of the Universities of Minho and Porto (CF-UM-UP); Portugal.
- ^f Also at CERN, Geneva; Switzerland.
- ^g Also at Département de Physique Nucléaire et Corpusculaire, Université de Genève, Genève; Switzerland.
- ^h Also at Departament de Física de la Universitat Autònoma de Barcelona, Barcelona; Spain.
- ⁱ Also at Department of Financial and Management Engineering, University of the Aegean, Chios; Greece.
- ^j Also at Department of Modern Physics and State Key Laboratory of Particle Detection and Electronics, University of Science and Technology of China, Hefei; China.
- ^k Also at Department of Physics, Ben Gurion University of the Negev, Beer Sheva; Israel.

- ^l Also at Department of Physics, Bolu Abant Izzet Baysal University, Bolu; Türkiye.
- ^m Also at Department of Physics, King's College London, London; United Kingdom.
- ⁿ Also at Department of Physics, Stellenbosch University; South Africa.
- ^o Also at Department of Physics, University of Fribourg, Fribourg; Switzerland.
- ^p Also at Department of Physics, University of Thessaly; Greece.
- ^q Also at Department of Physics, Westmont College, Santa Barbara; United States of America.
- ^r Also at Faculty of Physics, Sofia University, 'St. Kliment Ohridski', Sofia; Bulgaria.
- ^s Also at Faculty of Physics, University of Bucharest; Romania.
- ^t Also at Hellenic Open University, Patras; Greece.
- ^u Also at Henan University; China.
- ^v Also at Imam Mohammad Ibn Saud Islamic University; Saudi Arabia.
- ^w Also at Indian Institute of Technology (IIT), Jodhpur; India.
- ^x Also at Institutio Catalana de Recerca i Estudis Avancats, ICREA, Barcelona; Spain.
- ^y Also at Institut für Experimentalphysik, Universität Hamburg, Hamburg; Germany.
- ^z Also at Institute for Nuclear Research and Nuclear Energy (INRNE) of the Bulgarian Academy of Sciences, Sofia; Bulgaria.
- ^{aa} Also at Institute of Applied Physics, Mohammed VI Polytechnic University, Ben Guerir; Morocco.
- ^{ab} Also at Institute of Particle Physics (IPP); Canada.
- ^{ac} Also at Institute of Physics and Technology, Mongolian Academy of Sciences, Ulaanbaatar; Mongolia.
- ^{ad} Also at Institute of Physics, Azerbaijan Academy of Sciences, Baku; Azerbaijan.
- ^{ae} Also at Institute of Theoretical Physics, Ilia State University, Tbilisi; Georgia.
- ^{af} Also at Millennium Institute for Subatomic physics at high energy frontier (SAPHIR), Santiago; Chile.
- ^{ag} Also at National Institute of Physics, University of the Philippines Diliman (Philippines); Philippines.
- ^{ah} Also at The Collaborative Innovation Center of Quantum Matter (CICQM), Beijing; China.
- ^{ai} Also at TRIUMF, Vancouver BC; Canada.
- ^{aj} Also at Università di Napoli Parthenope, Napoli; Italy.
- ^{ak} Also at University of Chinese Academy of Sciences (UCAS), Beijing; China.
- ^{al} Also at University of Colorado Boulder, Department of Physics, Colorado; United States of America.
- ^{am} Also at University of Siena; Italy.
- ^{an} Also at Washington College, Chestertown, MD; United States of America.
- ^{ao} Also at Yeditepe University, Physics Department, Istanbul; Türkiye.
- * Deceased